Study on Elastic Buckling Strength of Steel Members with Bracing

The University of Kitakyushu

Graduate School of Environmental Engineering

Mao LIU

March, 2016

Contents

Chapter 1

Introduction

1.1 Purposes

This dissertation is concerned with the design methods for bracing of steel members and aimed at developing the methods for increasing the elastic buckling strength.

The design methods for bracing of steel structure are presented in Design Standard for Steel Structures[1)], Recommendation for Limit Design of Steel Structures[2)], Recommendations for the Plastic Design of Steel Structures[3)] and Recommendations for Stability Design of Steel Structures[4)].

This study referred to bracing of steel member consists of 1) bracing for compressive members to varying axial force in a staircase pattern, 2) relation between elastic buckling strength and bracing stiffness of H-shaped members with lateral bracing or torsional bracing when subjected to axial force, end moments and uniformly distributed load. The purposes of each part are shown as follows.

1) As for the members subjected to varying axial forces in a staircase pattern such as pony truss, the buckling strength of the members is larger than that of the members subjected to uniform axial force[4)]. In references 1) and 4), the equation is presented for calculating the effective length factor of members that has two parts subjected to different axial forces (Fig. 1(b-1) and (c-1)). When calculating the effective length factor of the member that has three parts subjected to different axial forces, the axial force in a staircase pattern is considered as that subjected to the axial force that varies continuously(Fig. 1(b-2) and (c-2)). The effective length can be calculating by using the equations for the effective length of the members subjected to axial force that varies

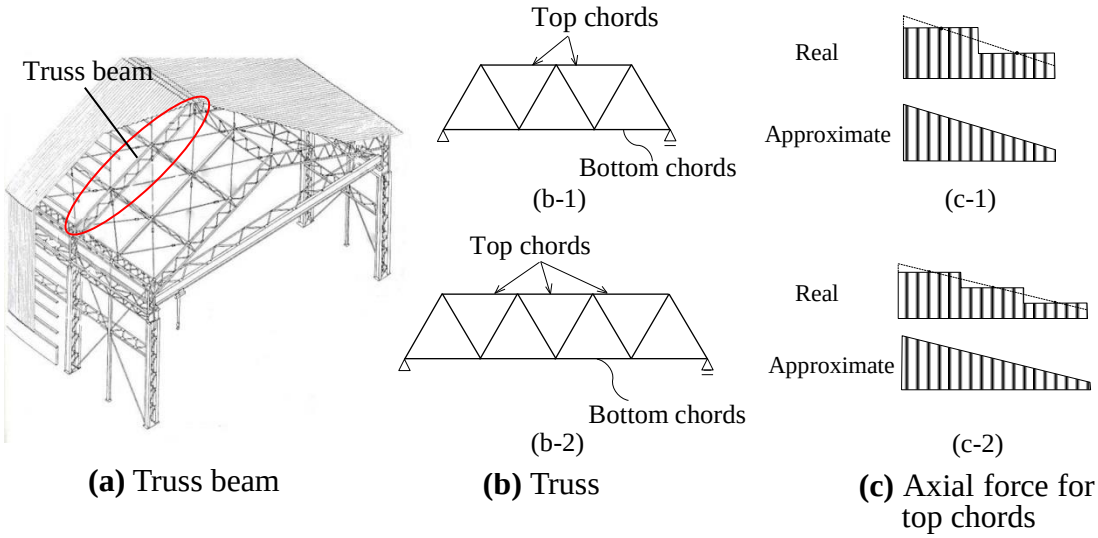

Fig. 1.1 Models of compressive members subjected to varying axial force in a staircase pattern

continuously which are presented in references 1) and 4).

The relation between the buckling strength and the bracing stiffness and the minimum bracing stiffness that the effective length can be taken as brace spacing are presented when the member is supported by equally spaced brace[4]. The required nondimensional bracing stiffness k is unity when there is one supporting point and k=1.5 and 1.7 when there are two or three supporting points respectively[4]. However, there are few studies about the buckling strength and bracing of members subjected to varying axial force in a staircase pattern.

The bracing frames should have sufficient stiffness and strength. In reference 4), the relation between the compressive force and bracing force of the elastic compressive members and the bracing force of the inelastic compressive members are presented. And the sufficient bracing force is 2% of the compressive force when the bracing stiffness k is greater than 3. However, this result was derived from the analytical and the experimental studies by using the compressive members subjected to uniform axial force and the relation between bracing force and axial force of the members subjected to varying axial force is not clear.

Therefore, as the first target of this dissertation, the problems of bracing for compressive member subjected to varying axial force in a staircase pattern will be discussed.

2) H-shaped beam or beam-column members are sometimes restrained laterally between their ends by elastic lateral supports to prevent lateral buckling and flexural-torsional buckling. Typical examples include (1) the beam-column members

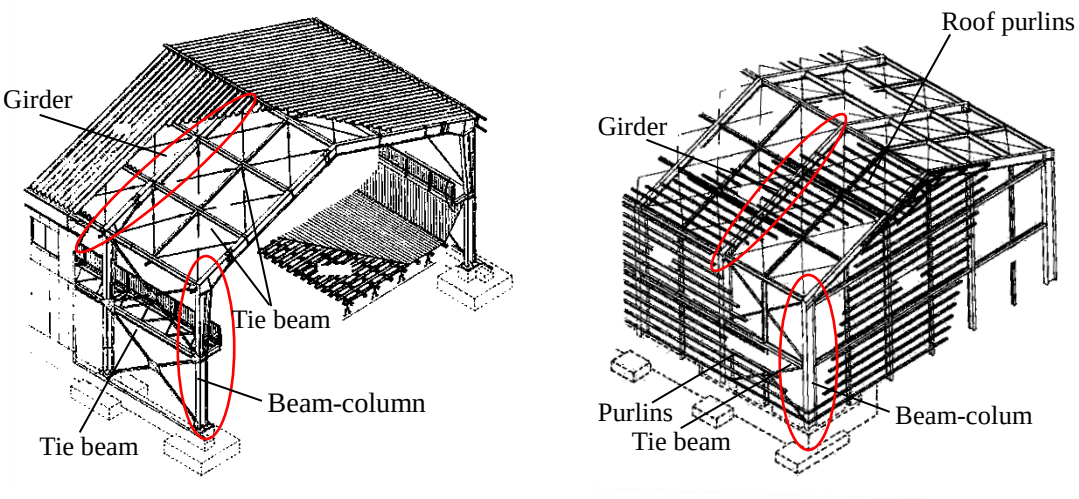

(a) **(b)**

Fig. 1.2 Examples of bracing used in industrial buildings

which are laterally restrained by tie beams used for industrial buildings and (2) the girders which are supported by secondary beams in general steel structures or tie beams in industrial buildings. Figure 1.2(a) presents a typical steel industrial building whose H-shaped beams and beam-columns are supported by tie beams as bracing. Figure 1.2(b) shows an example of continuous bracing that the H-shaped beams or beam-columns are supported by purlins.

In Recommendation for Limit State Design, the required bracing stiffness and the required bracing force are shown for flexural buckling of compressive members, lateral buckling of members subjected to bending moment and beam-columns respectively. These design methods for bracing are based on the study results of bracing for flexural buckling of compressive members subjected to the uniform axial force. Most of studies commencing with references 5) and 6) target the members subjected to uniform axial force although the studies investigated the flexural buckling of the members with multiple bracing, initial imperfection and inelastic buckling behavior.

As for the flexural-torsional buckling of H-shaped beam-columns or the lateral buckling of beams, the research results of bracing of compressive members subjected to uniform axial force are introduced by considering the flexural-torsional buckling or the lateral buckling as the flexural buckling of the compressive flange. Compressive member subjected to uniform axial force corresponds to the compressive flange of H-shaped beam which is subjected to uniform bending moment. However, the bending moment generally varies along the member axis.

Some studies have focused on the problems of bracing for beam-columns, such as references 7) and 8). The buckling equation of beam-columns with a sandwich section when single lateral bracing and single torsional bracing is attached at the midspan of the member was derived by using the Rayleigh-Ritz method. The effects of loading conditions, bracing stiffness and resistance by St. Venant torsion on the flexural-torsional buckling strength were presented[9)]. However, few studies show systematically the relation between buckling strength and bracing stiffness of the H-shaped member with lateral bracing or torsional bracing subjected to axial force, end moments concurrently. The effects of the size of cross section, the length of member and the position of bracing on the buckling strength are not clear.

As for the bracing for beams, most of studies referred to the lateral bracing when the beam members are subjected end moments and distributed load concurrently, such as references 10) ~14). However, all of these studies are about the continuous bracing, and the relation between buckling strength and bracing stiffness and the influence on

bracing force in the cases of discrete lateral bracing and discrete torsional bracing are not clarified. Although reference 15) relates to the influence of lateral bracing and torsional bracing on the lateral buckling strength of beams, and the relation between buckling strength and bracing stiffness is presented, the distributed load is not considered in the analytical model.

Hence, the problems on discrete lateral bracing and discrete torsional bracing for beam-columns and beams under the real loading conditions will be discussed and the influences of size of cross section, length of member and position of bracing will be taken as parameters.

1.2 Outline

This dissertation consists five chapters. Chapter 1 is the introduction of this dissertation and Chapter 5 summaries the results of this research. The abstract of other chapters are shown as follows.

Chapter 2 Bracing for Compressive Members Subjected to Varying Axial Force
Chapter 3 Relation between Elastic Buckling Strength and Bracing Stiffness of H-shaped Beam-column simply supported at Both Ends
Chapter 4 Bracing for buckling of members with pinned ends subjected to end moments and uniformly distributed load

Detail introduction for each chapter is shown as follows.

Chapter 2 is aimed to calculate the effective length factor of compressive member which is subjected to varying axial forces in a staircase pattern by using the buckling slope deflection method. The required bracing stiffness to take the effective length as brace spacing is presented. In addition, the behavior of deflection and the bracing force are shown when the member with initial deformation is subjected varying axial force in a staircase pattern.

Chapter 3 is concerned with the effect of the bracing stiffness on the elastic buckling strength of H-shaped members that are subjected to compressive force and end moments. The buckling equations are presented by Rayleigh-Ritz method when the H-shaped member is simply supported at both ends and discrete or continuous lateral bracing and torsional bracing are attached. The relation between elastic buckling strength and bracing stiffness are presented when the member is subjected to axial force and end moments and the bracing is attached at the midspan of the member. The relation between the compressive force and the required bracing stiffness in order that the deflection and the torsional angle at the bracing point are zero and the equation to obtain the required bracing stiffness is presented.

Chapter 4 focus on the effect of bracing stiffness on the elastic buckling strength of H-shaped members that are subjected to end moments and uniformly distributed load. The relation between the end moment ratio and the nondimensional bending moment are presented by taking the nondimensional distributed load ratio, the bracing stiffness, the cross section, the length and the position of bracing as parameters. Examples of the required bracing stiffness when the bracing strength equals the elastic buckling strength equals the elastic buckling strength when the member is subjected to end moment only is presented.

1.3 Published papers

The published papers referred to this thesis are presented as follows.

Papers

1) Mao Liu, Masae Kido: Bracing for Columns Subjected to Varying Axial Forces – Columns with One or Two braces Subjected to Axial Forces in a Staircase Pattern-, Journal of Structural Engineering, Vol.58B, pp. 357-363, March, 2012.
2) Mao Liu and Masae Kido: Bracing for Columns with Initial Deformation Subjected to Varying Axial Forces in a Staircase Pattern, Proceedings of Constructional Steel (JSSC), Vol.20, pp. 737-740, November, 2012.
3) Mao Liu and Masae Kido: Bracing Strength of Columns Braced Continuously with Different End Support Conditions Subjected to Linear Varying Axial Force, Proceedings of Constructional Steel (JSSC), Vol.22, pp. 652-659, November, 2014.
4) Mao Liu and Masae Kido: Elastic Buckling Strength of H-shaped Beam-column When Bracing is attached at Midspan of the Member- Relation between Elastic Buckling Strength and Bracing Stiffness of H-shaped Member Simply Supported at Both Ends-, Journal of Structural and Construction Engineering (AIJ), Vol.80, No. 712, pp. 927-937, June, 2015.
5) Mao Liu and Masae Kido: Bracing for Buckling of Members with Pinned Ends Subjected to End Moments and Uniformly Distributed Load, Proceedings of Constructional Steel (JSSC), Vol.23, pp. 697-704, November, 2015.

International conferences

6) Mao Liu and Masae Kido: Bracing for Columns with Initial Deformation Subjected to Varying Axial Forces in a Staircase Pattern, New Developments in Structural Engineering and Construction (ISEC-7), Honolulu, pp. 207-211, June, 2013

Internal conferences

7) Mao Liu and Masae Kido: Bracing for Columns Subjected to Varying Axial Forces -Columns with One or Two Braces Subjected to Axial Forces in a Staircase Pattern-, AIJ Kyushu Chapter Architectural Research Meeting, No.51, pp. 373-376, March, 2012.
8) Mao Liu and Masae Kido: Bracing for Columns Subjected to Varying Axial Forces -Columns with One or Two Braces Subjected to Axial Forces in a Staircase Pattern-, Summaries of Technical Papers of Annual Meeting AIJ, pp. 731-732, September, 2012.

9) Mao Liu and Masae Kido: Bracing for Buckling of Members with Pinned Ends Subjected to Bending Moment and Axial Force -Part 1 Analysis and Results of Member Subjected to Axial Force-, AIJ Kyushu Chapter Architectural Research Meeting, No.53, pp. 337-340, March, 2014.
10) Mao Liu and Masae Kido: Bracing for Buckling of Members with Pinned Ends Subjected to Bending Moment and Axial Force -Part 2 Results of Member Subjected to Axial Force and Bending Moment- AIJ Kyushu Chapter Architectural Research Meeting, No.53, pp. 341-344, March, 2014.
11) Mao Liu and Masae Kido: Bracing for Buckling of Members with Fixed Ends Subjected to Bending Moment and Axial Force –Analysis of Buckling Strength of Members Subjected to Axial Force and Bending Moment-, AIJ Kyushu Chapter Architectural Research Meeting, No.53, pp. 345-348, March, 2014.
12) Mao Liu and Masae Kido: Relation Between Elastic Buckling Strength of H-shaped Members Simply Supported at Both Ends and Bracing Stiffness -Analysis and Results When the Member is Subjected to Compressive Force or Bending Moment-, Summaries of Technical Papers of Annual Meeting AIJ, pp.937-938, September, 2014.
13) Mao Liu and Masae Kido: Relation Between Elastic Buckling Strength of H-shaped Members Simply Supported at Both Ends and Bracing Stiffness -Results When the Member is Subjected to Axial Force and End Moment-, Summaries of Technical Papers of Annual Meeting AIJ, pp.939-940, September, 2014.
14) Mao Liu and Masae Kido: Bracing for Buckling of Members with Pinned Ends Subjected to End Moments and Uniformly Distributed Load -Part 1 Analytical Method and Results-, AIJ Kyushu Chapter Architectural Research Meeting, No.54, pp. 397-400, March, 2015.
15) Mao Liu and Masae Kido: Bracing for Buckling of Members with Pinned Ends Subjected to End Moments and Uniformly Distributed Load -Part 2 Analytical Results and Required Bracing Stiffness of Members Subjected to End Moments When Bending Moment Equals Elastic Bending Moment-, AIJ Kyushu Chapter Architectural Research Meeting, No.54, pp. 401-404, March, 2015.
16) Masae Kido and Mao Liu: Bracing for Buckling of Members with Pinned Ends Subjected to End Moments and Uniformly Distributed Load Part 1, Summaries of Technical Papers of Annual Meeting AIJ, pp.849-850, September, 2015.
17) Mao Liu and Masae Kido: Bracing for Buckling of Members with Pinned Ends Subjected to End Moments and Uniformly Distributed Load Part 2, Summaries of Technical Papers of Annual Meeting AIJ, pp.851-852, September, 2015.

References for Chapter 1

1) Architectural Institute of Japan: Design Standard for Steel Structures -Based on Allowable Stress Concept-, 2005.09
2) Architectural Institute of Japan: Recommendation for Limit State Design of Steel Structures, 2010.02
3) Architectural Institute of Japan: Recommendations for the Plastic Design of Steel Structures, 2010.02
4) Architectural Institute of Japan: Recommendations for Stability Design of Steel Structures, 2009.11
5) Yokoo Yoshitsugu, Wakabayashi Minoru and Ueda Kenji: On the stiffness of an intermediate elastic support of a compression member, Transactions of the Architectural Institute of Japan, No.89, p.105, 1963.9
6) Suzuki Toshiro: Lateral bracing forces on beams and columns, Transactions of the Architectural Institute of Japan extra edition, p.295,1966.10
7) Suzuki Toshiro: Lateral buckling of braced columns and beams : I. Characteristics of effective bracing, Transactions of the Architectural Institute of Japan, No.65, pp.54-59, 1960.6
8) Kimura Junichi and Matsui Chiaki: 胴縁で補剛されたH形断面柱の弾性曲げねじれ座屈解析, AIJ Kyushu Chapter Architectural Research Meeting (Structure) , Vol.29, pp.285-288, 1986.3
9) Tsuda Keigo and Kido Masae: Flexural-torsional buckling of beam-columns restrained against sway and rotation at a center, Discussion of beam-columns that have sandwich sections, Journal of Structural and Construction Engineering Vol.78, No.684, pp.377- 385, 2013.02
10) Suzuki Toshiro: Lateral buckling of braced columns and beams : I. Characteristics of effective bracing, Transactions of the Architectural Institute of Japan, No.65, pp.54-59, 1960.6
11) Saisho Motoo and Tanaka Hisashi: Lateral bracing of steel beams (No.2) -Necessary strength and rigidity of lateral bracing, Transactions of the Architectural Institute of Japan, No.224, pp.19-24, 1974.10
12) Wakabayashi Minoru and Nakamura Takeshi: Numerical analysis of lateral buckling strength of H-shaped steel beams subjected to end moments and uniformly distributed load, Transactions of the Architectural Institute of Japan, No.208, pp. 7-13, 1973.6
13) Kato Ben and Akiyama Hiroshi: Lateral buckling of elastic H-section beams with continuous restraints on upper flange, Transactions of the Architectural Institute of

Japan, No.232, pp.41-50, 1975.6
14) Ono Tetsuro, Ishida Tomohiro and Hijikata Kazumi: A study on lateral bracing for steel beam considering lateral and local buckling , Journal of Structural and Construction Engineering, No.533, pp.159-166, 2000.7
15) Kimura Yoshihiro and Yoshino Yuki: Required bracing capacity on lateral buckling strength for H-shaped beams with bracings, Journal of Structural and Construction Engineering Vol.76, No.670, pp.2143-2152, 2011.12

Chapter 2

Bracing for Compressive Members Subjected to Varying Axial Force

2.1 Introduction

The buckling strength of the members in truss structures subjected to varying axial force in a staircase pattern is larger than that of the members subjected to uniform axial force [1)]. In references 1) and 2), the equation is presented for calculating the effective length factor of the member that has two parts subjected to different axial forces. When calculating the effective length factor of the member that has three parts subjected to different axial forces, the axial force in a staircase pattern is substituted to the axial force that varies continuously. The effective length can be calculated by using the equations for the effective length of the member subjected to axial force that varies continuously, which are presented in references 1) and 2).

As for the bracing of the compressive member, there are a lot of studies including reference 3). The relation between the buckling strength and the bracing stiffness and the minimum bracing stiffness that the effective length can be taken as brace spacing are presented when the member is supported by equally spaced brace [1)]. The required nondimensional bracing stiffness k is unity when there is one supporting point and k =1.5 and 1.7 when there are two and three supporting points respectively [1)]. However, there are few studies about the buckling strength and the bracing of the member which is subjected to varying axial force in a staircase pattern.

On the other hand, the bracing frames of the compressive members should have sufficient stiffness as well as sufficient strength. As to the problem about the stability of the top chord of the pony truss, the effective length factor for various values of the transverse frame and the brace spacing have been presented [4)].

In reference 1), the relation between the compressive force and the bracing force of the elastic compressive member and the bracing force of the inelastic compressive member are shown. And the sufficient bracing force is 2% of the compressive force when the nondimensional bracing stiffness k is greater than three. However, this result was derived from the analytical and the experimental study by using the compressive members subjected to uniform axial force and the relation between the bracing force and the axial force of the member subjected to varying axial force is not clear.

In this study, the effective length factor of the members subjected to varying axial force is calculated by using the buckling slope deflection method and the buckling modes are shown in Section 2.2. The axial force varies in a staircase pattern and the members have one and two supporting point. In addition, the required nondimensional bracing stiffness to take the effective length as brace spacing is presented.

Section 2.3 shows the basic findings about the bracing force at the member with initial deformation subjected to varying axial force in a staircase pattern. The

relationship between the axial force and the slope angle are calculated and the comparison among the axial force, the bracing force and the bracing stiffness are presented.

2.2 Bracing for compressive member subjected to varying axial force

2.2.1 Analytical model

Figure 2.1 shows the analytical model when the compressive member with brace is subjected to the axial forces that vary in a staircase pattern

Figure 2.1 (a) shows the model when there is one brace at the middle of the member. The axial force subjected to the right part is N_1 and the axial force subjected to the left part is $N_2=aN_1$ ($-1 \leqq a \leqq 1$). Figs. 2.1(b) and (c) show the model when there are two braces set in equal space along the whole member. The axial force pattern of the model shown in Fig. 2.1 (b) is a staircase pattern. The axial force subjected to the right part is N_1, to the middle part is $N_2=aN_1$ ($0 < a \leqq 1$) and to the left part is $N_3=bN_1$ ($-1 < b \leqq 1$). The axial force pattern of the model shown in Fig. 2.1 (c) is a convex pattern. The axial force subjected to the middle part is N_1 and to the right and the left parts are $N_2=aN_1$ ($0 < a \leqq 1$). In this study, N_i is the general expression for N_1, N_2 and N_3.

2.2.2 Buckling equations

The buckling equations are calculated by using the buckling slope deflection method. In this section, the procedure to obtain the buckling equation is presented.

a) When there is one brace [Fig. 2.1 (a)].

It is assumed that member 1 and 2 are subjected to the slope angles R and $-R$ respectively and joint 2 suffers a deflection angle θ_2 (Fig. 2.2), and we obtain Eq. (2.1.1)

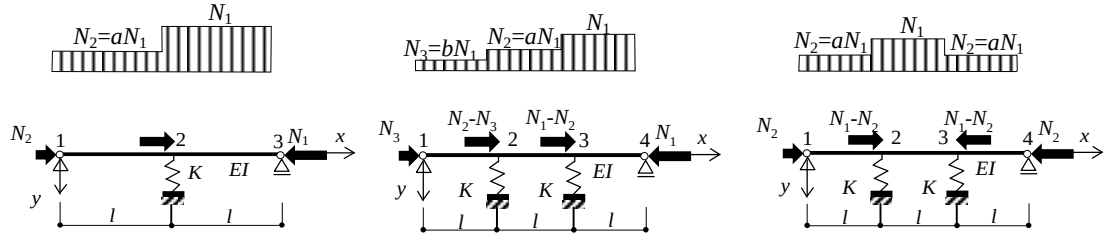

(a) One brace (staircase pattern) **(b)** Two braces (staircase pattern) **(c)** Two braces (convex pattern)

Fig. 2.1 Analytical model

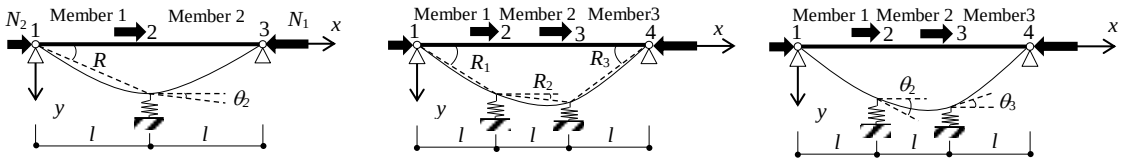

(b-1) Slope angle

(a) One brace **(b)** Two braces

Fig. 2.2 Calculating model

and Eq. (2.1.2) by applying the slope-deflection equation for stability.

$$M_{21}=\frac{EI}{l}(\xi_2\theta_2-\xi_2R)\qquad M_{23}=\frac{EI}{l}(\xi_1\theta_2+\xi_1R) \tag{2.1.1}$$

$$Q_{21}=-\frac{EI}{l^2}(\xi_2\theta_2-\omega_2R)\qquad Q_{23}=-\frac{EI}{l^2}(\xi_1\theta_2+\omega_1R) \tag{2.1.2}$$

In the equations mentioned above, E is the Young's modulus, I is geometrical moment of inertia. α_i, β_i, ξ_i, ω_i, γ_i and δ_i are the stability functions (i=1, 2, 3). Assuming $Z_i=l\sqrt{\frac{|N_i|}{EI}}$, their relations with Z_i are shown as follows.

1) When N_i is compressive force

$$\left.\begin{aligned}
&\alpha_i=\frac{Z_i\sin Z_i-Z_i^{\,2}\cos Z_i}{2(1-\cos Z_i)-Z_i\sin Z_i} && \beta_i=\frac{Z_i^{\,2}-Z_i\sin Z_i}{2(1-\cos Z_i)-Z_i\sin Z_i}\\
&\xi_i=\frac{\alpha_i^{\,2}-\beta_i^{\,2}}{\alpha_i} && \omega_i=\xi_i-Z_i^{\,2}\\
&\gamma_i=\alpha_i+\beta_i && \delta_i=2\gamma_i-Z_i^{\,2}
\end{aligned}\right\} \tag{2.2}$$

2) When N_i is tensile force

$$\left.\begin{aligned}
&\alpha_i=\frac{Z_i\sinh Z_i-Z_i^{\,2}\cosh Z_i}{2(\cosh Z_i-1)-Z_i\sinh Z_i} && \beta_i=\frac{Z_i^{\,2}-Z_i\sinh Z_i}{2(\cosh Z_i-1)-Z_i\sinh Z_i}\\
&\xi_i=\frac{\alpha_i^{\,2}-\beta_i^{\,2}}{\alpha_i} && \omega_i=\xi_i+Z_i^{\,2}\\
&\gamma_i=\alpha_i+\beta_i && \delta_i=2\gamma_i+Z_i^{\,2}
\end{aligned}\right\} \tag{2.3}$$

In which, suffix i corresponds to suffix of the axial force N_i.

Based on the force balance conditions, we get these equations as follows.

$$\begin{aligned}
&M_{21}+M_{23}=\frac{EI}{l}[(\xi_1+\xi_2)\theta_2-(\xi_1-\xi_2)R]=0\\
&\Rightarrow(\xi_1+\xi_2)\theta_2-(\xi_1-\xi_2)R=0
\end{aligned} \tag{2.4}$$

$$\begin{aligned}
&Q_{21}-Q_{23}+F=-\frac{EI}{l^2}(\xi_2\theta_2-\omega_2R)+\frac{EI}{l^2}(\xi_1\theta_2+\omega_1R)+KlR=0\\
&\Rightarrow(\xi_1-\xi_2)\theta_2+(\omega_1+\omega_2+2k\pi^2)R=0
\end{aligned} \tag{2.5}$$

In which, $F=KlR$, $k=\frac{Kl^3}{2\pi^2EI}$

F: the stiffening force, K: the bracing stiffness, k: the nondimensional bracing stiffness, M_{21} and M_{23}: the bending moment at joint 2 of member 1 and 2 respectively, Q_{21} and Q_{23}: the shear force of member 1 and 2 respectively.

In order that the equation-set that is made of Eq. (2.4) and Eq. (2.5) have nontrivial solution, the determinant as follows must be equal to zero, that is

$$\begin{vmatrix} \xi_1+\xi_2 & \xi_1-\xi_2 \\ \xi_1-\xi_2 & \omega_1+\omega_2+2k\pi^2 \end{vmatrix} = 0 \tag{2.6}$$

This is the buckling equation when there is one brace.

b) When there are two braces [Fig. 2.1 (b) and (c)]

As mentioned above, the procedure for the cases of with two braces are similar with the case of one brace, which is presented previously. The buckling equations when there are two braces are shown as follows.

i) Situation 1: the axial forces vary in a staircase pattern [Fig. 2.1 (b)].

$$\begin{vmatrix} \xi_3+\alpha_2 & \beta_2 & \gamma_2-\xi_3 & \gamma_2 \\ \beta_2 & \xi_1+\alpha_2 & \gamma_2 & \gamma_2-\xi_1 \\ \gamma_2-\xi_3 & \gamma_2 & \delta_2+\omega_3+2k\pi^2 & \delta_2 \\ \gamma_2 & \gamma_2-\xi_1 & \delta_2 & \delta_2+\omega_1+2k\pi^2 \end{vmatrix} = 0 \tag{2.7}$$

ii) Situation 2: the axial forces vary in a convex pattern [Fig. 2.1 (c)].

$$\begin{vmatrix} \xi_2+\alpha_1 & \beta_1 & \gamma_1-\xi_2 & \gamma_1 \\ \beta_1 & \xi_2+\alpha_1 & \gamma_1 & \gamma_1-\xi_2 \\ \gamma_1-\xi_2 & \gamma_1 & \delta_1+\omega_2+2k\pi^2 & \delta_1 \\ \gamma_1 & \gamma_1-\xi_2 & \delta_1 & \delta_1+\omega_2+2k\pi^2 \end{vmatrix} = 0 \tag{2.8}$$

The effective length factor for brace spacing γ and the effective length factor for whole length γ_0 are defined as below.

$$N_1 = \frac{\pi^2 EI}{{l_k}^2} = \frac{\pi^2 EI}{(\gamma l)^2} = \frac{\pi^2 EI}{(\gamma_0 nl)^2}\ ,\ \gamma = \frac{l_k}{l} \tag{2.9}$$

In which, *n* is the number of the members.

2.2.3 Buckling modes

The differential equation of the member subjected to axial force is shown as Eq. (2.10).

$$EIy^{\mathrm{IV}} + Ny'' = 0 \tag{2.10}$$

In general, the equations of buckling modes are represented as Eq. (2.11) and (2.12).

1) When *N* is compressive force:

$$y_j = C_{j1}\cos\frac{Z_i}{l}x + C_{j2}\sin\frac{Z_i}{l}x + C_{j3}\frac{x}{l} + C_{j4} \tag{2.11}$$

2) When *N* is tensile force:

$$y_j = C_{j1}\cosh\frac{Z_i}{l}x + C_{j2}\sinh\frac{Z_i}{l}x + C_{j3}\frac{x}{l} + C_{j4} \tag{2.12}$$

3) Specially, when N=0, Eq. (2.10) is rewritten as Eq. (2.13) and the deflection curve is given by Eq. (2.14)

$$EIy^{\mathrm{IV}} = 0 \tag{2.13}$$

$$y_j = \frac{1}{6}C_{j1}(\frac{x}{l})^2 + \frac{1}{2}C_{j2}(\frac{x}{l})^2 + C_{j3}(\frac{x}{l}) + C_{j4} \tag{2.14}$$

In which, j is the member number (j =1, 2, 3)

2.2.4 Analytical parameters

1) For Section 2.25~2.27, the ratio of axial force:

(i) One brace [Fig. 2.1(a)]: a = -1, -0.5, 0, 0.5, 1

(ii) Two brace :

staircase pattern[Fig. 2.1(b)]: (a, b) =(1,1), (3/5,1/5), (1/3, -1/3)

convex patten [Fig. 2.1(c)]: a= 2/5

2) For Section 2.2.8, the effective length fator: γ=1, 1.1, 1.2, 1.3, 1.4, 1.5

2.2.5 Relation between effective length factor γ_0 and nondimensional bracing stiffness k

Fig. 2.3 shows the relation between the effective length factor γ_0 and the nondimensional bracing stiffness k. Fig. 2.3(a) shows the case that there is one brace and Figs. 2.3(b) and (c) show the case that there are two braces.

According to Fig. 2.3(a), when the axial force is uniform (a=1) and the nondimensional bracing stiffness k is greater than unity, the effective length factor for the whole length γ_0 is 0.5 (in this case, the effective length factor for the brace spacing γ=1). According to Figs. 2.3(b) and (c), when the axial force is uniform (a,b=1) and the nondimensional bracing stiffness k is greater than 1.5, γ_0 is 0.333 (γ=1).

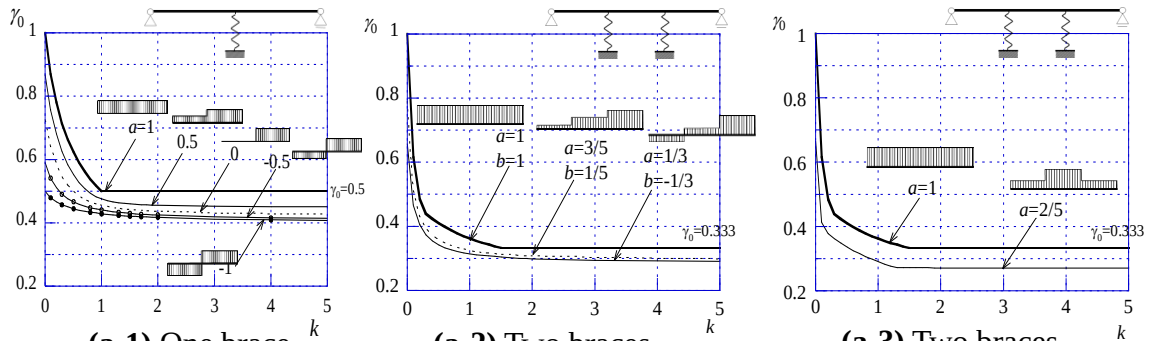

(a-1) One brace **(a-2)** Two braces (staircase pattern) **(a-3)** Two braces (convex pattern)

Fig. 2.3 Relation between bracing stirrness k and effective length factor γ_0

When the axial force is varying (a,b≠1) and the value of the nondimensional bracing stiffness k is the same, the effective length factor γ_0 becomes smaller as the axial force ratio decreases. That is to say, the ratio of axial forces is larger, the effective length factor γ_0 is larger when the nondimensional bracing stiffness k is the same value.

The effective length factor decreases as the nondimensional bracing stiffness increases, however, when the nondimensional bracing stiffness k is more than 2, the variation of the effective length factor γ_0 is very slight.

Fig. 2.4 and 2.5 show the buckling modes when there are one brace and two braces respectively. These are a series of buckling modes about the ratio of axial force, when

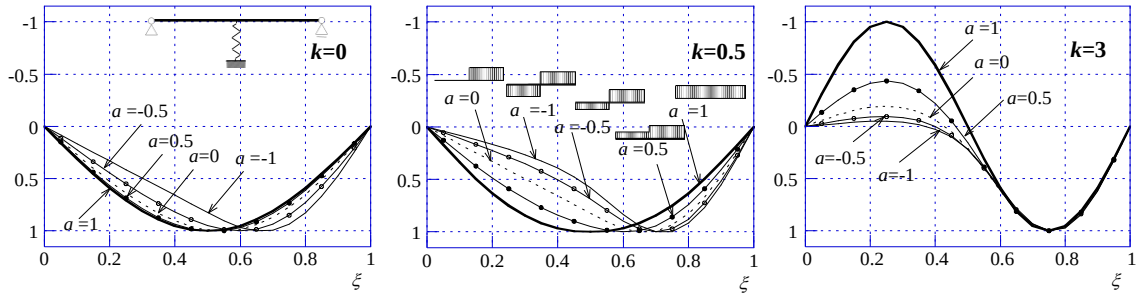

(a) k= 0 **(b)** k= 0.5 **(c)** k= 3

Fig. 2.4 Buckling mode (one brace)

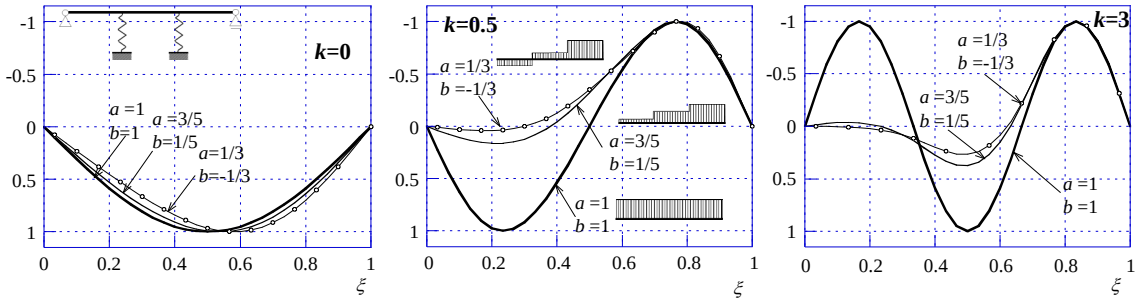

(a-1) k= 0 **(a-2)** k= 0.5 **(a-3)** k= 3

(a) Staircase pattern

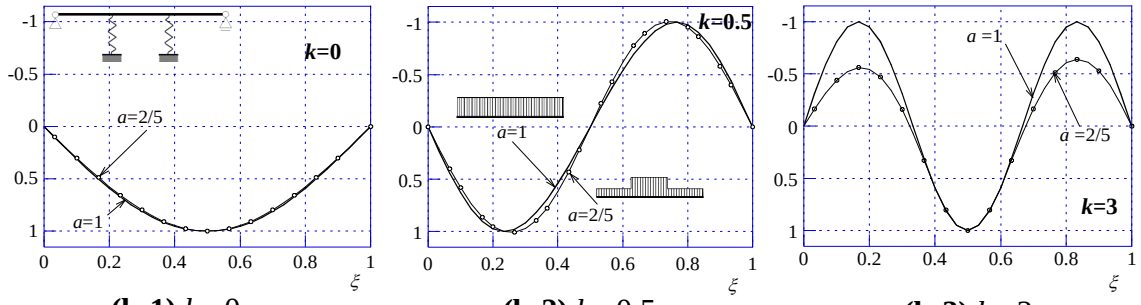

(b-1) k= 0 **(b-2)** k= 0.5 **(b-3)** k= 3

(b) Convex pattern

Fig. 2.5 Buckling mode (two braces)

the value of the nondimensional bracing stiffness k is defined. In Figs. 2.4 and 2.5, the horizontal axis ξ represents the position on the member. ξ is the nondimensional value obtained by normalizing the whole length of the member. When there is one brace $\xi = x/2l$,and when there are two braces, $\xi = x/3l$.

According to Fig. 2.4, when k equals 0 and 0.5, the position of maximum deflection moves from the center to the right side as the axial force ratio decreases. When k equals 3, the deflection decreases as the axial force ratio decreases in the left part.

According to Fig. 2.5(a), when k equals 0.5 and 3, the deflection at the right part is almost same without reference to the axial force ratio and the maximum deflection decreases as the axial force ratio decreases at the left part (Fig. 2.5(a-2)) and at middle part and the left part (Fig. 2.5(a-3)). When the axial force varies convexly (Fig. 2.5 (b)) and k equals 0 and 0.5, the buckling modes are similar regardless of the axial force ratio. When k equals 3, the deflection becomes smaller at the left and the right side as the axial force ratio decreases.

2.2.6 Comparison with design equations

According to reference 2), there is a rule for the design of the effective length l_k. When the two parts of the compressive member are subjected to different axial forces as shown in Fig. 2.1 (a), the member can be designed as the compressive member subjected to uniform axial force, which is the larger one. Remarkably, if one of the axial force is tensile, we should use the negative value of the tensile force to calculate.

$$\left.\begin{aligned} l_k &= l(0.75 + 0.25\frac{N_2}{N_1}) \\ l_k &\geq 0.5l \end{aligned}\right\} \qquad (2.15)$$

In which, l: the length of member

N_1: the larger axial force N_2: the smaller axial force

Table 2.1 shows the comparison of the effective length factor (γ_{01}) obtained by using

Table 2.1 Comparison of the effective length factor

N_2/N_1	γ_{01} (Eq. 2.6)	γ_{02} (Eq. 2.15)	$\frac{\gamma_{01}-\gamma_{02}}{\gamma_{01}}\times 100$ (%)
1	1.000	1.000	0.00
0.5	0.869	0.875	-0.69
0	0.727	0.750	-3.16
-0.5	0.591	0.625	-5.44
-1	0.500	0.500	0.00

the buckling slope deflection method and the effective length factor (γ_{02}) obtained by using Eq. 2.15 in reference 2). According to Table 1, the maximum error is 5.44% when the axial force ratio N_2/N_1=-0.5.

2.2.7 Required bracing stiffness

At this part, the required stiffness ${}_{req}k$ will be presented. ${}_{req}k$ is the bracing stiffness to take the effective length factor for the brace spacing γ. Fig. 2.6 shows the relation between the effective length factor for the brace spacing γ and the required stiffness ${}_{req}k$. Generally speaking, the value of ${}_{req}k$ decreases as the value of γ increases. Making γ as unity, the value of ${}_{req}k$ decreases as the ratio of axial force a becomes smaller. Remarkably, when there is one brace (Fig. 2.6(a)), the situation that the value of ${}_{req}k$ is zero occurred when a is smaller than zero. Tables 2.2 and 2.3 show the required stiffness when γ equals 1 in the cases of one brace and two braces respectively. When there is one brace, the effective length factor for the whole length γ_0 is equal to 0.5 and when there are two braces, γ_0 is equal to 0.333.

According to Table 2.2, ${}_{req}k$ decreases as the axial force ratio decreases and it is

Table 2.2 ${}_{req}k$ when there is one brace

Axial force ratio a	Required stiffness ${}_{req}k$
1	1.00
0.5	0.750
0	0.500
-0.5	0.250
-1	0

Table 2.3 ${}_{req}k$ when there are two brace

Axial force ratio		Required stiffness ${}_{req}k$
a	b	
1	1	1.50
3/5	1/5	0.818
1/3	-1/3	0.597
2/5		0.528

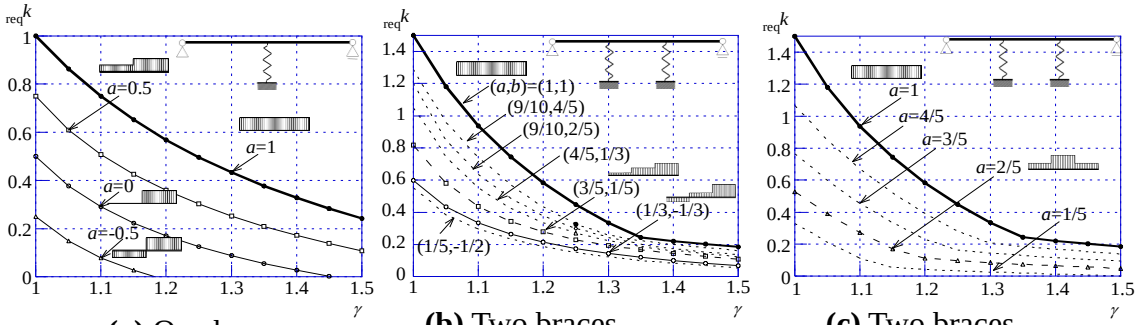

(a) One brace **(b)** Two braces (Staircase pattern) **(c)** Two braces (Convex pattern)

Fig. 2.6 Relation between ${}_{req}k$ and γ

found that the bracing stiffness is unnecessary when axial force ratio equals -1 in the case of one brace. According to Table 2.3, $_{req}k$ decreases as the axial force ratio decreases when there are two braces.

2.2.8 Design chart

Section 2.2.8 focused on the application of this study in design when there are two braces and the axial force varies in a staircase pattern. It consists of two parts. Part i) presents a series of figures on the ratio of axial force and the required stiffness k when the effective length factor for the brace spacing γ is constant. Then, Part ii) will give a specific example to show how to use these in design.

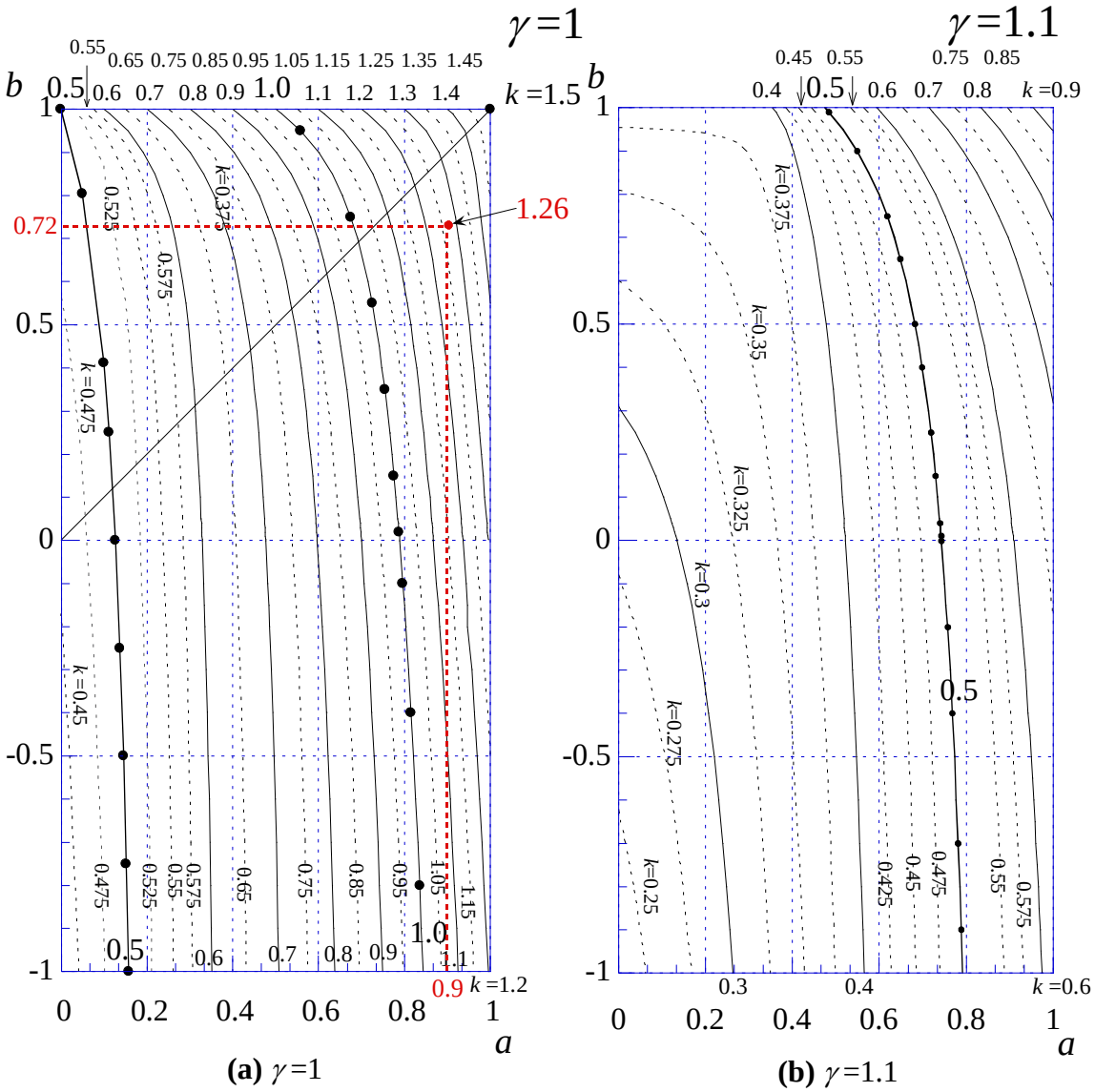

(a) γ=1 **(b)** γ=1.1

Fig. 2.7 Curves of required stiffness (staircase pattern)

i) Curves of required stiffness

Fig. 2.7 shows the required stiffness k corresponding to different ratio set of axial forces when the effective length factor γ is constant and the axial force varies in a staircase pattern. In these figures, the horizontal axis is the axial force ratio of the middle part which is from 0 to 1, and the vertical axis is the axial force ratio of the left part which is from -1 to 1.

Fig. 2.7(a) shows the case when the effective length factor γ is equal to unity. It is obvious that when the ratio set of the axial force (a, b) is equal to (1, 1), the required stiffness k equals 1.5 which has been proved in Fig. 2.6(b). The curves of the required stiffness k shown in this figure are from 0.45 to 1.5. When the axial force ratio of the

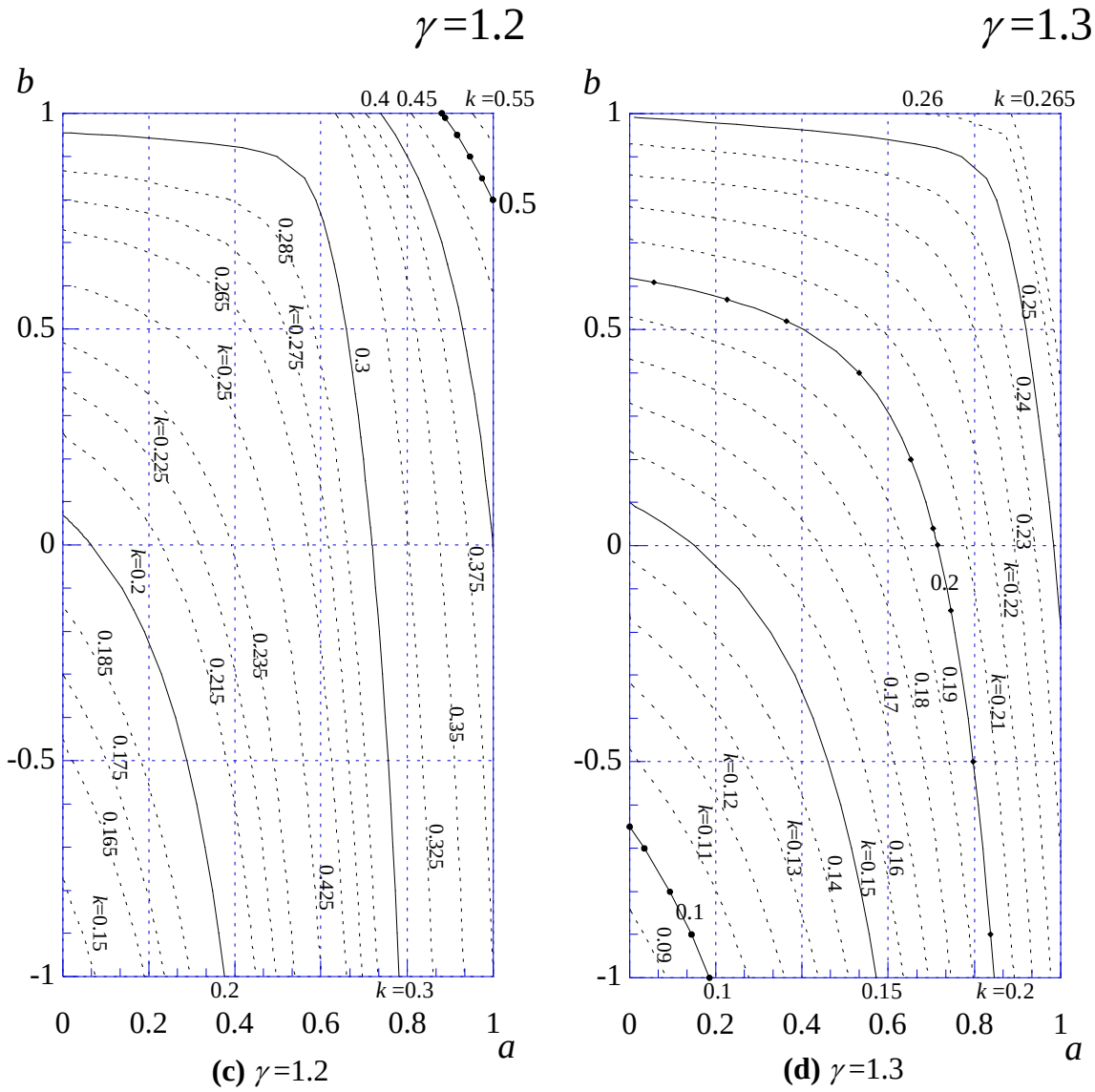

Fig. 2.7 Curves of required stiffness
(staircase pattern)

middle part *a* takes the same value, the larger the axial force ratio of the left part *b*, the larger the required stiffness *k* will be. For instance, assuming *a*=1, when the value of *b* equals 0.5, the value of *k* is between 1.35 and 1.4. However, when *b* equals 0.2, the value of *k* is between 1.3 and 1.35.

Fig. 2.7(b) is the situation when the effective length factor γ equals to 1.1. According to this figure, when the axial force ratio *a* of the middle part and *b* of the left part are both equal to unity, the required stiffness *k* is between 0.9 and 1 which is smaller than 1.5 when γ equals unity. The range of the curves of required stiffness *k* is from 0.25 to 0.9 which becomes smaller than the case when γ is equal to unity (Fig. 2.7(a)).

Fig. 2.7(c) and (d) present the curves of required stiffness *k* as the ratio set of axial

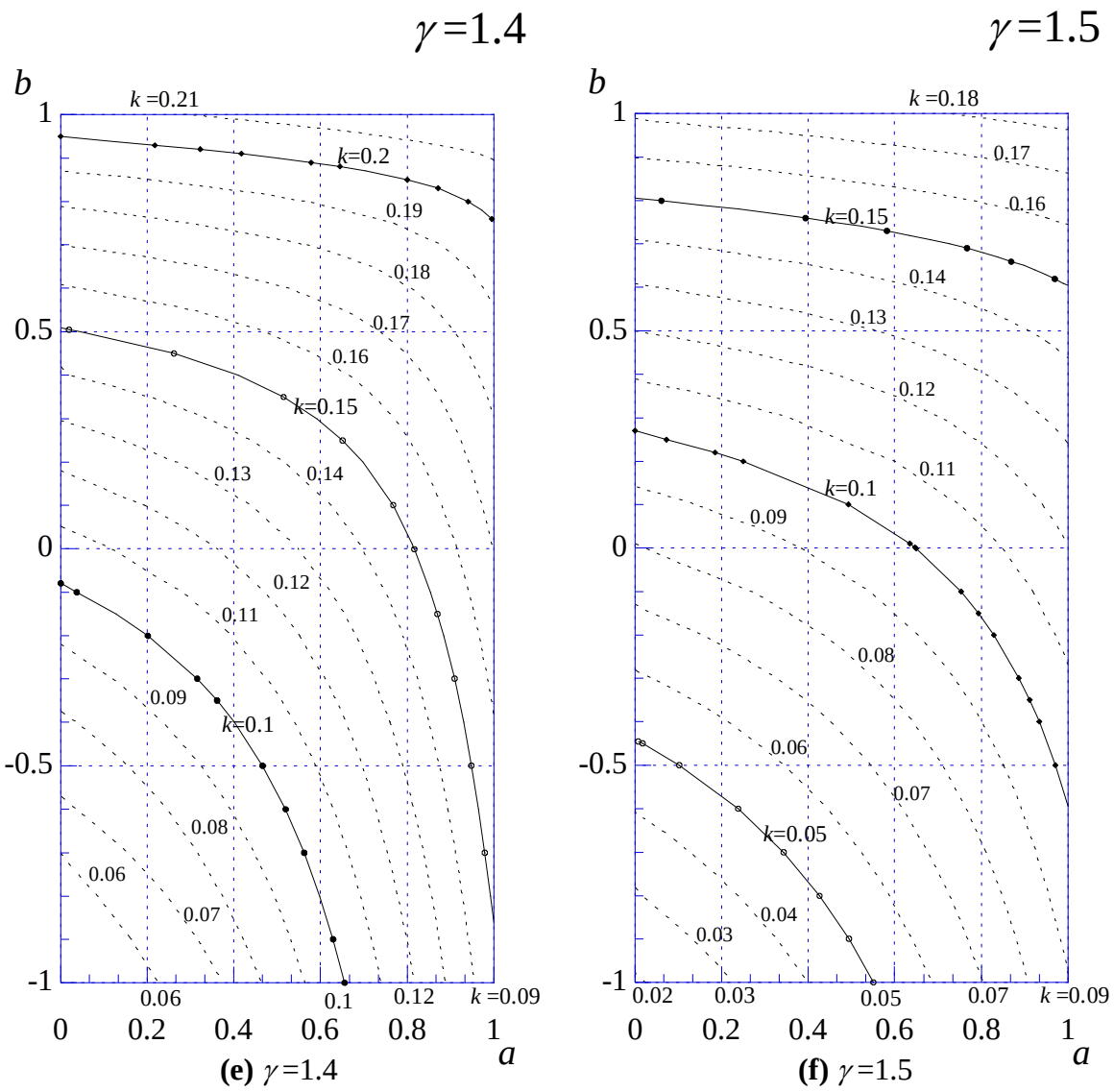

(e) γ=1.4 **(f)** γ=1.5

Fig. 2.7 Curves of required stiffness
(staircase pattern)

forces varies when the effective length factor γ is equal to 1.2 and 1.3 respectively. In Fig. 2.7(c), the range of the required stiffness k shown in this figure is from 0.15 to 0.55, while the range of curves in Fig. 2.7(d) is from 0.09 to 0.265.

Fig. 2.7(e) and (f) show the curves of required stiffness k as the ratio set of axial force varies when the effective length factor γ is equal to 1.4 and 1.5 respectively. In Fig. 2.7(e), the range of the required stiffness k shown in this figure is from 0.06 to 0.21, while the range of curves in Fig. 2.7(f) is from 0.02 to 0.18.

In these six figures about the curves of required stiffness k when the axial forces vary in a staircase pattern, the range of the curves of required stiffness k becomes smaller as the effective length factor γ increases. To the same ratio set of axial force, the larger the effective length factor γ is, the larger required stiffness k will be obtained. For example, assuming the ratio set of axial forces (a, b)=(1,0.5), required stiffness k is between 0.4 and 0.45 when the effective length factor γ is equal to 1.2, while in Fig. 2.7(d) the value is close to 0.265.

Fig. 2.8 presents the relation between the ratio of axial force and the required stiffness k when the axial force varies convexly. In this figure, the horizontal axis is the ratio of axial force a that is from 0 to 1, and the vertical axis represents the required stiffness k. According to Fig. 2.8, when the axial force ratio a is constant, the larger the effective length factor γ is, the larger the required stiffness k will be. As the value of γ increases, the effect of the axial force ratio a on the required stiffness k becomes smaller.

ii) Example for design

Figure 2.9 presents an example of truss beam which has 12 panels and the length of span is 12000mm. In Fig. 2.9(a), the left end of the beam is a pin end, while the right end is supported by a roller joint. To prevent the lateral deflection, five braces are set on Joint A~E at the top chord and Joint A'~E' at the bottom chord respectively. Each top-chord joint suffers 6kN in the vertical direction. The ends of the beam are subjected to the bending moment which is 60kN・m on the left and 100kN・m on the right in a clockwise direction. In addition, the height of the

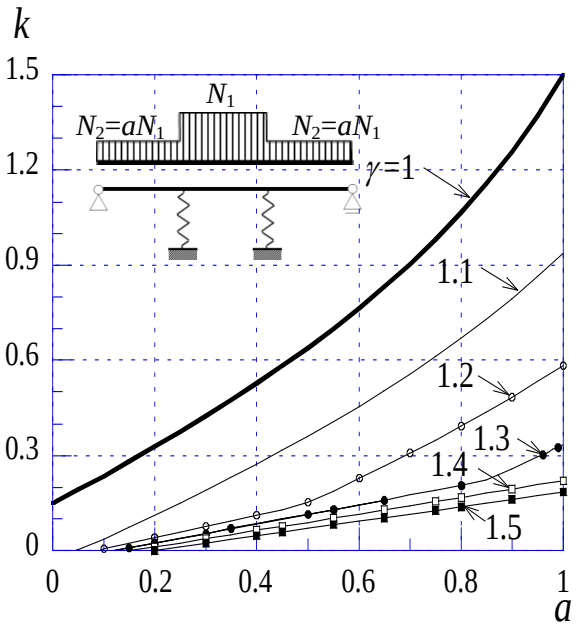

Fig. 2.8 Curves of required stiffness (convex pattern)

truss beam is 800mm.

Fig. 2.9(b) shows the material information about the cross section of each member. As the figure shown, the chord members are 114.3ϕ-4.5 and the web members are48.6ϕ-3.2.

The top chord between Joint A and B which is covered by dash line in Fig. 2.10(a) is chosen as the calculating model. The largest axial force N_1 is compressive force which is equal to 121.1kN on the right, the axial force N_2 in the middle is compressive force which is equal to 109.1kN, and the axial force N_3 on the left part is compressive force which is equal to 87.24kN. The ratio of axial force in each part is shown as Fig. 2.10(b). The ratio of axial force *a* in the middle is equal to 0.90, while the ratio of axial forces on the left *b* equals 0.72.

In this condition, the effective length factor γ can be gotten by the buckling slope deflection method when the nondimensional bracing stiffness *k* is equal to 0. In the same way, the required stiffness *k* can be obtained when the effective length factor γ is constant such as γ=1. The results by the buckling slope deflection method are shown as Table 2.4.

In addition, if using the figures presented in the preceding sections, the

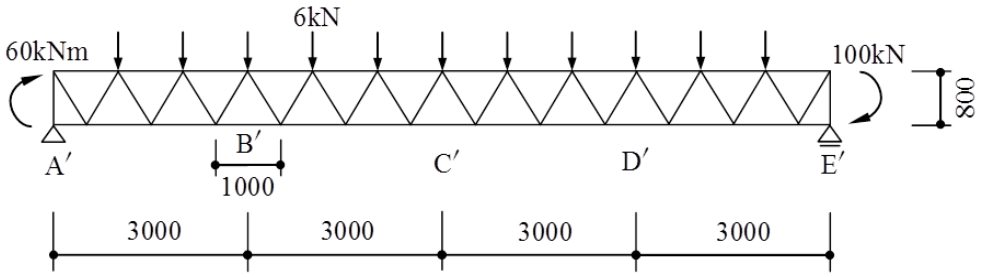

(a) Load condition

Chord: 114.3ϕ-4.5

A=1552 mm^2

I_c=2340 000 mm^4

i=38.9 mm

Web: 48.6 ϕ-3.2

A=456.2 mm^2

I_w=118 000 mm^4

i=16.1 mm

where, i: radius of gyration

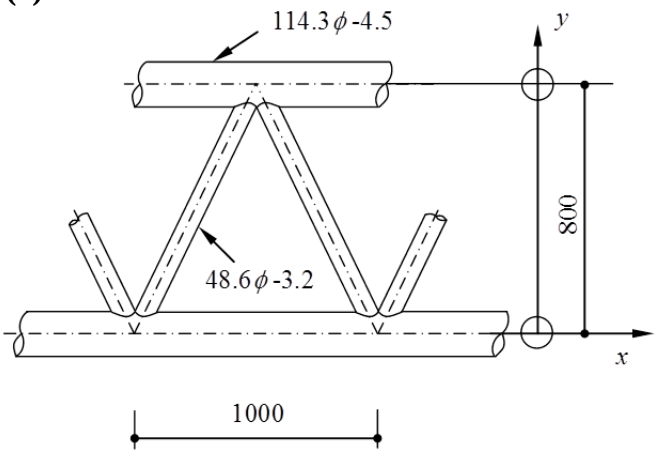

(b) Material information

Fig. 2.9 Example of truss beam

approximation of the results can be gotten quickly. When the bracing stiffness k is set to equal 0, we can look up Fig. 2.3(b) to find that, the effective length factor for the whole length γ_0 is close to 0.9. When the effective length factor for the brace spacing γ is decided to equal unity, we can use Fig. 2.7(a) to find that, the value of the required stiffness k is between 1.25 and 1.3.

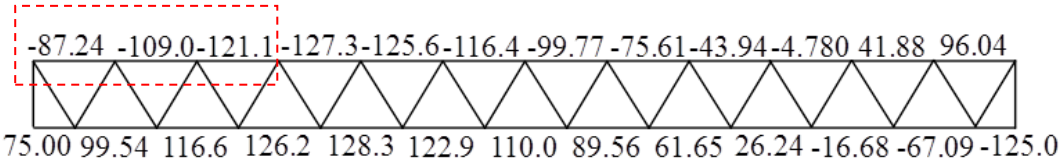

(a) Axial forces of chord members

N_1= -121.1kN

N_2= -109.0kN

N_3= -87.24kN

$$a = \frac{N_2}{N_1} = \frac{-109.0}{-121.1} = 0.90$$

$$b = \frac{N_3}{N_1} = \frac{-87.24}{-121.1} = 0.72$$

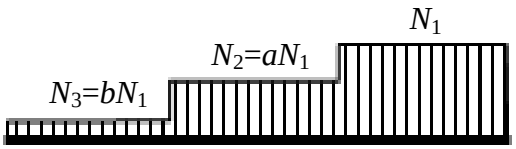

(b) Axial force ratios for calculating model

Fig. 2.10 Calculating model

Table 2.4 Results for the model by buckling slope deflection method

Axial force ratio		Bracing stiffness	Effective length factor for the brace spacing	Effective length factor for the whole length
$a = \frac{N_2}{N_1}$	$b = \frac{N_3}{N_1}$	k	$\gamma = \frac{l_k}{l}$	$\gamma_0 = \frac{l_k}{3l}$
0.90	0.72	0	2.79	0.930
		1.26	1	0.333

2.3 Bracing for columns with initial deformations subjected to varying axial force

Following is the procedure of the equilibrium equation about the load-deflection relationship obtained by the buckling slope deflection method.

2.3.1 Setting of problem

The analytical models are shown as Fig. 2.11 and 2.12. Fig. 2.11 presents the axial force pattern. Fig. 2.11(a) is the case of one brace. The axial force subjected to right part is N_1 and left part is $N_2=aN_1$ ($-0.5 \leqq a \leqq 1$). Fig. 2.11(b) and (c) show the cases of two braces when the axial force varies in a staircase pattern or convexly. In Fig. 2.11(b), the axial force subjected to the right part is N_1, the middle part is $N_2=aN_1$ ($0< a \leqq 1$) and the

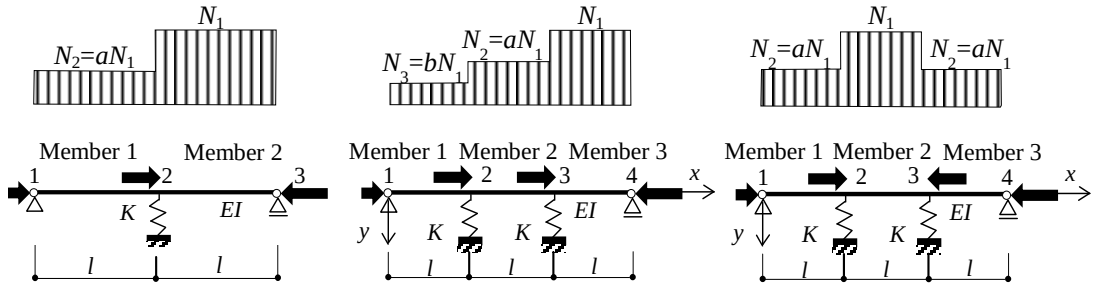

(a) One brace **(b)** Two braces (Staircase pattern) **(c)** Two braces (Convex pattern)

Fig. 2.11 Axial force pattern

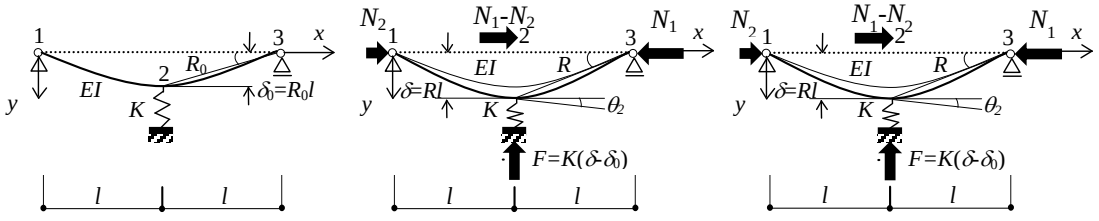

(a-1) Initial deformation (a-2) Slope angle (a-3) Deflection angle

(a) One brace

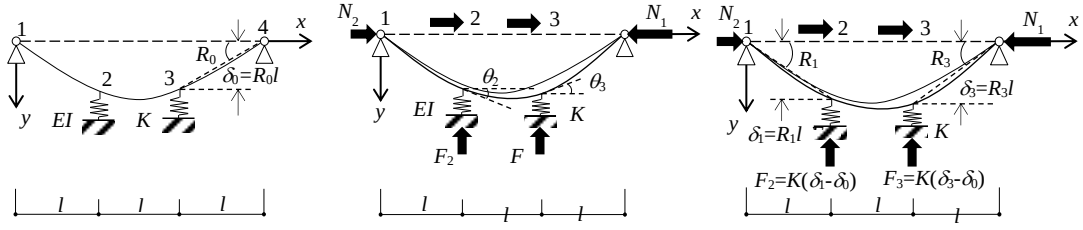

(b-1) Initial deformation (b-2) Slope angle (b-3) Deflection angle

(b) Two braces

Fig. 2.12 Deformation in different cases

left part is $N_3=bN_1$ ($-1 \leqq b \leqq 1$).in Fig. 2.11(c), the axial force subjected to middle part is N_1 and the right and the left parts are subjected to $N_2=aN_1$ ($0< a \leqq 1$).

Fig. 2.12 shows the deformation in different cases. Fig. 2.12(a) is the case of one brace. In Fig. 2.12(a-1), R_0 is the rotational angle before loading. δ_0 is the initial deformation at the middle point of the member. In Fig. 2.12(a-2), R and δ present the slope angle and the deformation under loading, respectively. F is the bracing force. The deflection angle θ_2 at Point 2 is shown as Fig. 2.12(a-3). Fig. 2.12(b) shows the case of two braces. In Fig. 2.12(b-1), R_0 is the rotational angle before loading. δ_0 is the initial deformation at supporting points of the members. In Fig. 2.12(b-2), R_1 and R_3 are the slope angles at the supporting ends. δ_2 and δ_3 are the deformation at points 2 and 3 respectively when the members are under loading. F_2 and F_3 are the bracing forces whose relation with deformation is shown in this figure. In Fig. 2.12(b-3), θ_2 and θ_3 are the deflection angle at Point 2 and Point 3.

Moreover, K represents the stiffness of brace, EI is the bending stiffness and l is the brace spacing. The initial deformation curve is not determined by any functions, however, it is assumed that the initial deformation is a symmetric shape and the initial rotational angle of the member at the middle point is zero.

2.3.2 Buckling equations

a) When there is one brace [Fig. 2.11(a)]

We can obtain Eq. (2.16) and Eq. (2.17) by applying the slope-deflection equation for stability which is also used in Section 2.2.

$$M_{21}=\frac{EI}{l}\{\xi_2\theta_2-\xi_2(R-R_0)\} \qquad M_{23}=\frac{EI}{l}\{\xi_1\theta_2+\xi_1(R-R_0)\} \tag{2.16}$$

$$Q_{21}=-\frac{EI}{l^2}(\xi_2\theta_2-\omega_2R+\xi_2R_0) \quad Q_{23}=-\frac{EI}{l^2}(\xi_1\theta_2+\omega_1R-\xi_1R_0) \tag{2.17}$$

In the equations mentioned above, ξ_i and ω_i are the stability functions (i=1, 2) which has been mentioned in Section 2.2 (Eq. (2.2) and Eq. (2.3)). θ_2 is the slope angle at point 2 and R is the rotational angle under loading.

Based on the force balance conditions, Eq. (2.18) and (2.19) are obtained.

$$\begin{aligned} &M_{21}+M_{23}=0 \\ &\therefore(\xi_1+\xi_2)\theta_2+(\xi_1-\xi_2)R=(\xi_1-\xi_2)R_0 \end{aligned} \tag{2.18}$$

$$\begin{aligned} &Q_{21}-Q_{23}+F=0 \\ &\therefore(\xi_1-\xi_2)\theta_2+(\omega_1+\omega_2+2k\pi^2)R \\ &=(\xi_1+\xi_2+2k\pi^2)R_0 \end{aligned} \tag{2.19}$$

In which,

$$F = Kl(R - R_0),\ k = \frac{Kl}{2N_E} = \frac{Kl^3}{2\pi^2 EI}, N_E = \frac{\pi^2 EI}{l^2}$$

F: the bracing force, k: the nondimensional bracing stiffness, N_E: the Euler's buckling load, M_{21} and M_{23}: the bending moment at Point 2 of Member 1 and 2 respectively, Q_{21} and Q_{23}: the shear forces of Member 1 and 2 respectively.

Eq. (2.20) is the buckling equation obtained by the buckling slope deflection method when the member with one brace has an initial deformation.

$$\begin{pmatrix} \xi_1 + \xi_2 & \xi_1 - \xi_2 \\ \xi_1 - \xi_2 & \omega_1 + \omega_2 + 2k\pi^2 \end{pmatrix} \begin{pmatrix} \theta_2 \\ R \end{pmatrix} = \begin{pmatrix} (\xi_1 - \xi_2)R_0 \\ (\xi_1 + \xi_2 + 2k\pi^2)R_0 \end{pmatrix} \tag{2.20}$$

b) When there are two braces [Fig.2.12(b) and (c)]

The procedure for the case of two braces is similar to that for the case of one brace. Therefore, the buckling equations when there are two braces are presented as follows.

i) Situation 1: the axial forces vary in a staircase pattern [Fig. 2.11(b)].

$$\begin{pmatrix} \xi_3 + \alpha_2 & \beta_2 & \gamma_2 - \xi_3 & \gamma_2 \\ \beta_2 & \alpha_2 + \xi_1 & \gamma_2 & \gamma_2 - \xi_1 \\ \beta_2 - \xi_3 + \alpha_2 & \beta_2 + \alpha_2 & \xi_3 + 2\gamma_2 - Z_2^{\,2} - Z_3^{\,2} + 2k\pi^2 & 2\gamma_2 - Z_2^{\,2} \\ \beta_2 + \alpha_2 & \alpha_2 - \xi_1 + \beta_2 & 2\gamma_2 - Z_2^{\,2} & -Z_2^{\,2} - Z_1^{\,2} + 2\gamma_2 + \xi_1 + 2k\pi^2 \end{pmatrix} \begin{pmatrix} \theta_2 \\ \theta_3 \\ R_1 \\ R_3 \end{pmatrix} = \begin{pmatrix} -\xi_3 R_0 \\ \xi_1 R_0 \\ (\xi_3 + 2k\pi^2)R_0 \\ -(\xi_1 + 2k\pi^2)R_0 \end{pmatrix} \tag{2.21}$$

ii) Situation 2: the axial forces vary convexly [Fig. 2.11(c)].

$$\begin{pmatrix} \xi_2 + \alpha_1 & \beta_1 & \gamma_1 - \xi_2 & \gamma_1 \\ \beta_1 & \alpha_1 + \xi_2 & \gamma_1 & \gamma_1 - \xi_2 \\ \beta_1 - \xi_2 + \alpha_1 & \beta_1 + \alpha_1 & \xi_2 + 2\gamma_1 - Z_2^{\,2} - Z_1^{\,2} + 2k\pi^2 & 2\gamma_1 - Z_1^{\,2} \\ \beta_1 + \alpha_1 & \alpha_1 - \xi_2 + \beta_1 & 2\gamma_1 - Z_1^{\,2} & -Z_2^{\,2} - Z_1^{\,2} + 2\gamma_1 + \xi_2 + 2k\pi^2 \end{pmatrix} \begin{pmatrix} \theta_2 \\ \theta_3 \\ R_1 \\ R_3 \end{pmatrix} = \begin{pmatrix} -\xi_2 R_0 \\ \xi_2 R_0 \\ (\xi_2 + 2k\pi^2)R_0 \\ -(\xi_2 + 2k\pi^2)R_0 \end{pmatrix} \tag{2.22}$$

2.3.3 Analytical parameters

The analytical parameters used to calculate in Section 2.3 are chosen as follows:

(1) The axial force ratio:

(i) One brace [Fig. 2.11(a)]: a = -0.5, 0, 0.5, 1

(ii) Two braces:

Staircase pattern [Fig. 2.11(b)]: (a, b) = (1, 1), (3/5, 1/5), (1/3, -1/3)

Convex pattern [Fig. 2.11(c)]: a = 1, 3/5, 2/5, 1/5

(2) The nondimensional bracing stiffness: k = 0.5, 1,2

(3) The initial rotational angle: R_0 = 0.001, 0.004

2.3.4 Relation between rotational angle *R* and nondimensional axial force *p*

a) When there is only one brace [Fig. 2.11(a)]

Fig. 2.13 shows some figures about the relation between rotational angle R and the nondimensional axial force p when there is only one brace. Fig. (a), (b) and (c) show the cases when the initial rotational angle R_0 equals 0.001 and the nondimensional bracing stiffness k equals 0.5, 1 and 2 respectively. While Fig. (d), (e) and (f) are the cases in different nondimensional bracing stiffness k which is equal to 0.5, 1 and 2 when the initial rotational angle R_0 is equal to 0.004 and the nondimensional bracing stiffness k equals 0.5, 1 and 2 respectively. In each figure, there are four curves shown in different axial force ratio a which is equal to 1, 0.5, 0 and -0.5 respectively.

Generally speaking, the value of the nondimensional axial force p becomes greater as the value of the rotational angle R increases, and the effect of the rotational angle R on the nondimensional axial force p becomes smaller as R increases. However, the value of

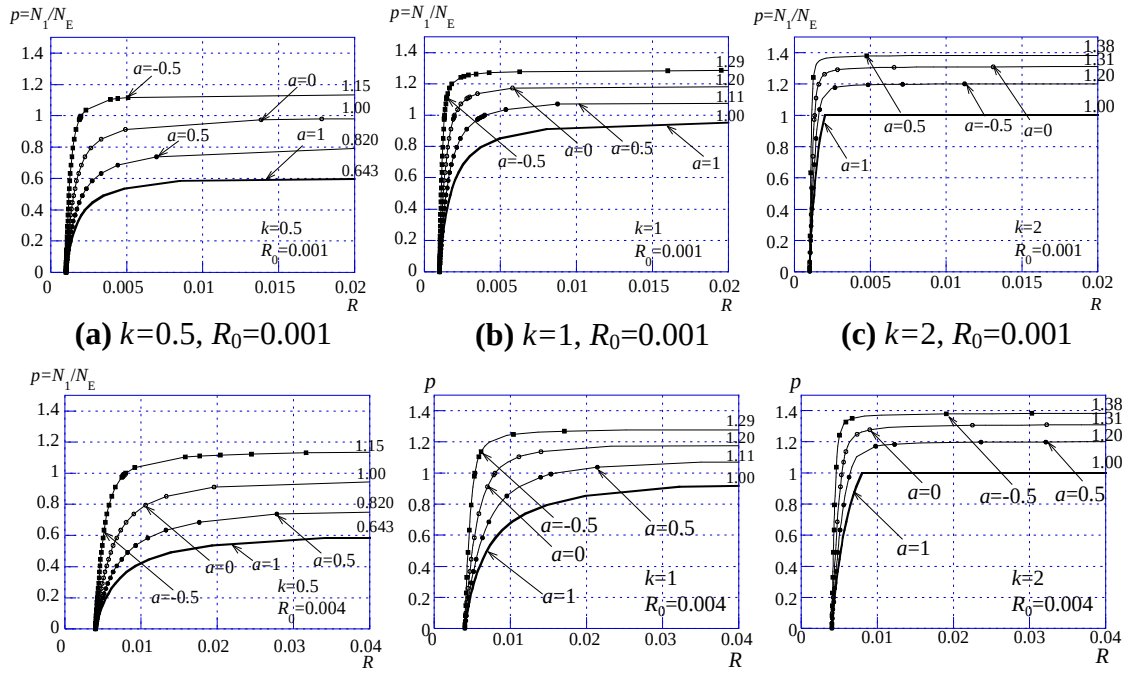

(a) k=0.5, R_0=0.001 **(b)** k=1, R_0=0.001 **(c)** k=2, R_0=0.001

(d) k=0.5, R_0=0.004 **(e)** k=1, R_0=0.004 **(f)** k=2, R_0=0.004

Fig. 2.13 Relation between rotational angle R and nondimensional axial force p (one brace)

p will not increase all the time, and it will approach constant as the value of *p* increases. the approached values in different axial force ratios are shown in the right side of each figure. When the rotational angle *R* is same, the value of the nondimensional axial force *p* becomes greater as the axial force ratio *a* decreases.

When the initial rotational angle R_0 and the axial force ratio *a* is same, the value of the nondimensional axial force *p* obtained under the greater nondimensional bracing stiffness *k* is greater than that obtained under the smaller *k*. For instance, Fig. 2.13(a) is the case when the nondimensional bracing stiffness *k* equals 0.5, while Fig. 2.13(b) is the case when the value of *k* is unity. The bold line represents the case when the axial force ratio *a* equals unity. In these two figures, the asymptotic value of *p* in Fig. 2.13(a) is 0.643 which is smaller than the value in Fig. 2.13(b) which is equal to 1.00.

When the initial rotational angle R_0 is different and other parameters are consistent, the value of the nondimensional axial force *p* of the case with smaller initial rotational angle approaches the final asymptotic value faster than that of the case when the nondimensional axial force *p* is larger. For example, the value of the nondimensional axial force *p* approches the asymptotic value when the rotitional angle *R* is 0.02 in Fig. 2.13(a), while the nondimensional axial force *p* hasn't reached the asymptotic value, even though the value of the rotational angle *R* has been over 0.03 in Fig. 2.13(d).

It should be metioned, when the axial force ratio *a* and the nondimensional bracing stiffness *k* are same, the asymptotic value is consistent even if the initial rotational angle R_0 changes. For example, when the axial force ratio *a* is equal to 1 in Fig. 2.13(a) and Fig. 2.13(d), the asymptotic value of the nondimensional axial force *p* is 0.643, whatever the initial rotational angle R_0 is.

b) when there are two braces

i) Situation 1: the axial force varies in a staircase pattern [Fig. 2.11(b)].

Fig. 2.14 shows the relation between the rotational angle *R* and the nondimensional axial force *p* when there are two braces and the axial force varies in a staircase pattern. Fig. 2.14(a), (b) and (c) show the cases when the initial rotational angle R_0 equals 0.001 and the nondimensional bracing stiffness *k* equals 0.5, 1 and 2 respectively. While Fig. 2.14(d), (e) and (f) are the cases in different nondimensional bracing stiffness *k* which is equal to 0.5, 1 and 2 when the initial rotational angle R_0 is equal to 0.004 and the nondimensional bracing stiffness *k* equals 0.5, 1 and 2 respectively.In each figure, there are three curves shown in different axial force ratio set (*a*, *b*) which is equal to (1, 1), (0.6, 0.2) and (1/3, -1/3) respectively.

The basic features of the figures are similar with the situation when there is only one brace. the value of the nondimensional axial force *p* becomes greater as the value of the

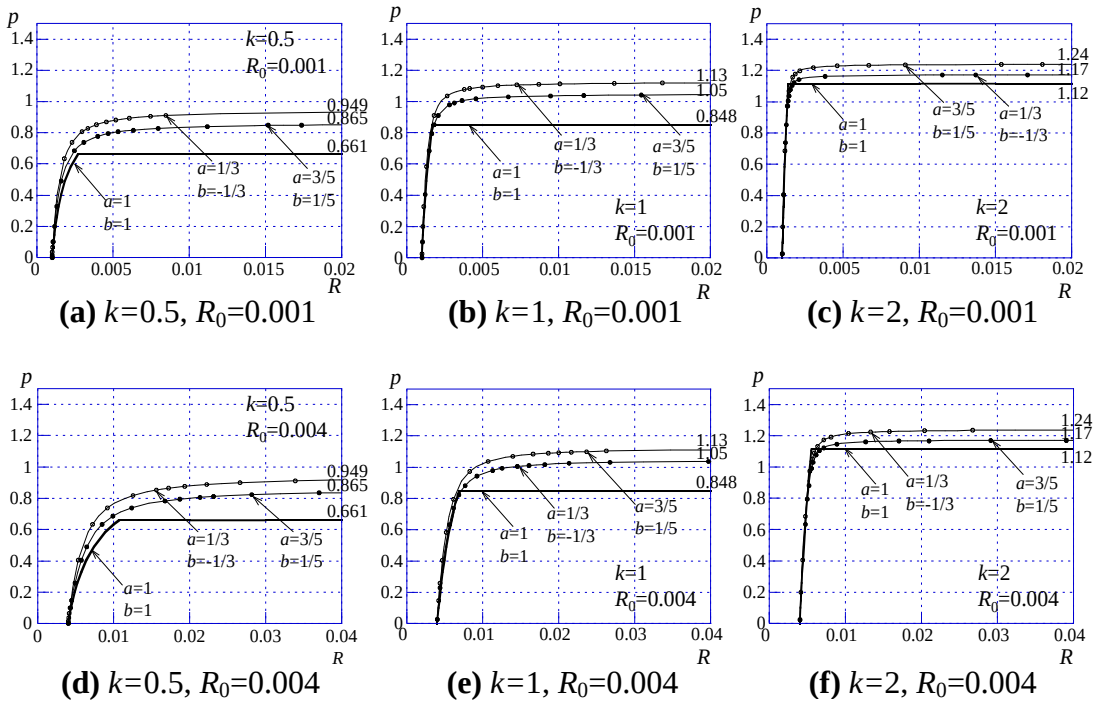

Fig. 2.14 Relation between rotational angle R and nondimensional axial force p (two braces for staircase pattern)

rotational angle R increases, and the effect of the rotational angle R on the nondimensional axial force p becomes smaller as R increases. The value of p will not increase all the time, and it will approach constant as the value of p increases. the approached values in different axial force ratios are shown in the right side of each figure.

ii) Situation 2: the axial force varies convexly [Fig. 2.11(c)]

Fig. 2.15 shows the relation between the rotational angle R and the nondimensional axial force p when there are two braces and the axial force varies in a staircase pattern. Fig. 2.15(a), (b) and (c) show the cases when the initial rotational angle R_0 equals 0.001 and the nondimensional bracing stiffness k equals 0.5, 1 and 2 respectively. While Fig. 2.15(d), (e) and (f) are the cases in different nondimensional bracing stiffness k which is equal to 0.5, 1 and 2 when the initial rotational angle R_0 is equal to 0.004 and the nondimensional bracing stiffness k equals 0.5, 1 and 2 respectively.In each figure, there are three curves shown in different axial force ratio a which is equal to 1, 0.6, 0.4 and 0.2 respectively.

Because the calculating model used in this part is symmetrical, there is a special boundary condition than others. That is to say, the buckling load can be reached in some conditions. For example, in Fig. 2.15(a), there is a salient point in each curve and the

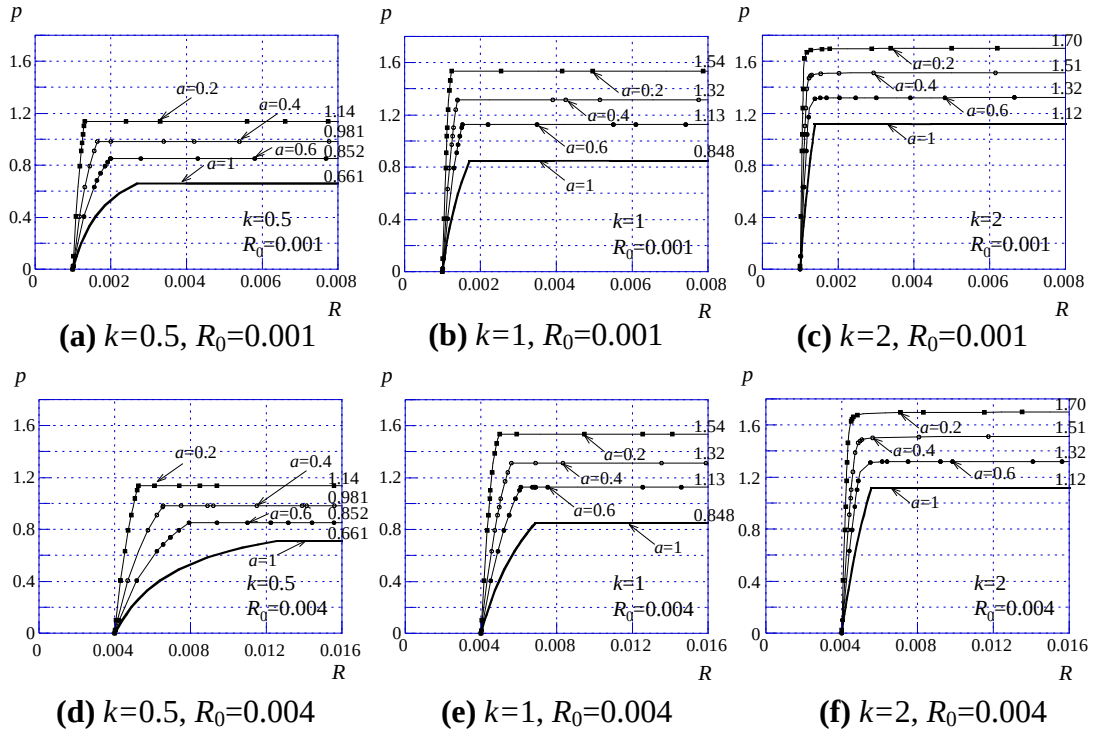

(a) k=0.5, R_0=0.001 **(b)** k=1, R_0=0.001 **(c)** k=2, R_0=0.001

(d) k=0.5, R_0=0.004 **(e)** k=1, R_0=0.004 **(f)** k=2, R_0=0.004

Fig. 2.15 Relation between rotational angle R and nondimensional axial force p (two braces for convex pattern)

axial force N_1 corresponding to that point is the buckling load. When the initial rotational angle R_0 is different and other parameters are consistent, the value of the rotational angle R to obtained the buckling load in Fig. 2.15(a) is larger than that in Fig. 2.15(d).

2.3.5 Relation between nondimensional axial force *p* and bracing force *F*

a) when there is only one brace [Fig. 2.11(a)]

Figure 2.16 is made of six firgures which are about the relation between the nondimensional axial force p and the bracing force F. In these firgures, the horizontial axis is the ratio between the bracing force F and the larger axial force N_1, and the vertical axis represents the nondimensional axial force p. Fig. 2.16(a), (b) and (c) show the cases that the initial rotational angle R_0 equals 0.001 when the nondimensional bracing stiffness k equals 0.5, 1 and 2 respectively. Fig. 2.16(b), (d) and (f) show the cases that the initial rotational angle R_0 equals 0.004 when the nondimensional bracing stiffness k equals 0.5, 1 and 2 respectively. In each figure, there are four curves shown in different axial force ratio a which is equal to 1, 0.5, 0 and -0.5 respectively.

In general, the value of the nondimensional axial force p increases and becomes constant as the value of the nondimensional axial force p increases. when the value of F/N_1 is same, the value of the nondimensional axial force p becomes greater as the axial

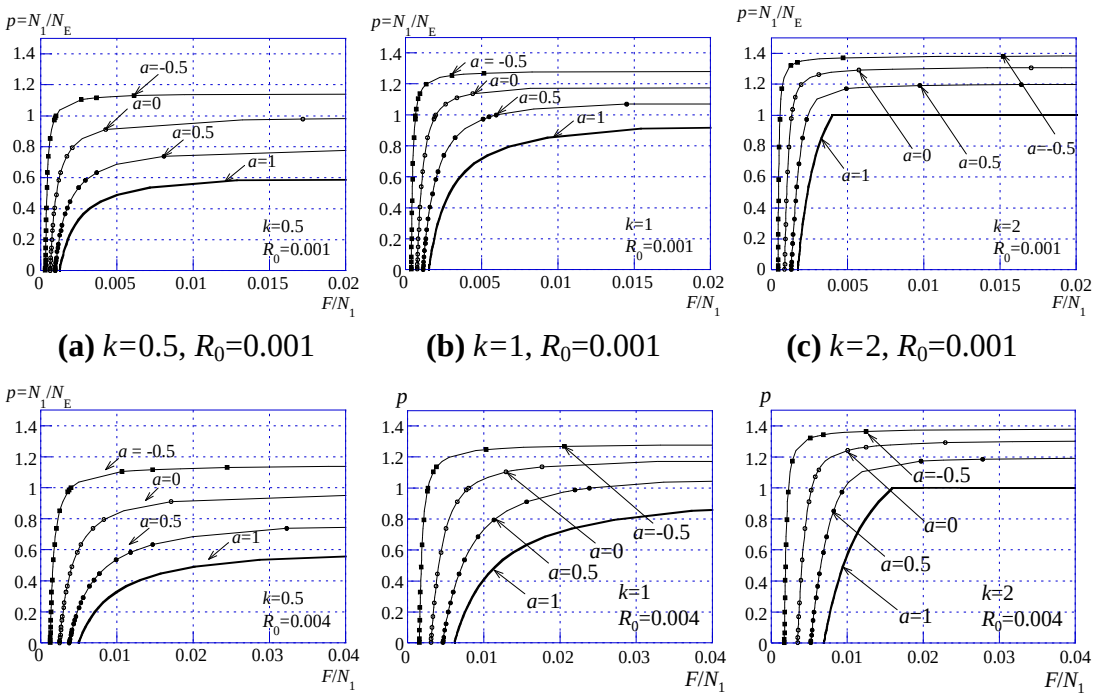

(a) k=0.5, R_0=0.001 **(b)** k=1, R_0=0.001 **(c)** k=2, R_0=0.001

(d) k=0.5, R_0=0.004 **(e)** k=1, R_0=0.004 **(f)** k=2, R_0=0.004

Fig. 2.16 Relation between nondimensional axial force p and F/N_1 (one brace)

force ratio a decreases.

When the initial rotational angle R_0 is same, the value of the nondimensional axial force p obtained under the greater nondimensional bracing stiffness k is greater than that obtained under the smaller k with the same axial force ratio. For instance, Fig. 2.16(a) is the case when the nondimensional bracing stiffness k equals 0.5, while Fig. 2.16(b) is the case when the value of k is unity. The positions of the curves in Fig. 2.16(b) are higher than those shown in Fig. 2.16(a) with the same axial force ratio.

b) when there are two braces

i) Situation 1: the axial force varies in a staircase pattern [Fig. 2.11(b)].

Fig. 2.17 shows some figures about the relation between the nondimensional axial force p and the stiffening force F when there are two braces and the axial forces vary in a staircase pattern. The parameters in these figures are same with that set in Fig. 2.14.

The basic features of the figures are similar with the situation when there is only one brace. The value of F/N_1 increases as the value of the nondimensional axial force p increases obviously at the beginning, then approaches some constant in final.In addition, the asymptotic value of the nondimensional axial force p becomes greater as the ratio set of axial force (a, b) decreases in the same figure.

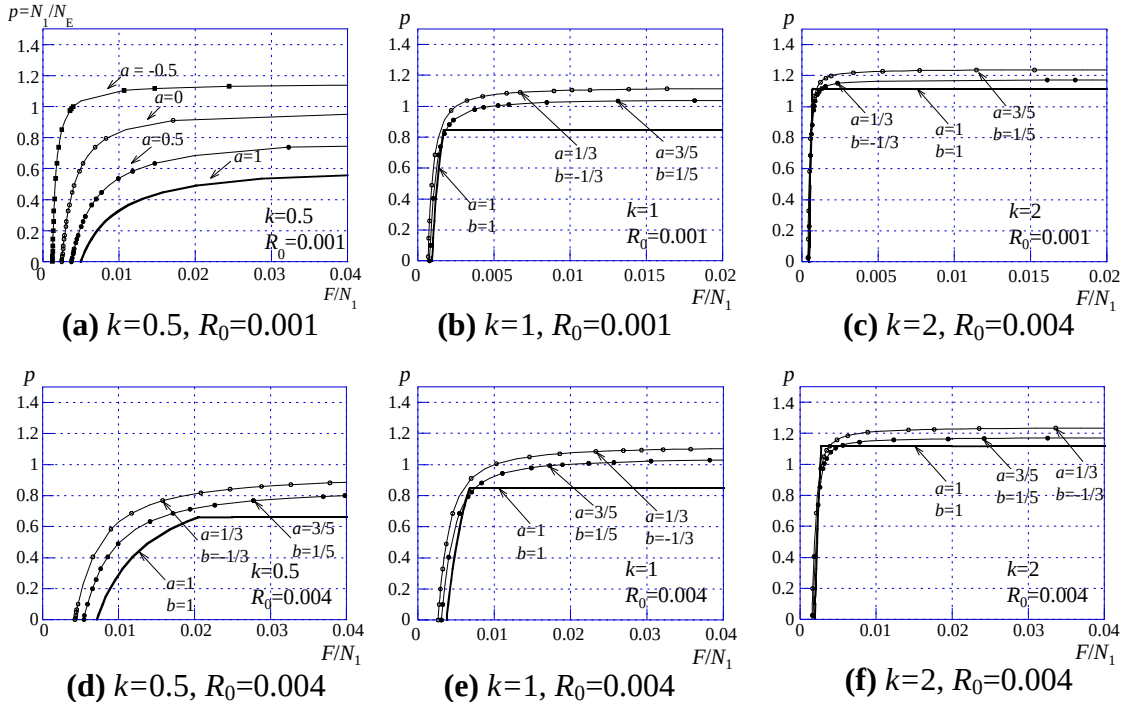

Fig. 2.17 Relation between nondimensional axial force p and F/N_1 (two braces for staircase pattern)

ii) Situation 2: the axial force varies convexly [Fig. 2.11(c)]

Fig. 2.18 shows the relation between the nondimensional axial force p and the bracing force F when there are two braces and the axial force varies convexly. The parameters in Fig. 2.18 are same with these shown in Fig. 2.15.

When R_0 takes the same one, the value of F/N_1 obtained under the greater nondimensional bracing stiffness k is greater than that obtained under the smaller k corresponding to the nondimensional axial force p with the same axial force ratio. For instance, Fig. 2.20(a) is the situation when the nondimensional bracing stiffness k equals 0.5, while Fig. 2.20(c) is the situation when the value of k is unity. In these two figures, the approximation of F/N_1 corresponding to Fig. 2.20(a) is 0.002 which is smaller than the value in Fig. 2.20(c) which is equal to 0.012 when the nondimensional axial force p is equal to 0.4.

The calculating model used in Fig. 2.18 that is same with the case used in Fig. 2.15 is symmetrical and there is a special boundary condition than others. So that the axial force N_1 corresponding to the salient point is the buckling load. Comparing Fig. 2.18(a) and (d), the buckling load is same when the axial force ratio is consistent. However, the value of F/N_1 in Fig. 2.18(b) is larger than that in Fig.2.18(a) when the buckling load is obtained.

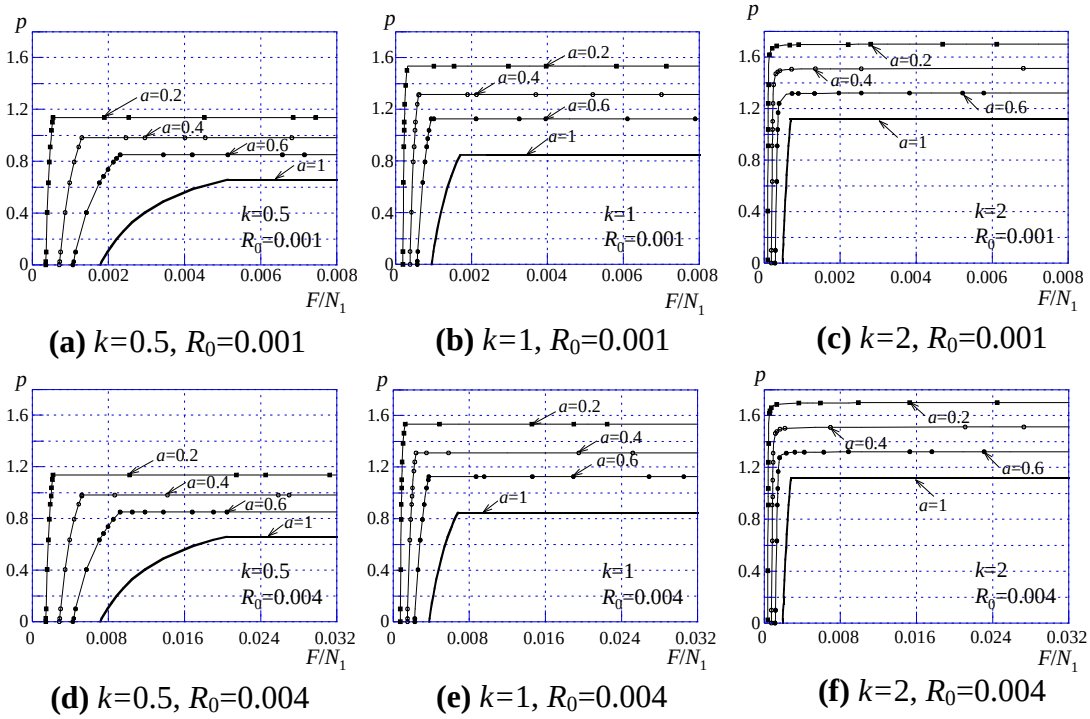

(a) k=0.5, R_0=0.001 **(b)** k=1, R_0=0.001 **(c)** k=2, R_0=0.001

(d) k=0.5, R_0=0.004 **(e)** k=1, R_0=0.004 **(f)** k=2, R_0=0.004

Fig. 2.18 Relation between nondimensional axial force p and F/N_1 (two braces for convex pattern)

2.3.6 Relation between bracing force F and nondimensional bracing stiffness k

Fig. 2.19 shows the relation between the bracing force F and the nondimensional bracing stiffness k when the nondimensional axial force p is unity. The vertical axis is the ratio between the bracing force F and the Euler's buckling load N_E. The horizontial axis is the bracing stiffness k. Fig. 2.21(a) shows the cases when there is only one brace. Fig. 2.21(b) and (c) show the cases of two braces when the axial force varies in a staircase pattern or convexly. The initial rotational angle R_0 equals 0.001 or 0.004.

According to these figures, the value of F/N_E decreases as the nondimensional bracing stiffness k increases. In Fig. 2.19(a) and (c), when the nondimensional bracing stiffness k is same, the value of F/N_E increases as the axial force ratio a increases, while the value of F/N_E decreases as the axial force ratio a increases in Fig.2.19. Moreover, the value of F/N_E is almost same even if the axial force ratio a is different when the nondemensional bracing stiffness k is larger than 3 in Fig.(b-1) and 8 in Fig.(b-2). That is to say, as the nodimensional bracing stiffness k increases, the effect of the axial force ratio on the value of F/N_E becomes smaller when the axial force varies in a staircase pattern.

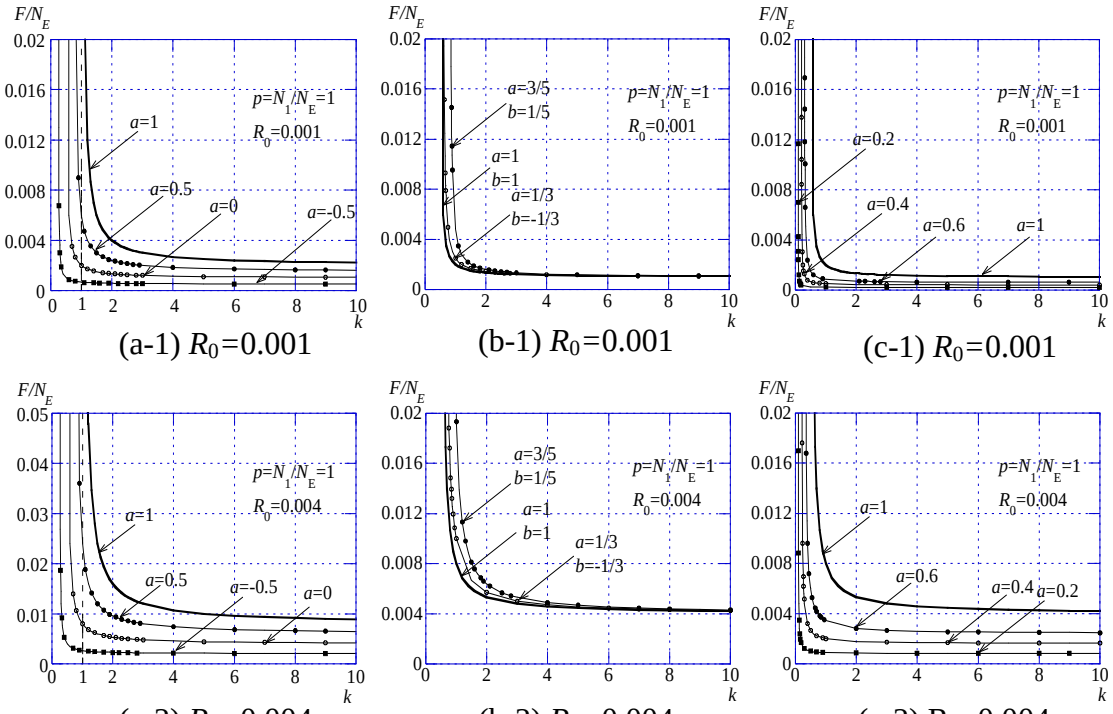

(a-1) R_0=0.001 (b-1) R_0=0.001 (c-1) R_0=0.001

(a-2) R_0=0.004 (b-2) R_0=0.004 (c-2) R_0=0.004

(a) One brace

(b) Two braces for staircase pattern

(c) Two braces for convex pattern

Fig. 2.19 Relation between nondimensional bracing stiffness k and F/N_E

2.4 Conclusions

The buckling equations when the compressive member with one or two braces is subjected to varying axial force have been calculated by the buckling slope deflection method. The main findings are summarized as follows.

i) For Section 2.2

(1) When the ratio of axial forces is larger, the effective length factor γ_0 is larger when the nondimensional bracing stiffness k is the same value.

(2) Buckling modes are presented when the value of the nondimensional bracing stiffness k is equal to 0, 0.5 and 3. The ratio of axial forces plays an important role in the variation of buckling mode.

(3) Required bracing stiffness to take the effective length as the brace spacing is calculated and it decreases as the axial force ratio decreases.

(4) A specific example about the truss beam has been shown in the final part of this section in order to present the application of this study in structural design.

ii) For Section 2.3

(1) The value of the nondimensional axial force p becomes larger as the value of the rotational angle R increases. The effect of the rotational angle R on the nondimensional axial force p becomes smaller as R increases. However, the value of p will not increase at all times, and it will approach constant as the value of p increases.

(2) When the value of F/N_1 is same, the value of the nondimensional axial force p increases as the axial force ratio a decreases and the value of p with k =1 is greater than that the value of p with k =0.5, in the case that the axial force ratio is same.

(3) According to Fig. 2.19(a) and (c), when the nondimensional bracing stiffness k is same, the value of F/N_E increases as the axial force ratio a increases, while the value of F/N_E decreases as the axial force ratio a increases. Moreover, as the nondimensional bracing stiffness k increases, the effect of the axial force ratio on the value of F/N_E becomes smaller when the axial force varies in a staircase pattern.

References for Chapter 2

1) Architectural Institute of Japan (AIJ): Recommendations for Stability Design of Steel Structures, 2009.11.
2) Architectural Institute of Japan: Design Standard for Steel Structures -Based on Allowable Stress Concept-, 2005.9.
3) Y. Yokoo, M. Wakabayashi, and K. Ueda: On the stiffness of an Intermediate elastic support of a compression member, Transactions of the Architectural Institute of Japan, Vol. 89, p.105, 1963.9.
4) Ronald D. Ziemian (editor): Guide to Stability Design Criteria for Metal Structures 6th edition Chapter 15, 2010

Chapter 3

Relation between Elastic Buckling Strength and Bracing Stiffness of H-shaped Beam-Column Simply Supported at Both Ends

3.1 Introduction

The design methods for bracing of steel structure are presented in Design Standard for Steel Structures [1)], Recommendation for Limit State Design of Steel Structures [2)], Recommendations for the Plastic Design of Steel Structures [3)] and Recommendations for Stability Design of Steel Structures [4)].

In Recommendation for Limit State Design, the required bracing stiffness and the required bracing force are shown for flexural buckling of compressive members, lateral buckling of members subjected to bending moment and beam-columns respectively. These design methods for bracing are based on the study results of bracing for flexural buckling of compressive members subjected to the uniform axial force. That is to say, most of the studies, including the references 5) and 6), target the members subjected to the uniform axial force although the studies investigated the flexural buckling of the members with multiple bracing and with initial imperfection and the inelastic buckling behavior.

As for the lateral buckling of beams or flexural-torsional buckling of H-shaped beam-columns, the research results of bracing of compressive members subjected to the uniform axial force are introduced by considering the lateral buckling and the torsional buckling as the flexural buckling of the compressive flange. Compressive members subjected to the uniform axial force correspond to the compressive beam flanges when the beam and the beam-columns are subjected to the constant bending moment. However, the bending moment generally varies along the member axis.

In reference 7)~13), problems of bracing of beams and beam-columns are treated, however, the lateral bracing stiffness and the torsional bracing stiffness, and the relationship between loading conditions and flexural-torsional buckling strength are not clear.

The buckling equation of beam-columns which have sandwich section and which have one lateral and one torsional bracing at the middle of the member was derived by using the Rayleigh-Ritz method and the effects of loading conditions, bracing and resistance by St. Venant torsion on the flexural-torsional buckling strength were presented[14)]. However, few studies show systematically the relation between the buckling strength and the bracing stiffness of the H-shaped member with the lateral bracing or the torsional bracing subjected to axial force and end moments.

The purpose of this study is to calculate the buckling equation of H-shaped beam-columns by using the Rayleigh-Ritz method and show the relation between elastic buckling strength and the lateral and the torsional bracing stiffness. The member is simply supported at both ends and subjected to compressive force, end moments and

uniformly distributed load.

3.2 Analysis

3.2.1 Analytical model

In this Chapter, the flexural-torsional buckling force of H-shaped cross section which is subjected axial load and bending moment around the strong axis is presented when the lateral defection and the torsion are fixed by the brace. The loading conditions and the boundary conditions are shown as Fig. 3.1. The left end of the member is a hinge joint and subjected to bending moment M_1. The right end is supported by a pin and subjected to bending moment $M_2=\kappa M_1$ (κ is the end moment ratio, $|\kappa| \leqq 1$). Both ends are subjected to equal compressive load N and the axial load is constant. w is the uniformly distributed load. There are four kinds of the bracing attached to the member, discrete lateral bracing, continuous lateral bracing, discrete torsional bracing and continuous torsional bracing whose bracing stiffness are denoted by K_{ivd}, K_{vc}, $K_{i\phi d}$ and $K_{\phi d}$ respectively (the subscript i represents the number of the bracing). When the number of the bracing i=1, the bracing is attached at the midspan of the member, and when i=2, the bracing is attached at the trisection of the member. This study is to

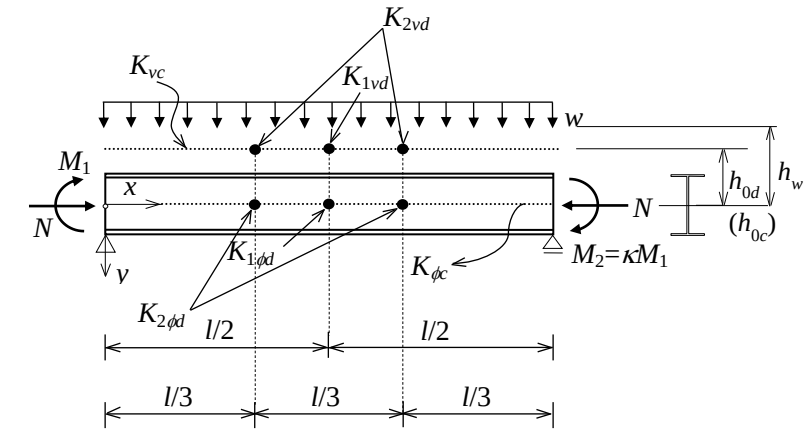

(a) Loading conditions and boundary conditions

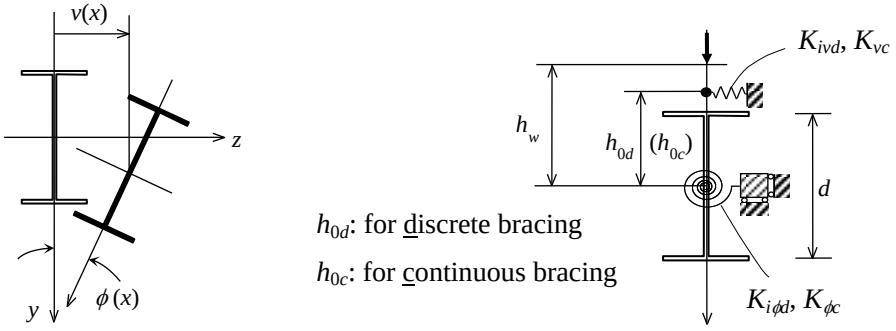

(b) Lateral deflection and torsional angle

(c) Position of bracing and uniform distributed load

Fig. 3.1 Analytical model

analysis the situation when the both ends of the member are simply supported. The boundary conditions in this situation are different from the conditions in fact. However, the boundary conditions of this study are the most basic so that the safe side can be evaluated.

In Fig. 3.1(b), v(x) and ϕ(x) represent the lateral deflection and the torsional angle of the center of the cross section respectively. The left supporting point of the member is selected as the original point and x axis is set along the member as Fig. 3.1(a) shown. The geometric boundary conditions are $v(0)=v(l)=\phi(0)=\phi(l)=0$ and the mechanical boundary conditions are $v''(0)=v''(l)=\phi''(0)=\phi''(l)=0$. In Fig. 1(c), h_{0d} and h_{0c} represent the distance from the center of the cross-section to the discrete lateral bracing and the continuous lateral bracing. h_w is the distance from the center of the cross-section to the position subjected to the uniformly distributed load. The torsional bracing is attached at the center of the cross-section.

In this study, the Rayleigh-Ritz method is used to calculate the approximate value of the buckling strength, because the exact solution of this problem is hard to obtain.

3.2.2 Total-potential energy

The total-potential energy of this model is shown in Eq. (3.1). In addition, $v(x)$ and $\phi(x)$ represent the lateral deflection and the torsional angle along x axis, respectively. The symbols v', ϕ', v'' and ϕ'' in Eq. (3.1) represent the first and the second derivatives of $v(x)$ and $\phi(x)$ with respect to x.

$$\begin{aligned}\Pi[v,\phi]=&\int_0^l \frac{EI_y v''^2}{2}dx+\frac{1}{2}\int_0^l\left(GJ-N\frac{I_y+I_z}{A}\right)\phi'^2dx+\int_0^l\frac{EI_w\phi''^2}{2}dx+\int_0^l Mv''\phi dx\\&-\frac{1}{2}\int_0^l Nv'^2dx+\int_0^l\frac{wh_w\phi^2}{2}dx+\frac{1}{2}\sum_{i=1}^n K_{ivd}\{v(x_i)-h_{0d}\phi(x_i)\}^2+\frac{1}{2}\int_0^l K_{vc}(v-h_{0c}\phi)^2dx\\&+\frac{1}{2}\sum_{i=1}^n K_{i\phi d}\phi^2(x_i)+\frac{1}{2}\int_0^l K_{\phi c}\phi^2dx\end{aligned}\qquad(3.1)$$

In Eq. (3.1), the first term is the strain energy of deflection along x axis, the second term is the strain energy of St.Venant torsion reduced by the axial force effect [15], the third term is the strain energy of warping, the fourth, the fifth and the sixth terms are the potential energy of external loads corresponding to bending moment M, axial force N and uniformly distributed load w respectively, other four terms are the strain energy of discrete lateral bracing, continuous lateral bracing, discrete torsional bracing and continuous torsional bracing. Definitions of notations are as follows: l is the length of the member, A is the area of the cross-section, I_y and I_z are the second moments of inertia around y and z axes, J is the St.Venant torsional constant, I_w is the warping constant, E is the elastic modulus and G is the shear modulus. In this paper we define as

follows:

$$M_e = \frac{1}{2} N_e d\sqrt{1+R},\ N_e = \frac{\pi^2 EI_y}{l^2},\ i_0 = \sqrt{\frac{I_y + I_z}{A}},\ m \equiv \frac{M_1}{M_e},\ n \equiv \frac{N}{N_e},\ \beta \equiv \frac{wl^2}{8M_1},\ \kappa \equiv \frac{M_2}{M_1},$$

$$\eta_{0c} \equiv \frac{h_{0c}}{d},\ \eta_{0d} \equiv \frac{h_{0d}}{d},\ R \equiv \frac{GJl^2}{\pi^2 EI_w},\ r \equiv \frac{1}{\sqrt{1+R}},\ d_{i_0} \equiv \frac{i_0}{d},\ d_l \equiv \frac{l}{d}$$

M_e is the elastic lateral buckling moment when the member is subjected to equal end moments, N_e is the elastic buckling load for out-of-plane bending around the weak axis, i_0 is the polar radius of gyration of area, m is the nondimensional bending moment, n is the nondimensional compressive force, β is the uniformly distributed load ratio, κ is the end moment ratio, d is the distance between the two centroids of the flanges of the H-shaped cross-section.

Referring the method used in reference 16), the nondimensional bracing stiffness is defined as follows:

One lateral bracing: $k_{1vd} = \dfrac{K_{1vd} l^3}{16\pi^2 EI}$ (3.2)

Two lateral bracing: $k_{2vd} = \dfrac{2K_{2vd} l^3}{16\pi^2 EI}$ (3.3)

Continuous lateral bracing: $k_{vc} = \dfrac{K_{vc} l^4}{16\pi^2 EI}$ (3.4)

One torsional bracing: $k_{1\phi d} = \dfrac{K_{1\phi d} l}{\pi^2 EI}$ (3.5)

Two torsional bracing: $k_{2\phi d} = \dfrac{2K_{2\phi d} l}{\pi^2 EI}$ (3.6)

Continuous torsional bracing: $k_{\phi c} = \dfrac{K_{\phi c} l^2}{\pi^2 EI}$ (3.7)

3.2.3 Assumption of buckling mode and buckling equation

The buckling modes that satisfy the geometrical boundary conditions and the mechanical boundary conditions are assumed as follows.

$$v(x) = \sum_{i=1}^{m^*} a_i \cdot d \cdot \sin i\pi\xi = d \begin{pmatrix} a_1 & a_2 & \cdots & a_{m^*} \end{pmatrix} \begin{pmatrix} \sin \pi\xi \\ \sin 2\pi\xi \\ \vdots \\ \sin m^*\pi\xi \end{pmatrix} \quad (3.8)$$

$$\phi(x)=\sum_{i=1}^{m^*} b_i \cdot \sin i\pi\xi = \begin{pmatrix} b_1 & b_2 & \cdots & b_{m^*} \end{pmatrix} \begin{pmatrix} \sin \pi\xi \\ \sin 2\pi\xi \\ \vdots \\ \sin m^*\pi\xi \end{pmatrix} \tag{3.9}$$

where $\xi \equiv x/l$. By substituting Eq. (3.8) and (3.9) into Eq. (3.1), Eq. (3.10) is obtained.

$$\Pi\left(a_1, a_2 \cdots a_{m^*}, b_1, b_2, \cdots b_{m^*}\right) = \frac{M_e d}{2l} \boldsymbol{a}^{\mathrm{T}} \boldsymbol{K} \boldsymbol{a} \tag{3.10}$$

where $a^{\mathrm{T}}=(a_1,\ a_2,\ldots,\ a_{m*},\ b_1,\ b_2,\ldots,\ b_{m*})$. Based on the Rayleigh-Ritz method, the following equation is obtained by partially differentiating Eq. (3.10) by a_i, b_i (i=1, 2,…, m^*) and making it equal to 0.

$$\boldsymbol{K}_{aa} = \begin{pmatrix} r\left\{\pi^2(1-n)+16k_{vc} \right. & 0 & -32rk_{1vd} & 0 & 8r\left(4k_{1vd}-3k_{2vd}\right) \\ \left. +32k_{1vd}+24k_{2vd}\right\} & & & & \\ 0 & r\left\{4\pi^2(4-n)+16k_{vc} \right. & 0 & -24rk_{2vd} & 0 \\ & \left. +24k_{2vd}\right\} & & & \\ -32rk_{1vd} & 0 & r\left\{9\pi^2(9-n)+16k_{vc} \right. & 0 & -32rk_{1vd} \\ & & \left. +32k_{1vd}\right\} & & \\ 0 & -24rk_{2vd} & 0 & r\left\{16\pi^2(16-n)+16k_{vc} \right. & 0 \\ & & & \left. +24k_{2vd}\right\} & \\ 8r\left(4k_{1vd}-3k_{2vd}\right) & 0 & -32rk_{1vd} & 0 & r\left\{25\pi^2(25-n)+16k_{vc} \right. \\ & & & & \left. +32k_{1vd}+24k_{2vd}\right\} \end{pmatrix} \tag{3.12}$$

$$\boldsymbol{K}_{ba}{}^{\mathrm{T}} = \boldsymbol{K}_{ab} = \begin{pmatrix} {}_{ab}k_{11} & -\frac{8}{9}m(1+\kappa) & \frac{3}{4}m\beta+32\eta_{0d}rk_{1vd} & \frac{-16}{225}m(1+\kappa) & \frac{5}{36}m\beta-\eta_{0d}r(32k_{1vd}-24k_{2vd}) \\ -\frac{32}{9}m(1+\kappa) & {}_{ab}k_{22} & -\frac{96}{25}m(1+\kappa) & \frac{32}{9}m\beta+24\eta_{0d}rk_{2vd} & -\frac{160}{441}m(1+\kappa) \\ \frac{27}{4}m\beta+32\eta_{0d}rk_{1vd} & -\frac{216}{25}m(1+\kappa) & {}_{ab}k_{33} & -\frac{432}{49}m(1+\kappa) & \frac{135}{16}m\beta+32\eta_{0d}rk_{1vd} \\ -\frac{256}{225}m(1+\kappa) & \frac{128}{9}m\beta+24\eta_{0d}rk_{2vd} & -\frac{768}{49}m(1+\kappa) & {}_{ab}k_{44} & -\frac{1280}{81}m(1+\kappa) \\ \frac{125}{36}m\beta-\eta_{0d}r\left(32k_{1vd}-24k_{2vd}\right) & -\frac{1000}{441}m(1+\kappa) & \frac{375}{16}m\beta+32\eta_{0d}rk_{1vd} & -\frac{2000}{81}m(1+\kappa) & {}_{ab}k_{55} \end{pmatrix} \tag{3.13}$$

Where, ${}_{ab}k_{ii} = -\frac{1}{3}m\beta\left(3+i^2\pi^2\right)-\frac{1}{4}i^2m\pi^2\left(1-\kappa\right)-8r\left[2\eta_{0c}k_{vc}+2\left\{1+(-1)^{i+1}\right\}\eta_{0d}k_{1vd}+3\eta_{0d}k_{2vd}\right],\ (i\neq 3)$

${}_{ab}k_{ii} = -\frac{1}{3}m\beta\left(3+9\pi^2\right)-\frac{9}{4}m\pi^2\left(1-\kappa\right)-16r\left(\eta_{0c}k_{vc}+2\eta_{0d}k_{1vd}\right),\ (i=3)$

$$\boldsymbol{K}_{bb} = \begin{pmatrix} {}_{bb}k_{11} & 0 & -2r\left(16\eta_{0d}^2k_{1vd}+d_l{}^2k_{1\phi d}\right) & 0 & \frac{1}{2}r\left(64\eta_{0d}^2k_{1vd}-48\eta_{0d}{}^2k_{2vd} \right. \\ & & & & \left. +4d_l{}^2k_{1\phi d}-3d_l{}^2k_{2\phi d}\right) \\ 0 & {}_{bb}k_{22} & 0 & -\frac{3}{2}r\left(16\eta_{0d}^2k_{2vd}+d_l{}^2k_{2\phi d}\right) & 0 \\ -2r\left(16\eta_{0d}^2k_{1vd}+d_l{}^2k_{1\phi d}\right) & 0 & {}_{bb}k_{33} & 0 & -2r\left(16\eta_{0d}^2k_{1vd}+d_l{}^2k_{1\phi d}\right) \\ 0 & -\frac{3}{2}r\left(16\eta_{0d}^2k_{2vd}+d_l{}^2k_{2\phi d}\right) & 0 & {}_{bb}k_{44} & 0 \\ \frac{1}{2}r\left(64\eta_{0d}^2k_{1vd}-48\eta_{0d}^2k_{2vd} \right. & 0 & -2r\left(16\eta_{0d}{}^2k_{1vd}+d_l{}^2k_{1\phi d}\right) & 0 & {}_{bb}k_{55} \\ \left. +4d_l{}^2k_{1\phi d}-3d_l{}^2k_{2\phi d}\right) & & & & \end{pmatrix} \tag{3.14}$$

Where, ${}_{bb}k_{ii} = r\left[\frac{1}{4}i^2\pi^2(i^2+R)-i^2\pi^2d_{i0}{}^2n+16\eta_{0c}^2k_{vc}+d_l{}^2k_{\phi c}+\left\{1+(-1)^{i+1}\right\}(16\eta_{0d}^2k_{1vd}+d_l{}^2k_{1\phi d})+\frac{3}{2}(16\eta_{0d}^2k_{2vd}+d_l{}^2k_{2\phi d})\right]+4m\beta\eta_w,\ (i\neq 3)$

${}_{bb}k_{ii} = r\left\{\frac{9}{4}\pi^2(9+R)-9\pi^2d_{i0}{}^2n+16\eta_{0c}^2k_{vc}+d_l{}^2k_{\phi c}+32\eta_{0d}^2k_{1vd}+2d_l{}^2k_{1\phi d}\right\}+4m\beta\eta_w,\ (i=3)$

$$\frac{M_e d}{2l} \times \boldsymbol{K}\boldsymbol{a} = \frac{M_e d}{2l} \times \begin{pmatrix} \boldsymbol{K}_{aa} & \boldsymbol{K}_{ab} \\ \boldsymbol{K}_{ba} & \boldsymbol{K}_{bb} \end{pmatrix} \boldsymbol{a} = 0 \tag{3.11}$$

In this study, Eq.(10) is calculated by setting m^* in Eq. (3.8) and (3.9) equal to 5. And m^* is set equal to 7 when the effect of torsional bracing is considered for the preservation of accuracy. The matrix of $\boldsymbol{K}_{aa}$, $\boldsymbol{K}_{ab}$, $\boldsymbol{K}_{ba}$ and $\boldsymbol{K}_{bb}$ are presented as Eq. (3.12) ~ (3.14). In these equations, i is the row position of diagonal elements. In order that Eq. (3.11) has a nontrivial solution, the buckling equation is presented as follows.

$$|\boldsymbol{K}| = 0 \tag{3.15}$$

By analyzing Eq. (3.12) ~ (3.15), we find that the parameters which have effects on the buckling load n and m are the end moment ratio κ, the uniformly distributed load ratio w, the position of the bracing η_{0d} and η_{0c}, the position of the uniformly distributed load η_w and R, d_{i0}, d_l which are the various amounts about the section size and the length. The buckling load can be obtained when these parameters are determined.

3.3 Analytical results

In this section, the case when one lateral bracing or one torsional bracing is attached at the member is presented. That is to say, k_{2vd}, k_{vc}, $k_{2\phi d}$ and $k_{\phi c}$ in Eq. (3.12) ~ (3.14) are equal to 0. When the bracing is considered as the brace for the beam-column, the discussion about the case of plural bracing is important. However, the results for the cases of two bracing and continuous bracing are similar to that for the case of one bracing. Therefore, the discussion on two bracing and continuous bracing will be presented in future.

3.3.1 Analytical parameters

The analytical parameters are set as follows:

1) The end moment ratio: κ=-1, 0, 1
2) The position of the bracing: η_{0d}=-0.6, 0, 0.6
3) The section size: H-600×200×11×17 (narrow width)
   H-588×300×12×20
   H-488×300×11×18
   H-300×300×10×15 (wide width)
4) The length of the member: l=6m, 16m
5) The kind of the bracing: lateral bracing and torsional bracing

The section properties for analyzing are shown as Table 3.1. The slenderness ratio λ_y corresponding to the weak axis when the buckling effective length is the whole length of the member is presented. In Reference 1, the upper limit of the slenderness ratio λ_y is 200 and the lower limit of λ_y is calculated by $\sqrt{\pi^2 E/(0.6F)}$ (when F=235N/mm^2, the lower limit is about 120). In Table 1, the values of λ_y which are over the upper and lower limit are chosen as the analytical parameters. That is because it is easy to compare the results when the length of the member is constant.

3.3.2 Relation between buckling strength and bracing stiffness

The interactions between the nondimensional bending moment m and the nondimensional axial force n on the buckling load are presented by taking the nondimensional bracing stiffness as a parameter. The cases of the lateral bracing and the torsional bracing are presented respectively.

i) Case of lateral bracing

(a) Effect of end moment ratio (Fig. 3.2)

Figure 3.2 shows the m-n interactions when the lateral bracing is attached at the midspan of the member by taking the bracing stiffness k_{1vd} as a parameter. The cross

Table 3.1 Section properties and member length

	H-600×200	H-588×300	H-488×300	H-300×300
A (mm^2)	13170	18720	15920	11850
I_z(mm^4)	7.56×10^8	1.14×10^9	6.89×10^8	2.02×10^8
I_y(mm^4)	2.27×10^7	9.01×10^7	8.11×10^7	6.75×10^7
i_0 (mm)	243	257	220	151
J (mm^4)	9.14×10^5	1.93×10^6	1.37×10^6	7.70×10^5
I_w (mm^6)	1.93×10^{12}	7.27×10^{12}	4.48×10^{12}	1.37×10^{12}
l (mm)	6000	6000	6000	6000
	16000	16000	16000	16000
λ_y	144	86.5	84.1	79.5
	385	231	224	212
R	0.663	0.372	0.431	0.788
	4.72	2.65	3.06	5.60

NOTE For λ_y, R, the upper and lower values correspond to the cases of l=6000 and l=12000, respectively.

section is H-600×200×11×17 and the length of the member is 6m. The bracing is attached at the middle of the cross section (η_{0d}=0). Fig. 3.2(a) shows the case when the end moment ratio κ=-1 (symmetric bending). According to this figure, as the bracing stiffness increases, the field covered by the m-n curve and the axes of coordinates becomes wider. When m=0 or n=0, the maximum value is n=2.39 and m=3.35 respectively.

When the H-shaped beam supported simply is subjected to the compressive load, the buckling load is determined by the torsional buckling force or the bending buckling force around the strong or weak axis. The buckling load when n=2.39 is determined by the torsional buckling force (referred to Appendix 2). In this situation, when the section size and the length are constant and the member is subjected to the axial load, the buckling load will not be larger than the torsional buckling force even though the bracing stiffness increases. As shown in Eq. (3.2), when the nondimensional bracing stiffness k_{1vd} =1, the required bracing stiffness is equal to the required stiffness bracing of the compressive member attaching one bracing at the midspan and subjected to uniform axial force only when the buckling mode becomes the second order distribution of a sine wave. And when n=2.39, the minimum value of the bracing stiffness k_{1vd} is 0.441 which is smaller than unity. The maximum value of the nondimensional bending moment m is 3.35 when the effective length is half of the whole length of the member (referred to Appendix 2).

In Fig. 3.2(a), LineA means the buckling modes of the deflection and the torsional

angle are both second order distribution of a sine wave. And as shown in this figure, the larger the bracing stiffness is, the wider the same part with LineA is.

Figure 3.2(b) shows the case of κ=0. According to Fig. 3.2(b), the case of κ=0 has the same tendency as the case of κ=-1. However, there is not the obvious limit like LineA in Fig. 2(b).

Figure 3.2(c) shows the case of κ=1 (antisymmetric end moment). According to this figure, two kinds of the buckling mode (modeA and modeB) can be observed. As shown in Fig. 3.2(c), modeA is the case that the torsional angle at the bracing point is zero and modeB is the case that the lateral deflection at the bracing point is zero. When the nondimensional bracing stiffness is smaller than 0.441, the effect of the bracing can be observed under large axial force. While the nondimensional bracing stiffness is larger than 0.441, the buckling mode is modeB and the curves of the *m*-*n* interactions are same whatever the bracing stiffness equals.

(b) Effect of bracing point (Fig. 3.3)

Figure 3 shows the relation of the *m*-*n* interaction on the elastic flexural-torsional buckling strength by taking the nondimensional bracing stiffness k_{1vd} as a parameter when the bracing is attached at the upper or lower side of the cross section. The size of the cross section is H-600×200×11×17 and the length of the member is set to 6m. In Fig. 3, the first quadrant shows the case of the bracing at the upper side (η_{0d}=-0.6) and the second quadrant shows the case of the bracing at the lower side (η_{0d}=0.6). This model can be considered as the furring strips attaching at the beam-column. The position of the bracing is determined by the size of the cross section of the member, the size of the cross section of the bracing and the way of connection. In this study, we assume the bracing is attached at the surface of the flanges when η_{0d}=±0.6.

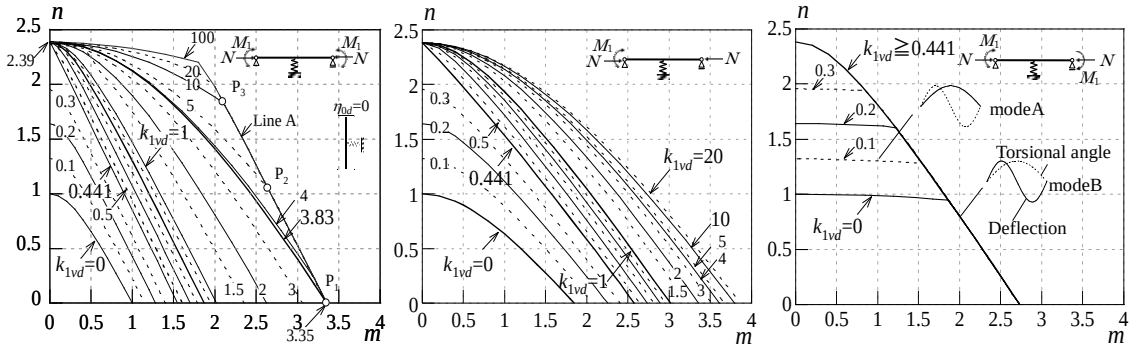

(a) κ=-1 **(b)** κ=0 **(c)** κ=1

Fig. 3.2 *m*-*n* interaction (with one lateral bracing at center of the section)

In Fig. 3.3(a), when the member is subjected to axial load only (m=0), the nondimensional axial force n becomes larger as the bracing stiffness increases. However, the maximum value n=2.39 shown in Fig. 3.2(a) cannot be reached when the bracing is attached at the surface of the flanges. And according to the first quadrant in Fig. 3.2(a), there are two buckling strengths m to the same buckling strength n when the bracing is attached at the member. For example, when k_{1vd}=0.420 and n=2.0, the value of m is 0.592 and 1.76 (see Point A1 and A2). When the bracing stiffness and the axial force are constant, two different values of the bending moment are obtained. That is because the buckling modes corresponding to these two values are different (referred to Appendix 3). Fig. 3.3(b) shows the case of κ=0, the curves of the m-n interaction have the same tendency with these shown in Fig. 3.3(a).

Figure 3.3(c) shows the case of κ=1. The curves of the m-n interaction are symmetric about the x-axis. When the axial force and the bracing stiffness are same, there is only one value of m to correspond that is different with the cases of κ=-1 and κ=0.

(c) Effect of size of cross section and length of member (Fig. 3.4)

In Fig. 3.4(a), the relation of the m-n interaction with different size of the cross section are presented when κ=-1 and η_{0d}=0. The sizes of the cross section are included H-588×300×12×20, H-488×300×11×18 and H-300×300×10×15 (wide width). The length of the member is set to 6m. As shown in Fig. 3.4(a), the difference of the size of the cross section has a little effect on the relation between the m-n interaction and the bracing stiffness. Fig. 3.4(a) shows the same tendency as Fig. 3.2(a) and the values of the bracing stiffness when the curve has the same part with LineA are different. The values are equal to 4.57, 4.37 and 3.61 in Fig. 3.4(a-1), (a-2) and (a-3), respectively. And the value corresponding to the size of wide width is smaller than the others.

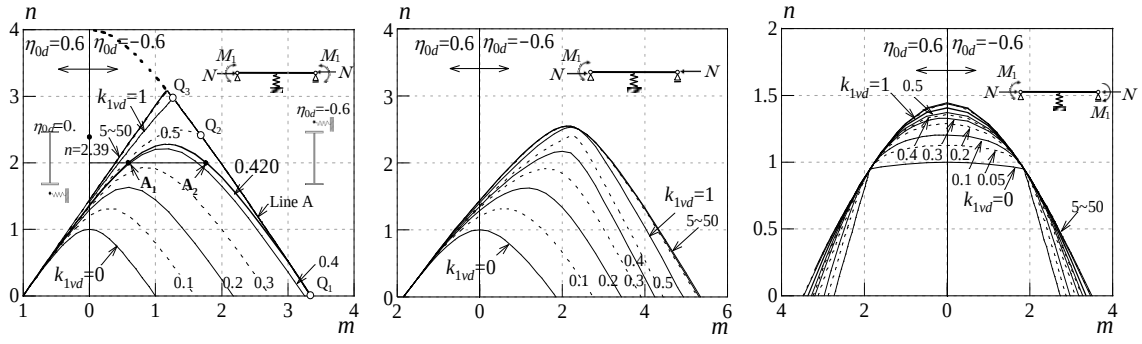

(a) κ=-1 **(b)** κ=0 **(c)** κ=1

Fig. 3.3 m-n interaction (with one lateral bracing at upper side and lower side)

To present the effect of the length of the member, the cases when the length of the member l=16m and the end moment ratio κ=-1 (symmetric end moment) are shown in Fig. 3.4(b). The sizes of the cross sections are H-588×300×12×20, H-488×300×11×18 and H-300×300×10×15 (wide width) corresponding to Fig. 3.4(b-1), (b-2) and (b-3), respectively. As shown in Fig. 3.4(b), when the member is subjected to the axial load only, the maximum value of the nondimensional axial force n is equal to 4. This value corresponds to the flexural buckling strength around the weak axis when the effective length equals half of the whole length (l_k =l/2). Therefore, we can find the length of the member has effects on the relation of the m-n interaction that the buckling strength is determined by the flexural buckling strength around the weak axis or the torsional buckling strength when the member is subjected to the axial load only. The discussion about the conditions to determining the buckling form is shown as Appendix 4. For this study, we define the buckling mode when the flexural buckling occurred (shown as the case of l=16m) is the flexural buckling mode and the buckling mode when the torsional

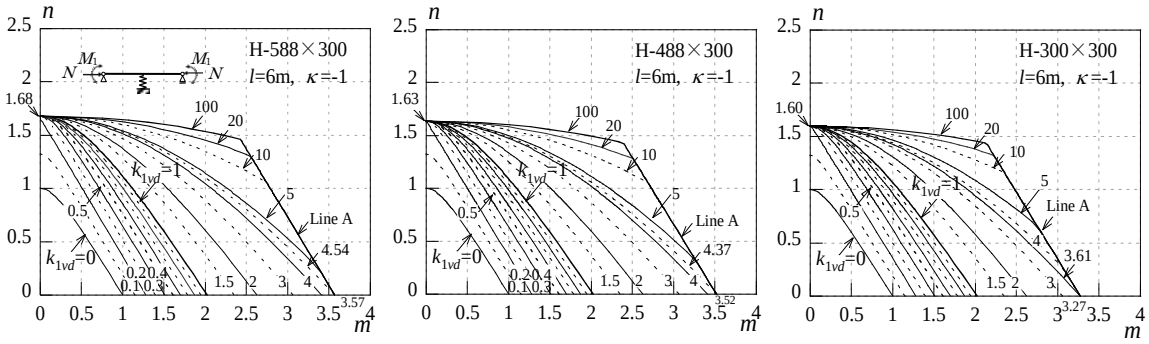

(a-1) H-588×300 (a-2) H-488×300 (a-3) H-300×300

(a) Member length 6m (η_{0d}=0)

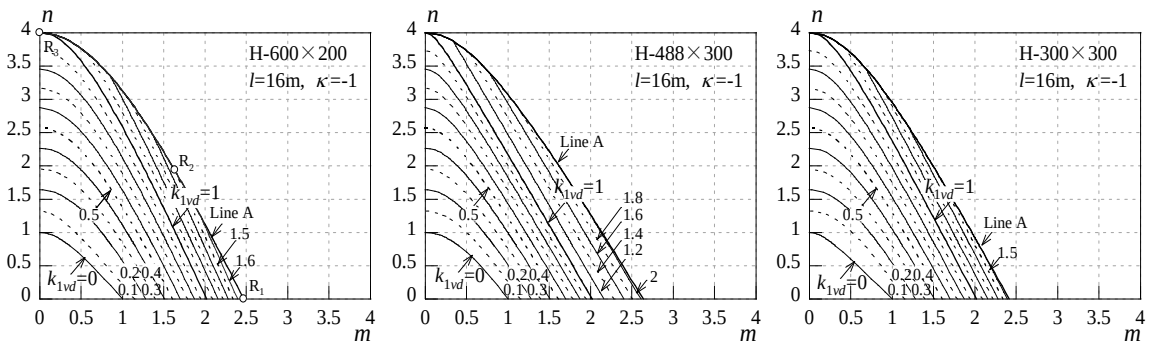

(b-1) H-600×200 (b-2) H-488×300 (b-3) H-300×300

(b) Member length 16m (η_{0d}=0)

Fig. 3.4 *m*-*n* interaction (effect of section size and member length)

buckling occurred (shown as the case of l=6m) is the torsional buckling mode. When the member is subjected to the axial load only, the nondimensional bracing stiffness k_{1vd} to obtain the maximum value of n is 0.441<1 in Fig. 3.2(a) (l=6m, n_{max}=2.39), while the value of k_{1vd} in the same condition in Fig. 3.4(b-1) (l=16m, n_{max}=4) is exactly equal to unity. On the effect of the size of the cross section, when the curve has the same part with LineA and n=0, the value of m is not constant in Fig. 3.4(b-1) that is different from the situation shown in Fig. 3.2(a) (when n=0, m_{max}=3.35).

ii) Case of torsional bracing (Fig. 3.5)

Fig. 3.5 shows the relation of the m-n interaction when the torsional bracing is attached at the midspan of the member. The size of the cross section is H-600×200×11×17 and the length of the member is set to 6m. As shown in Fig. 3.5, the value of the nondimensional axial force is constant (n=1) even if the bracing stiffness increases when the member is subjected to the axial load only (m=0). And it is the same as the case of the lateral bracing, as the bracing stiffness increases, the field covered by the m-n curve and the axes of coordinates becomes wider. When κ=-1 (Fig. 3.5(a)), as the bracing stiffness increases, the same part with LineA whose deflection and torsional angle at the bracing point are both zero becomes larger. When κ=1 (Fig. 3.5(c)), modeA when the torsional angle at the bracing point is zero and modeB when the deflection at the bracing point is zero can be observed. When $k_{1vd} \geqq 0.156$, the buckling mode is modeB and the curves are constant even if the bracing stiffness increases. According the analysis about the lateral bracing, we can find that the buckling strength has relations with the buckling form when the member is subjected to the axial load only, so the effect of the length of the member has a little effect on the buckling strength when the torsional bracing is attached at the midspan of the member. However, the term about the nondimensional bracing stiffness k_{1vd} has a coefficient $d_l^2 = (l/d)^2$ in Eq. (12)~(15), so

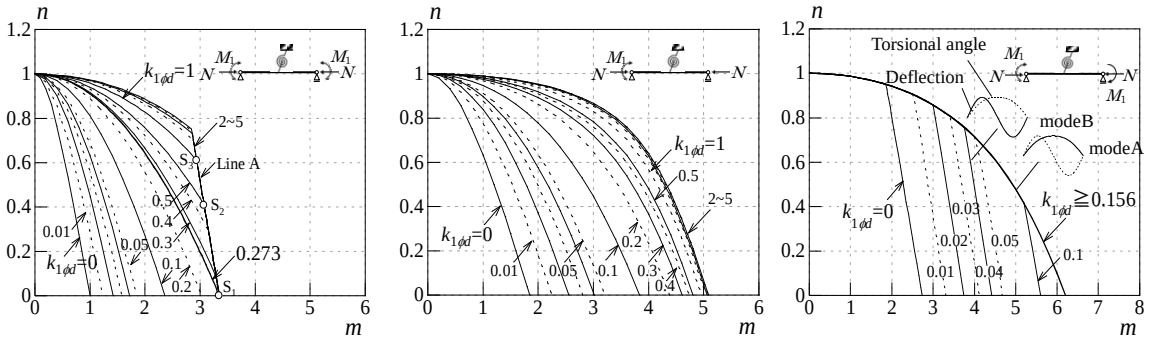

(a) κ=-1 **(b)** κ=0 **(c)** κ=1

that there is a large efficiency of the bracing when the value of l/d is large. Therefore, when the bracing stiffness is constant, as the value of l/d increases, the field covered by the m-n curve and the axes of coordinates becomes wider.

3.3.3 Required bracing stiffness to be full-bracing

i) Relation between required bracing stiffness and nondimensional axial force

(a) Case of lateral bracing

In this chapter, when the lateral bracing or the torsional bracing is attached at the midspan of the member, the buckling mode that the deflection and the torsional angle at the bracing point are zero is referred to as full-bracing, just like the cases when the curve has the same part with LineA shown as Fig. 3.2(a) and Fig. 3.4(a). Fig. 3.6 shows the required bracing stiffness to be full-bracing ${}_{req}k_{1vd}$ by taking the position of the bracing as a parameter when the lateral bracing is attached at the midspan of the member and the end moment ratio κ=-1. The horizontal axis represents the nondimensional axial force n and the vertical axis represents the required bracing stiffness ${}_{req}k_{1vd}$. Because the curves of the m-n interaction has no same part with LineA when the bracing is attached at the lower side of the cross section shown as the second quadrant in Fig. 3.3, the parameter $\eta_{0d} \leqq 0$ in Fig. 3.6. Fig. 3.6(a), (b) show the cases when the length of the member is 6m and 16m respectively. The size of the cross section is set to H-600×200×11×17 or H-300×300×10×15. The points P1, P2, P3, Q1, Q2 and Q3 in Fig. 3.6(a-1) correspond to the same points shown in Fig. 3.2(a) and Fig. 3.3(a). And the points R1, R2 and R3 in Fig. 3.6(b-1) correspond to the same points shown in Fig. 3.4(b-1).

According to Fig. 3.6(a), when n<2.65 in Fig. 3.6(a-1) and n<2.5 in Fig. 3.6(a-2), the required bracing stiffness decreases as the bracing point is far away from the center of the cross section. And this decrease becomes slow when the value of η_{0d} is smaller than -0.2. Comparing Fig. 3.6(a-1) and (a-2), when the required stiffness bracing ${}_{req}k_{1vd}$ abruptly increases, the value of the nondimensional axial force n corresponding to the case of the cross section of the narrow width (Fig. 3.6(a-1)) is larger than that corresponding to the wide width (Fig. 3.6(a-2)). In Fig. 3.6(b), when n<3.0, as the bracing point is far away from the center of the cross section, the value of ${}_{req}k_{1vd}$ decreases. Comparing Fig. 3.6(b-1) and (b-2), it is not obvious for the effect of the size of the cross section when the length of the member is 16m. And when the bracing is attached at the center of the cross section (η_{0d}=0), as the nondimensional axial force n increases, the required bracing stiffness ${}_{req}k_{1vd}$ becomes smaller. As the bracing point is far away from the center of the cross section, the value of n is close to 4, the required bracing stiffness abruptly increases. Comparing Fig. 3.6(a) and (b), we can find that the

relation between $_{req}k_{1vd}$ and n will be different if the length of the member is different.

(b) Case of torsional bracing

The required bracing stiffness when the torsional bracing is attached at the midspan of the member is shown as Fig. 3.7. In Fig. 3.7(a), the points S_1, S_2 and S_3 correspond to the same points in Fig. 3.5(a). As mentioned before, the position of the torsional bracing has no effect on the elastic buckling strength, so that we take the size of the cross section as a parameter to show the required bracing stiffness in Fig. 3.7. Fig. 3.7(a) and (b) show the cases when the length of the member is set to 6m and 16m respectively. According to Fig. 3.7(a), the required bracing stiffness when the size of the cross section belongs to the type of the wide width is smaller than that when the size of the cross section belongs to the type of the narrow width. According to Fig. 3.7(b), the tendency of the curve with the different size of the cross section is similar when the value of the nondimensional axial force n is smaller than 0.6. We have discussed the coefficient $d_l=l/d$ has effects on the case of the torsional bracing in Section 3.2.2.

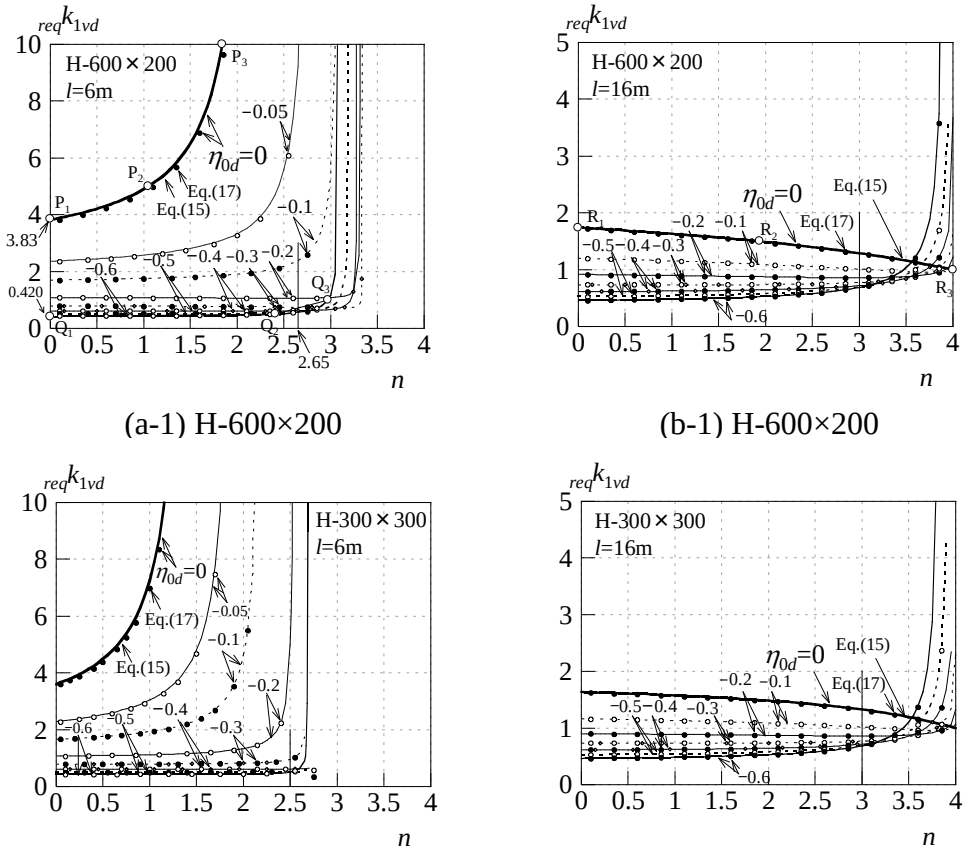

(a-1) H-600×200　　(b-1) H-600×200

(a-2) H-300×300　　(b-2) H-300×300

(a) l=6m（lateral bracing）　　**(b)** l=16m（lateral bracing）

Fig. 3.6 Required bracing stiffness for full bracing (lateral bracing)

Because the value of d_l is large, the required bracing stiffness corresponding to the cross section H-300×300×10×15 is small. While the value of d_l is small, the required bracing stiffness corresponding to the cross section H-600×200×11×17 is large.

ii) Equations to obtain required bracing stiffness

(a) Equations and accuracy

In this study, the simple equations to obtain the required bracing stiffness are presented. The relation of the *m*-*n* interaction to be the full-bracing (LineA) is presented as Eq. (3.16).

$$m = r\sqrt{(4-n)\left(4+R-4{d_{i0}}^2 n\right)} \equiv r m_b \tag{3.16}$$

Equation (3.16) is calculated by the buckling equation whose number of the terms m^* in Eq. (3.8) and (3.9) is set to equal to three. The required bracing stiffness to be the full-bracing can be calculated by Eq. (3.17) which uses m_b defined by Eq. (3.16).

The relation of ${}_{req}k_{1vd}$-*n* calculated by Eq. (3.16) is shown as the marks ● and ○ in

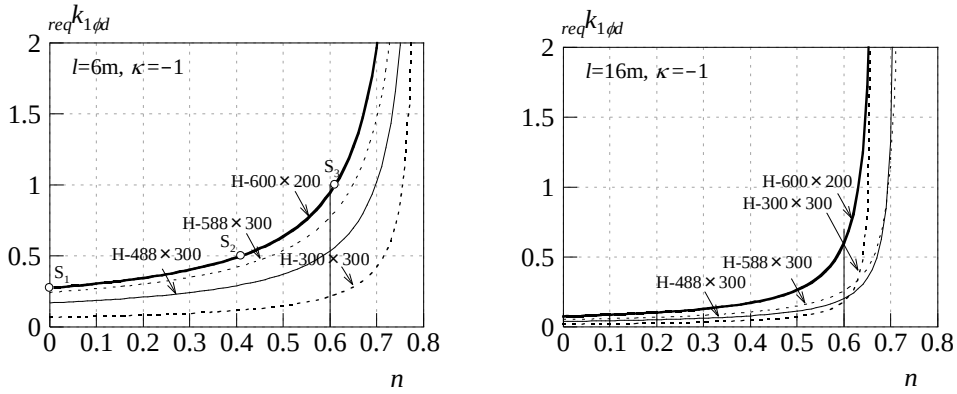

(a) *l*=6m (b) *l*=16m

Fig. 3.7 Required bracing stiffness for full bracing (torsional bracing)

Fig. 3.6. According to Fig.3.6, the difference with the result calculated by Eq. (17) when the bracing is attached at the center of the cross section (η_{0d}=0) is larger than the others whose accuracy is good enough to be used for evaluating.

In the same way, the equation to obtain the required bracing stiffness to be the full-bracing when the torsional bracing is attached at the midspan of the member is shown as Eq. (3.18). However, the number of the terms m^* in Eq. (3.8) and (3.9) to obtain Eq. (3.18) is set equal to 5 which is the same as that used for calculating the buckling equation shown as before. Because of this, the results obtained by Eq. (3.18) are consistent with the curves in Fig. 3.7.

Figure 3.8 shows the accuracy of the case of the lateral bracing. The horizontal axis is the nondimensional axial force *n* and the vertical axis is the accuracy which is

$$ {}_{req}k_{1vd} = \frac{45\pi^2}{64} \frac{n^2\left(4d_{I_0}^2+1\right)^2 - 2n\left(4d_{I_0}^2+1\right)(R+9)+(R+13)(R+5)}{28n^2\left(4d_{I_0}^2+1\right)\left(d_{I_0}^2+\eta_{0d}^2\right) - n\left\{-28m_b\eta_{0d}\left(4d_{I_0}^2+1\right)+48d_{I_0}^2\eta_{0d}^2+56(R+7)d_{I_0}^2+28(R+14)\eta_{0d}^2+7R+3\right\} - 4m_b\eta_{0d}(7R+95)+12(R+25)\eta_{0d}^2+7R^2+98R+75} \quad (3.17) $$

$$ {}_{req}k_{1\phi d} = \frac{1575\pi^2}{8d_l^2} \frac{n^3\left(4d_{I_0}^2+1\right)^3 - n^2\left(4d_{I_0}^2+1\right)^2(3R+47)+n\left(4d_{I_0}^2+1\right)\left(3R^2+94R+587\right)-(R+29)(R+13)(R+5)}{487n^3\left(4d_{I_0}^2+1\right)^2 - n^2\left(4d_{I_0}^2+1\right)\left\{540d_{I_0}^2+487(2R+43)\right\}+n\left\{1080d_{I_0}^2(R+37)+487R^2+21080R+202600\right\}-45\left(3R^2+222R+3275\right)} \quad (3.18) $$

calculated by Eq. (3.19). In Eq. (3.19), ${}_{5req}k_{1vd}$ represents the required bracing stiffness when the number of the terms m^* in Eq. (3.8) and (3.9) is set equal to 5.

$$ \text{Accuracy} = \frac{{}_{req}k_{1vd} - {}_{5req}k_{1vd}}{{}_{5req}k_{1vd}} \times 100\ (\%) \quad (3.19) $$

Fig. 3.8(a) and (b) show the cases when the length of the member is set equal to 6m and 16m respectively. According to Fig. 3.8(a), when $\eta_{0d} \geqq$-0.4, the accuracy becomes better as the bracing point is far away from the center of the cross section. while when $\eta_{0d} \leqq$-0.5, the accuracy becomes worse as the value of η_{0d} decreases. When $\eta_{0d} \leqq$-0.2, the accuracy is not larger than 5% and the accuracy when η_{0d} =-0.05, -0.1 is quite bad. According to Fig. 3.8(b), except the case of η_{0d}=0, the accuracy becomes worse as the bracing point becomes far away from the center of the cross section. When $\eta_{0d} \leqq$-0.5, the accuracy is not larger than 5% and when $n \leqq$-0.5, the accuracy is not larger than 2%.

(b) Correction for equations

About the equations to obtain the required bracing stiffness (Eq. (3.17) and (3.18)), it should be mentioned that if the nondimensional axial force is large enough, the required bracing stiffness will increase abruptly. Because of this, the accuracy at this moment becomes exceeding bad. As the bracing point becomes far away from the center of the cross section the accuracy becomes worse, especially the case when the torsional buckling mode occurred (Fig. 3.8(a)). The analytical method used for this study is the Rayleigh-Ritz method which cannot keep the evaluation safety. Therefore, there is necessary to set a correction coefficient for the required bracing stiffness and define the range of application. The required bracing stiffness corrected is shown as Eq. (3.20).

$$ {}_{req}k_{1vd}{}^{*} = {}_{req}k_{1vd} \times 1.1 \quad (3.20) $$

The scope of application is shown as follows.

(1) When the torsional buckling mode occurred and the buckling load n is smaller than the torsional buckling load, if $\eta_{0d} \geqq$-0.05, the required bracing stiffness should be confined to the range of ${}_{req}k_{1vd} \leqq 10$.

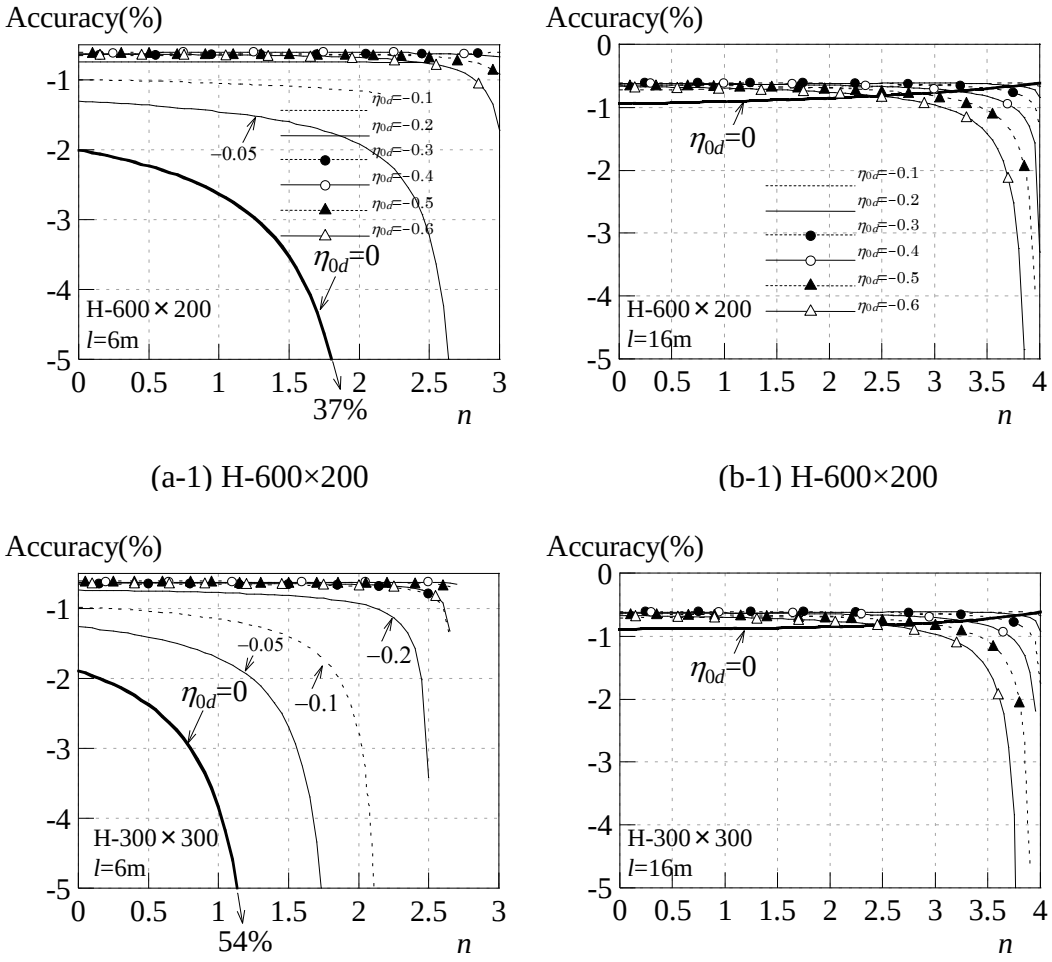

(a) *l*=6m **(b)** *l*=16m

Fig. 3.8 Accuracy of required stiffness obtained by Eq.(3.17) compared with the required stiffness obtained by Eq. (3.15)

(2) When the flexural buckling mode occurred, if $\eta_{0d} \leqq$-0.3, the buckling load *n* should be satisfied with the condition of n$\leqq$3.

When the torsional buckling mode occurred and the buckling load *n* is smaller than the torsional buckling load, the results calculated by Eq. (3.17) include the part of bold dashes which cannot be obtained in fact. So that Limit (1) is necessary for the simple equation to evaluate th

e required bracing stiffness. About Limit (2), when the flexural buckling mode occurred and $\eta_{0d} \neq 0$, as the bracing point becomes far away from the center of the cross section, the required bracing stiffness becomes larger. And the situation when *n*=4 cannot be come true even if the required bracing stiffness becomes infinite. Therefore, the part when the required bracing stiffness increases abruptly shown as Fig. 3.6(b) should be

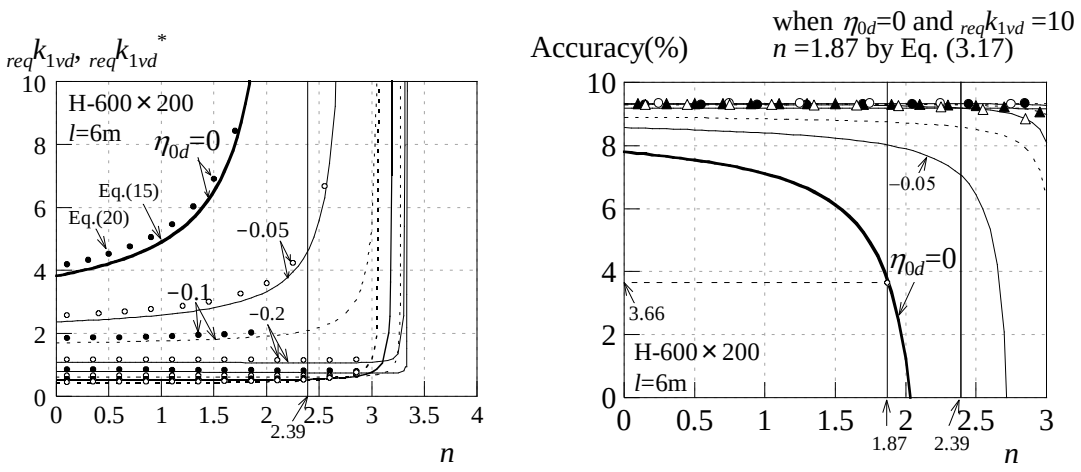

(a-1) modified $_{rea}k_{1vd}^{*}$ (a-2) difference after modification

(a) H-600×200

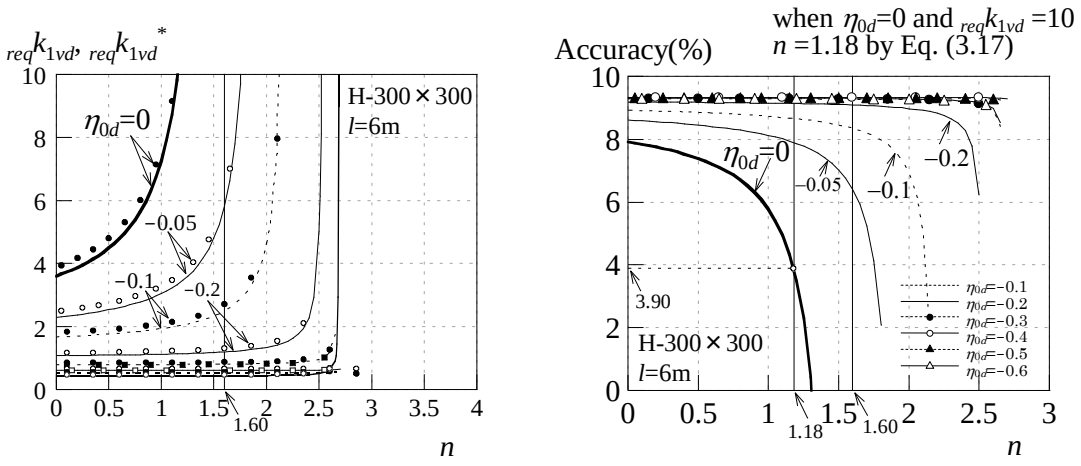

(b-1) modified $_{rea}k_{1vd}^{*}$ (b-2) difference after modification

(b) H-300×300

Fig. 3.9 Relation between n and required bracing stiffness $_{req}k_{1vd}$ obtained by modified equation (3.20) and accuracy

deleted.

Fig. 3.9 shows the accuracy which has been corrected by Eq. (3.20) and Limit (1). The sizes of the cross section are set to H-600×200×11×17 and H-300×300×10×15 and the length of the member is set equal to 6m. According to Fig. 3.9, when η_{0d}=0 and $_{req}k_{1vd}$=10, the accuracy of the cases of n=1.87, 1.18 is 3.66% and 3.9% respectively. In the scope of application, the results calculated by these equations are in safety.

On the bracing attached at the beam-column used in real structure, the Recommendation for Stability Design of Steel Structures published in 1980 presents an example for the evaluation of the bracing which is attached at the midspan of the

H-shaped steel beam-column. We calculated the same case by the method used in that example and the procedure of the calculation is not presented there. However, the results are larger than the required bracing stiffness shown in Fig. 3.6.

3.4 Conclusions

The general buckling equation of the H-shaped member pinned at both ends and subjected to the axial load, the end moments and the uniformly distributed load with the lateral bracing and torsional bracing is calculated by using the Rayleigh-Ritz method. The moment – axial force interaction of the elastic buckling strength when the lateral bracing or the torsional bracing are attached at the midspan of the member is presented. The conclusions derived from this chapter are shown as follows:

1) When the lateral bracing is attached at the midspan of the member, the deflection and the torsional angle at the bracing point are zero as the bracing stiffness increases in case of the end moment ratio κ=-1 (symmetric end moment, Fig. 3.2(a)). As for the case of κ=1 (antisymmetric end moment), bracing is effective when the compressive force is large. However, the *m*-*n* interaction is same when the bracing stiffness is above a certain value (Fig. 3.2(c)).
2) There are two different buckling moments for one buckling axial force when the bracing is attached at the compressive flange (Fig. 3.3(a)).
3) When the length of the member is same, the effect of the cross section on the m-n interaction is not so remarkable (Fig. 3.4(a)). As for the influence of the member length, the difference of bucking modes affects the *m*-*n* interaction. The weak axis buckling or torsional buckling occurs depending on the member length when the member is subjected to axial force and the bracing stiffness increases.
4) About the effect of the torsional bracing, the deflection and the torsional angle at the bracing point are zero as the bracing stiffness increases in case of the end moment ratio κ=-1 (Fig. 3.5(a)).
5) When the lateral bracing or the torsional bracing is attached at the midspan of the member, the buckling mode that the deflection and the torsional angle at the bracing point are zero is referred to as full-bracing. The relation between the nondimensional buckling axial force and the required bracing stiffness for full-bracing is presented by Fig. 3.6 and Fig. 3.7. The simple equations to obtain the required bracing stiffness and the scope of the application are presented (Eq. (3.17), (3.18) and (3.20)).

Reference for Chapter 3

1) Architectural Institute of Japan: Design Standard for Steel Structures -Based on Allowable Stress Concept-, 2005.09
2) Architectural Institute of Japan: Recommendation for Limit State Design of Steel Structures, 2010.02
3) Architectural Institute of Japan: Recommendations for the Plastic Design of Steel Structures, 2010.02
4) Architectural Institute of Japan: Recommendations for Stability Design of Steel Structures, 2009.11
5) Kimura Junichi and Matsui Chiaki: 胴縁で補剛されたH形断面柱の弾性曲げねじれ座屈解析，AIJ Kyushu Chapter Architectural Research Meeting (Structure) , Vol.29, pp.285-288, 1986.03
6) Tsuda Keigo and Kido Masae: Flexural-torsional buckling of beam-columns restrained against sway and rotation at a center, Discussion of beam-columns that have sandwich sections, Journal of Structural and Construction Engineering Vol.78, No.684, pp.377- 385, 2013.02
7) Kimura Yoshihiro and Yoshino Yuki: Required bracing capacity on lateral buckling strength for H-shaped beams with bracings, Journal of Structural and Construction Engineering Vol.76, No.670, pp.2143-2152, 2011.12
8) Architectural Institute of Japan: Stability Problems of Steel Structures 2013, 2013.07
9) Kimura Yoshihiro, Matuso takeshi and Yoshino Yuki: Estimation of elasto-plastic lateral buckling stress for h-shaped beams with lateral-rotational braces on subjected to axial force and flexural moment, Journal of Structural and Construction Engineering Vol.79, No.703, pp.1299-1308, 2014.09
10) Theodore V. Galambos: Structural Members and Frames (Interpreted by Yushi Fukumoto and Fumio Nishino), 1970.10
11) Tsuda Keigo and Kido Masae: Buckling strength of columns braced continuously with varying axial force, Flexural buckling of compressive flange of H-sharped steel restrained by web or slab, Journal of Structural and Construction Engineering Vol.78, No.690, pp.1513- 1521, 2013.08
12) Architectural Institute of Japan: Recommendation for Limit State Design of Steel Structures, 1980.09
13) Trinh Van Quang and Idota Hideki: Buckling strength and Rigidity Requirement of Lateral Support for H-shaped Steel Column Supported by Furring Strips, AIJ Toukai Chapter Architectural Research Meeting, No.50, pp.137-140, 2012.02

Appendix 3.1 Discussion about accuracy of analysis

In this chapter, the number of the terms m^* in Eq. (3.8) and (3.9) is set equal to 5 to analysis. When the torsional bracing is attached at the midspan of the member and the nondimensional axial force n is set equal to 0.8, the accuracy is shown as Fig.A1 by taking the bracing stiffness k_{1vd} as a parameter. In Fig.A1, the length of the member is 6m and the value of k_{1vd} is equal to 0.05 or 1000. The vertical axis is the value of ${}_im/{}_7m$ and the horizontal axis is the number of the terms. ${}_im$ means the buckling strength of the member subjected to the end moments only when $m^*=i$ (i =1, 2, 3, 4, 5, 6, 7) and ${}_7m$ is the nondimensional bending moment when the number of the terms m^* equals 7 to calculate. According to Fig.A1, the maximum difference between the cases of m^*=7 and m^*=5 is 1.1% when the size of the cross section is H-600×200×11×17 (Fig. A1(a)) and the maximum difference is 1.4% when size of the cross section is H-300×300×10×15 (Fig. A1(b)).

Therefore, we think the accuracy of the analysis is sufficient by taking m^*=5 to analysis.

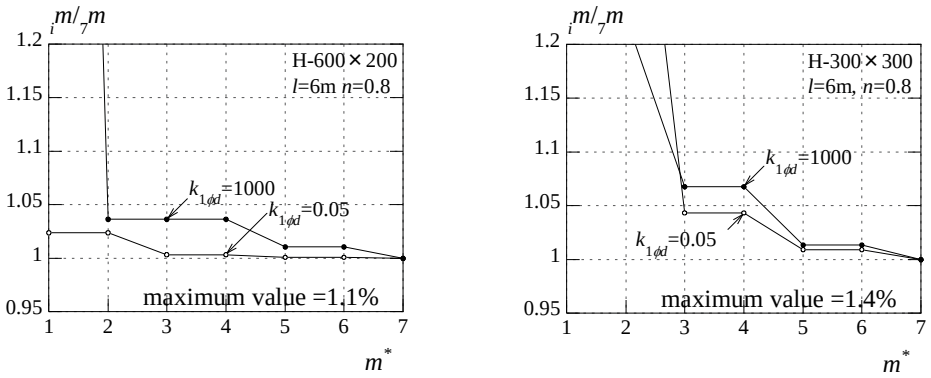

(a) H-600×200 **(b)** H-300×300

Fig. A3.1 Difference by the number of terms of basis

Appendix 3.2 Buckling load when the end moment ratio κ=-1 (H-600×200×11×17)

The value of R can be calculated by the equations shown as follows, when the length of the member is set to 3m and 6m respectively.

$$\left.\begin{aligned} R_{l=3} &= \frac{GJl^2}{\pi^2 EI_w} = \frac{78846\times 9.14\times 10^5\times 3000^2}{\pi^2\times 205000\times 1.93\times 10^{12}} = 0.1661 \\ R_{l=6} &= \frac{78846\times 9.14\times 10^5\times 6000^2}{\pi^2\times 205000\times 1.93\times 10^{12}} = 0.6644 \end{aligned}\right\} \quad \text{(A.3.1)}$$

The torsional buckling load can be calculated the equation shown as follows.

$$P_{crw} = \frac{1}{{i_0}^2}\left(\frac{\pi^2 EI_w}{l^2} + GJ\right) \tag{A.3.2}$$

Then the nondimensional axial force can be calculated by Eq. (A.3.3) in which P_e represents the elastic buckling load for out-of-plane bending around the weak axis. And the result calculated by this equation is consistent with the maximum value of n shown in Fig. 3.2(a).

$$P_{crw}/P_e = \frac{1+R}{4{d_{i0}}^2} = \frac{1+0.6644}{4\times(243.1/583)^2} \cong 2.39 \tag{A.3.3}$$

The elastic lateral buckling moment M_e when the member is subjected to symmetric end moment only is calculated by Eq. (A.3.4).

$$M_e = \frac{1}{2} N_e d\sqrt{1+R} \tag{A.3.4}$$

The elastic buckling load when the length of the member is 3m is four times of that when the length of the member is 6m. The ratio of the elastic lateral buckling moment in these two situations is presented as Eq. (A.3.5).

$$\frac{{}_{l=3}N_e\sqrt{1+{}_{l=3}R}}{{}_{l=6}N_e\sqrt{1+{}_{l=6}R}} = 4\frac{\sqrt{1+0.1661}}{\sqrt{1+0.6644}} \cong 3.35 \tag{A.3.5}$$

This value obtained by Eq. (A.3.5) is consistent with the maximum value of m shown in Fig. 3.2(a) when the member is subjected to the symmetric end moment only (κ=-1).

Appendix 3.3 Buckling modes when lateral bracing is attached at upper side of cross section

Figure A3.2 shows the buckling modes corresponding to Point A1 and A2 (Fig. 3.3(a)) when the lateral bracing is attached ate the upper side of the cross section. The

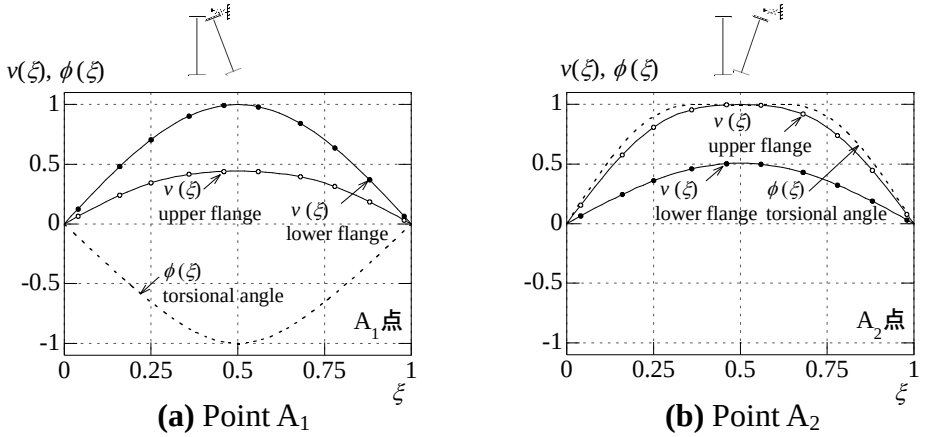

(a) Point A_1 **(b)** Point A_2

Fig. A3.2 Buckling mode at point A_1 and point A_2 in Fig. 3.3(a)

horizontal axis represents the position along the member and the vertical axis represents the lateral deflection or the torsional angle. The lateral deflection of upper and borrow flange is defined as Eq. (A.3.6).

$$\text{Values calculated by Eq.}(1) \pm \phi(\xi)/2 \tag{A.3.6}$$

According to Fig. A3.2, the deflection of borrow flange is larger than that of upper flange at Point A1, while the opposite result is obtained at Point A2. Moreover, the deflection of the torsional angle is opposite at Point A1 and A2.

Appendix 3.4 Discussion about buckling modes when the member is subjected to axial load only

When the member is subjected to axial load only and the lateral bracing is attached at the midspan of the member, if the bracing stiffness is large than some value, the torsional buckling or the flexural buckling around the weak axis whose buckling length equals half of the length of the member will occur. The critical value of the nondimensional axial force to determine the flexural buckling or the torsional buckling will occur (Eq. (A.3.2)) is equal to 4. Therefore, the conditions to determine the types of the buckling are shown as follows.

$$\text{Flexural buckling mode}: \quad 16{d_{i0}}^2 - R \le 1 \tag{A.3.7}$$

$$\text{Tosional buckling mode}: \quad 16{d_{i0}}^2 - R \ge 1 \tag{A.3.8}$$

Table A3.1 Slenderness ratio and Length of members when torsional buckling and bending buckling occur simultaneously

	H-600×200	H-588×300	H-488×300	H-300×300
λ_y	237	214	203	167
l(mm)	9833	14813	14459	15101

The values of the slenderness ratio around the weak axis λ_y and the length of the member l when the situation $16{d_{i0}}^2$-R=1 is satisfied are shown in Table A3.1. According to this table, the value of λ_y corresponding to the narrow width is larger than the others. The cross section of H-300×300×10×15 is the only one whose slenderness ratio is not over the critical value 200 in Table A1. If the real length of the member is shorter than that shown in this Table, the torsional buckling will occur, while if the real length is longer than that shown in Table A1, the flexural buckling will occur. Moreover, when the lateral bracing is attached at the midspan of the member and the slenderness ratio is not over the critical value 200, the flexural buckling is easy to occur for the case of the

wide width and the torsional buckling is easy to occur for the narrow width.

Chapter 4

Bracing for Buckling of Members with Pinned Ends Subjected to End Moments and Uniformly Distributed Load

4.1 Introduction

The design methods for bracing of steel structure are presented in Design Standard for Steel Structures [1)], Recommendation for Limit State Design of Steel Structures [2)], Recommendations for the Plastic Design of Steel Structures [3)] and Recommendations for Stability Design of Steel Structures [4)].

As the lateral bracing for beam members, it is often considered to be discrete corresponding to the case of secondary beams and continuous corresponding to the case of floor slabs or purlins. In these situations, the lateral deflection and torsion can be restrained by the bracing. In addition, the position attached bracing has an influence on the effect of bracing in practice. The beam members subjected to symmetric end moments only is considered as the most simply loading condition. In fact, the end moments are not symmetric and the effect of distributed load should be taken into account. For this complexity of loading condition, there are a small number of studies related to the lateral bracing for beam members.

Some studies on the lateral bracing for beam members under the complex loading condition mentioned above have been provided. In references 7) and 8), the lateral buckling strength was calculated by the Energy method when the beam members with the continuous bracing are subjected to end moments and distributed loading. The lateral buckling strength of H-shaped steel beam member with two axes of symmetry was calculated by numerical analysis when the beam members subjected to end moments and distributed load in reference 9), and the relation between buckling strength and end moments is also presented when the lateral deflection of upper flange is restrained by the continuous bracing. The equation of equilibrium to calculate lateral buckling strength has been given by Reference 10), when the lateral deflection and torsion of the upper flanges of H-shaped beam members are restrained by continuous bracing. However, these studies all are about the continuous bracing, and the relation between buckling strength and bracing stiffness and the influence on bracing force are not clarified when the lateral deflection and torsion of beam members are restrained by the discrete bracing such as secondary beams. In this situation, the influence of the number of bracing should be discussed when the bracing is not single.

Moreover, reference 11) relates to the influence of lateral bracing and torsional bracing on the lateral buckling strength, and the relation between buckling strength and bracing stiffness and the influence on bracing force are presented. However, the distributed load is not included in the loading condition for analysis. For the combination of end moments and distributed load, the position of bracing is not always the compressive or tensional side. Therefore, there is necessary to clarify the relation

between buckling strength and bracing stiffness for the design of bracing when the distributed load is in general condition. In addition, because the calculation of buckling strength and the design for bracing are complicated, it is necessary to develop evaluative methods as easy as possible for design.

In this chapter, I aim to clarify the relation between buckling strength and bracing stiffness when the beam member with lateral bracing or torsional bracing is subjected to end moments and uniformly distributed load. The number of bracing is one or two and the bracing is attached at equal space along the length of the beam member. in addition, the required bracing stiffness is presented in order that the buckling strength of the beam member subjected to end moments and uniformly distributed load is equal to the buckling strength of the beam member which is subjected to end moments only.

4.2 Analysis

This section presents the method to calculate the buckling equations which has been shown in Chapter 3 when the H-shaped member simply supported at both ends is subjected to axial load, end moments and uniformly distributed load.

4.2.1 Analytical model

The analytical model is shown as Fig. 4.1. The member is simply supported at both ends. The left end is subjected to bending moment M_1 and the right end is subjected to bending moment $M_2=\kappa M_1$ (κ is the end moment ratio). Both ends are subjected to equal compressive force N. the uniformly distributed load is w. there are two kinds of bracing, lateral bracing and torsional bracing whose stiffness are denoted by k_{ivd} and $k_{i\phi d}$ respectively. The number of bracing is one or two and the bracing is attached at equal space along the length of the beam member. In this study, the warping restraint is not considered. Both ends are pinned and turn free around the weak axis.

In Fig. 4.1(b) which has been shown in Chapter 3, $v(x)$ and $\phi(x)$ represent the lateral deflection and the torsional angle of the center of the cross section respectively. The left supporting point of the member is selected as the original point and x axis is set along

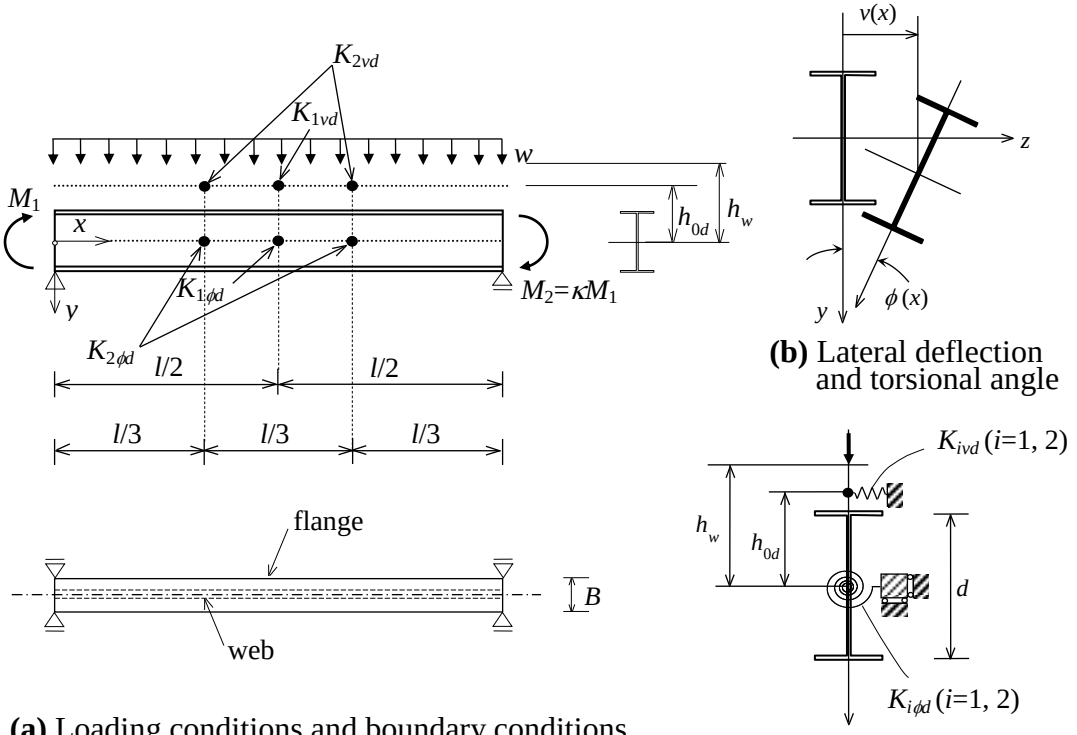

(a) Loading conditions and boundary conditions

(b) Lateral deflection and torsional angle

(c) Position of bracing and uniform distributed load

Fig. 4.1 Analytical model

the member as Fig. 4.1(a) shown. The geometric boundary conditions are $v(0)=v(l)=\phi(0)=\phi(l)=0$ and the mechanical boundary conditions are $v''(0)=v''(l)=\phi''(0)=\phi''(l)=0$. In Fig. 4.1(c), h_{0d} represents the distance from the center of the cross-section to the discrete lateral bracing. h_w is the distance from the center of the cross-section to the position subjected to the uniformly distributed load. The torsional bracing is attached at the center of the cross-section.

In this study, the Rayleigh-Ritz method is used to calculate the approximate value of the buckling strength, because the exact solution of this problem is hard to obtain.

4.2.2 Total-potential energy

The total-potential energy of this model is shown in Eq. (4.1). In addition, $v(x)$ and $\phi(x)$ represent the lateral deflection and the torsional angle along x axis, respectively. The symbols v', ϕ', v'' and ϕ'' in Eq. (3.1) represent the first and the second derivatives of $v(x)$ and $\phi(x)$ with respect to x.

$$\Pi[v,\phi]=\int_0^l \frac{EI_y v''^2}{2}dx+\frac{1}{2}\int_0^l\left(GJ-N\frac{I_y+I_z}{A}\right)\phi'^2 dx+\int_0^l \frac{EI_w\phi''^2}{2}dx+\int_0^l Mv''\phi dx$$
$$-\frac{1}{2}\int_0^l Nv'^2 dx+\int_0^l \frac{wh_w\phi^2}{2}dx+\frac{1}{2}\sum_{i=1}^{n}K_{ivd}\{v(x_i)-h_{0d}\phi(x_i)\}^2+\frac{1}{2}\sum_{i=1}^{n}K_{i\phi d}\phi^2(x_i) \tag{4.1}$$

In Eq. (4.1), the first term is the strain energy of deflection along x axis, the second term is the strain energy of St.Venant torsion reduced by the axial force effect, the third term is the strain energy of warping, the fourth, the fifth and the sixth terms are the potential energy of external loads corresponding to bending moment M, axial force N and uniformly distributed load w respectively, other two terms are the strain energy of discrete lateral bracing and discrete torsional bracing. Definitions of notations are as follows: l is the length of the member, A is the area of the cross-section, I_y and I_z are the second moments of inertia around y and z axes, J is the St.Venant torsional constant, I_w is the warping constant, E is the elastic modulus and G is the shear modulus. In this paper we define as follows:

$$M_e=\frac{1}{2}N_e d\sqrt{1+R},\ N_e=\frac{\pi^2 EI_y}{l^2},\ m\equiv\frac{M_1}{M_e},\ n\equiv\frac{N}{N_e},\ \beta\equiv\frac{wl^2}{8M_1},\ \kappa\equiv\frac{M_2}{M_1},$$
$$\eta_{0d}\equiv\frac{h_{0d}}{d},\ \eta_w\equiv\frac{h_w}{d}$$

M_e is the elastic lateral buckling moment when the member is subjected to equal end moments, N_e is the elastic buckling load for out-of-plane bending around the weak axis, m is the nondimensional bending moment, n is the nondimensional compressive force, β is the uniformly distributed load ratio, κ is the end moment ratio, d is the distance

between the two centroids of the flanges of the H-shaped cross-section.

The nondimensional bracing stiffness is defined as follows:

For lateral bracing: $k_{1vd} = \dfrac{K_{1vd} l^3}{16\pi^2 EI}$ (one brace) $k_{2vd} = \dfrac{2K_{2vd} l^3}{16\pi^2 EI}$ (two braces)

For torsional bracing: $k_{1\phi d} = \dfrac{K_{1\phi d} l}{\pi^2 EI}$ (one brace) $k_{2\phi d} = \dfrac{2K_{2\phi d} l}{\pi^2 EI}$ (two braces)

The buckling modes that satisfy the geometrical boundary conditions and the mechanical boundary conditions are assumed as follows.

$$v(x) = \sum_{i=1}^{m^*} a_i \cdot d \cdot \sin i\pi\xi = d \begin{pmatrix} a_1 & a_2 & \cdots & a_{m^*} \end{pmatrix} \begin{pmatrix} \sin \pi\xi \\ \sin 2\pi\xi \\ \vdots \\ \sin m^*\pi\xi \end{pmatrix} \tag{4.2}$$

$$\phi(x) = \sum_{i=1}^{m^*} b_i \cdot \sin i\pi\xi = \begin{pmatrix} b_1 & b_2 & \cdots & b_{m^*} \end{pmatrix} \begin{pmatrix} \sin \pi\xi \\ \sin 2\pi\xi \\ \vdots \\ \sin m^*\pi\xi \end{pmatrix} \tag{4.3}$$

where $\xi \equiv x/l$. By substituting Eq. (4.2) and (4.3) into Eq. (4.1), the buckling equation for this model can be obtained.

4.3 Results and discussion

4.3.1 Analytical parameters

The analytical parameters are set as follows:

1) The end moment ratio: κ=-1 ~ 1

2) The uniformly distributed load ratio: β=0, 0.5, 1, 1.5 and 2

3) The position of the bracing: η_{0d}=-0.6~ 0.6

4) The section size: H-600×200×11×17 (narrow width, referred to as cross-section 1)
H-300×300×10×15 (wide width, referred to as cross-section 2)

5) The length of the member: l=6m, 12m

6) The kind of the bracing: lateral bracing and torsional bracing

The moment diagrams corresponding to different composition of κ and β are shown as Fig. 4.2.

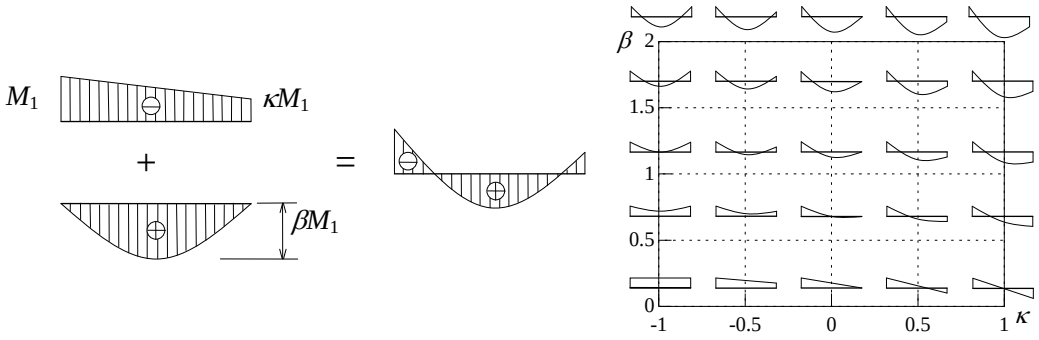

Fig. 4.2 Moment diagrams

4.3.2 Relation between end moment ratio and nondimensional bending moment

i) Effect of number of bracing

Figure 4.3 and Figure 4.4 respectively shows the relation between end moment ratio κ and nondimensional bending moment m by taking the uniformly distributed load ratio β as a parameter, when the length of the member (cross-section 1) is 6m and the lateral bracing is attached at the upper side of the cross section.

Figure 4.3 presents the case when there is no bracing attached at the member and the results are identical with that shown in reference 9). The effect of end moment ratio κ when $\beta \geqq 1$ is smaller than that when β<1.

Figure 4.4 includes the cases with different bracing stiffness for one or two braces. Figures

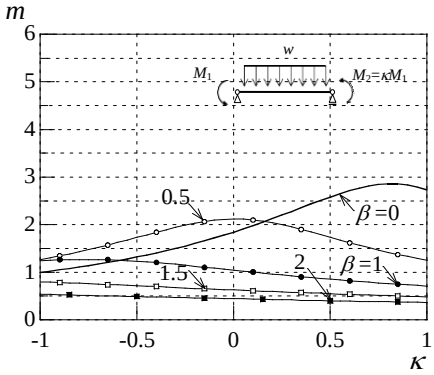

Fig. 4.3 Case of no bracing

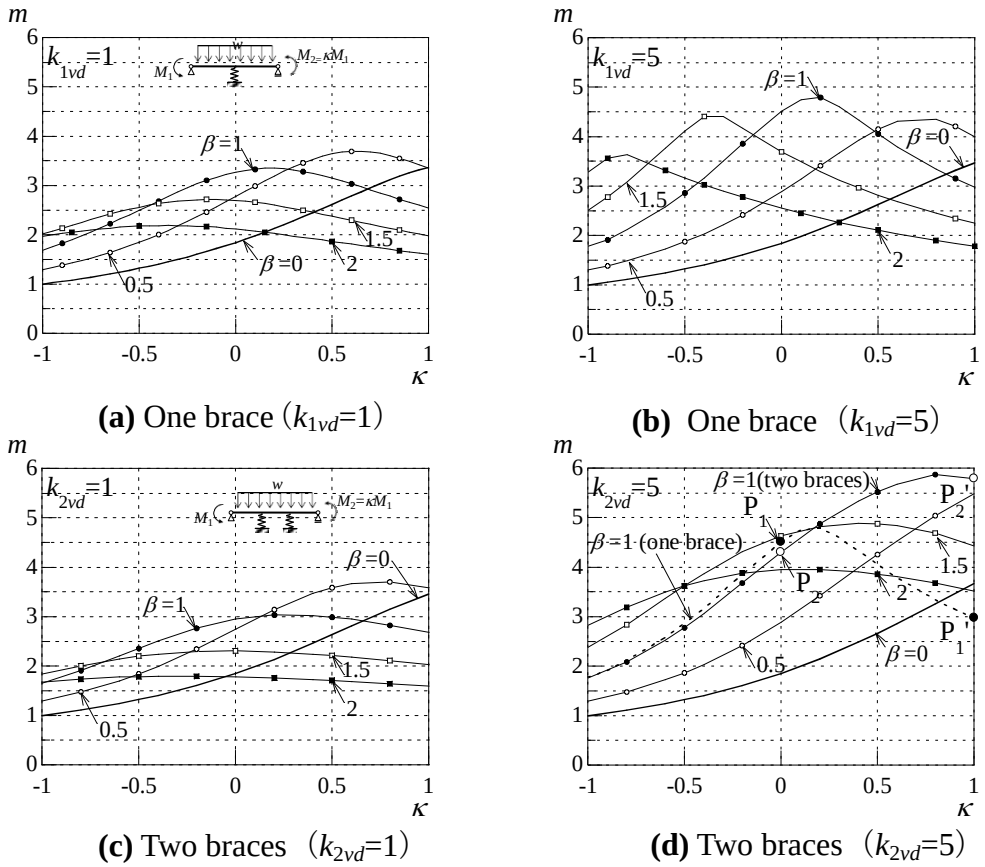

(a) One brace（k_{1vd}=1）　**(b)** One brace （k_{1vd}=5）

(c) Two braces （k_{2vd}=1）　**(d)** Two braces （k_{2vd}=5）

Fig. 4.4 Case of lateral bracing（η_{0d}=-0.6 upper side）

(a), (b) show the cases of one brace whose bracing stiffness k_{1vd} equals 1and 5 respectively. In the situation of $\beta \neq 0$, the end moment ratio κ has much effect on the buckling strength m when the bracing stiffness is large. For the same uniformly distributed load β, the value of κ when buckling strength m becomes maximum value in Fig. 4.4(a) is larger than that with the same conditions in Fig. 4.3.

Figures 4.4(c), (d) present the cases of two braces and the nondimensional bracing stiffness in these figures corresponds to that in Figures 4.4(a), (b). The result of the case of two braces is similar with the case of one brace that the end moment ratio κ has much effect on the buckling strength m when the bracing stiffness is large.

Comparing the cases of one brace and two braces, the value of κ obtained in the case of one brace when buckling strength m becomes maximum value is larger than that obtained in the case of two braces. In the situation with the same β, κ and k_{1vd} (i=1, 2), the relation of magnitude of m between the cases of one brace and two braces is not constant. For instance, the dash line in Fig. 4.4(d) shows the case of one brace when β=1 and k_{1vd}=5. When the end moment ratio κ is approximately smaller than 0.2, the buckling strength of the case of one brace is larger than that of the case of two braces;

when κ is approximately larger than 0.2, the relation of magnitude of m is opposite. Figure 4.5 shows the buckling modes corresponding to the points P_1, P_2, P_1' and P_2' in Figure 4.4(d). Fig. 4.5(a) shows the lateral deflection and the torsional angle when κ=0 (<0.2). According to Fig. 4.5(a), the buckling mode of the case of one brace is similar to that of the case of two braces. Fig. 4.5(b) shows the buckling mode when κ=1 (>0.2). The lateral deflection and the torsional angle in the case of one brace are completely different with those in the case of two braces. That is to say, the effect of bracing on the buckling strength depends on the number of bracing in some way, even though the bracing stiffness is identical. Therefore, the effect of the number of bracing should not be ignored in the design of bracing for beam members.

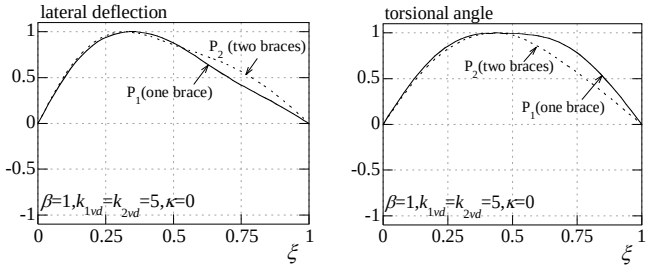

(a-1) Lateral deflection (a-2) Torsional angle

(a) κ=0

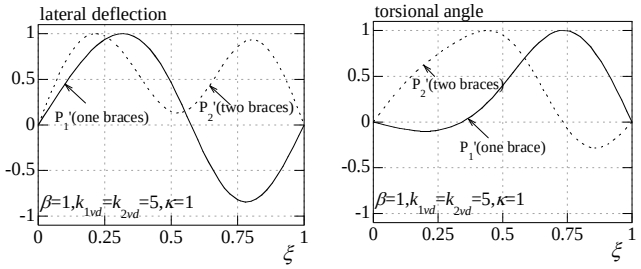

(b-1) Lateral deflection (b-2) Torsional angle

(b) κ=1

Fig. 4.5 Buckling modes

Figure 4.6 shows the relation of m-κ when torsional bracing is attached at the member. Fig. 4.6(a), (b) shows the case of one brace when the bracing stiffness k_{1vd} equals 0.005 and 0.05 respectively. Fig. 4.6(c), (d) shows the case of two braces and the bracing stiffness k_{2vd} corresponding to the case of one brace is equal to 0.005 and 0.05 respectively. According to Fig. 4.6, the buckling strength m of the case of one brace is larger than that of the case of two braces in the situation with the same β, κ and $k_{1\phi d}$ (i=1, 2). For example, the dash line in Fig. 4.6(d) presents the case of one brace when β=1 and $k_{1\phi d}$=0.05.

ii) Effect of bracing stiffness

Figure 4.7 shows the effect of bracing stiffness on the relation of m-κ when one brace is attached at the member (H-600×200×11×17, l=6m). The uniformly distributed load ratio β is set to equal 0.5. Fig. 4.7(a) shows the case of lateral bracing. In the situation of κ=-1 (symmetric end moment), the buckling strength m has little change even though the bracing stiffness increases. However, as the end moment ratio κ increases, the

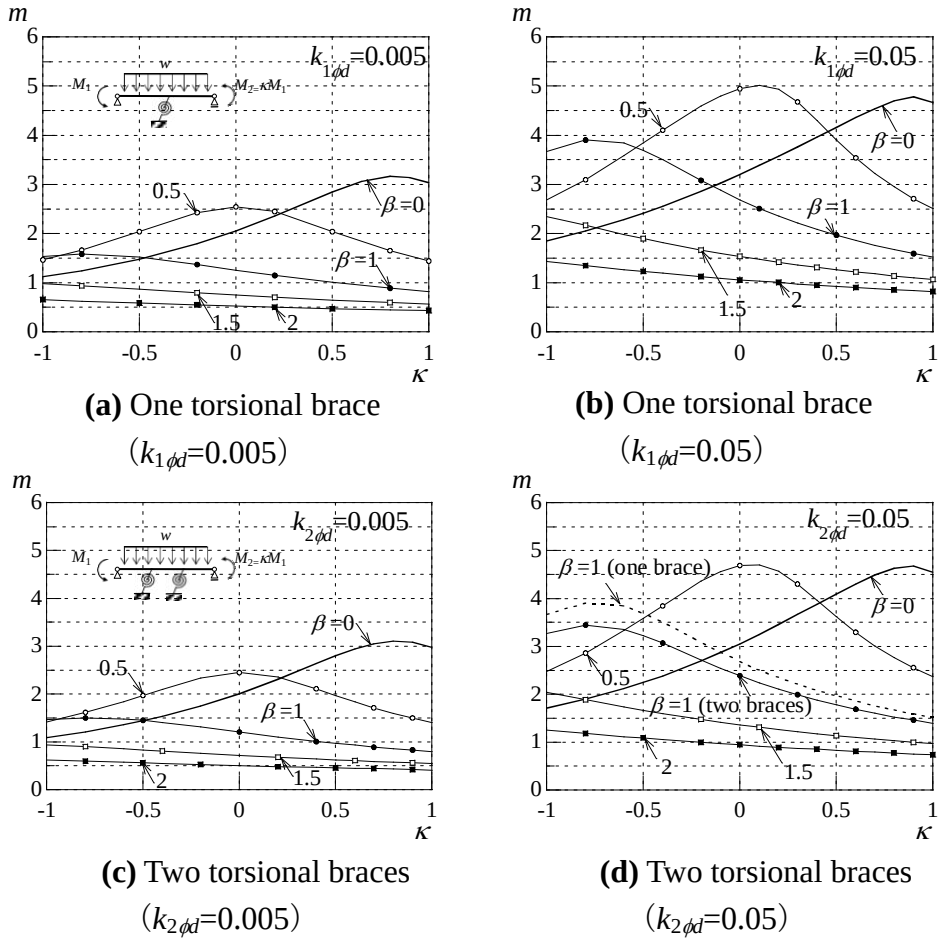

(a) One torsional brace ($k_{1\phi d}$=0.005)

(b) One torsional brace ($k_{1\phi d}$=0.05)

(c) Two torsional braces ($k_{2\phi d}$=0.005)

(d) Two torsional braces ($k_{2\phi d}$=0.05)

Fig. 4.6 Case of torsional bracing

buckling strength m increases and the effect of bracing stiffness becomes larger. This is because that when the lateral bracing is attached at the compressive side, the buckling strength will be developed, while the buckling strength has a little change when the lateral bracing is attached at the tensile side. According to Fig. 4.2, the strength of the bracing point is not identical and it depends on the composition of κ and β. Therefore, to increase the lateral bracing cannot always develop the buckling strength when the member is subjected to end moments and distributed load currently.

Figure 4.7(b) shows the result of torsional bracing in the same conditions with the case of lateral bracing. Because the position of torsional bracing has no influence on the buckling strength, as the bracing stiffness increases ($k_{1\phi d} \leqq 0.5$, approximately), the value of m increases regardless of the end moment ratio κ.

Compared Fig. 4.7(a) and Fig. 4.7(b), setting torsional bracing is more efficiency to increase the buckling strength than setting lateral bracing. Fig. 4.8 presents the comparison between lateral bracing and torsional bracing when the bracing stiffness is

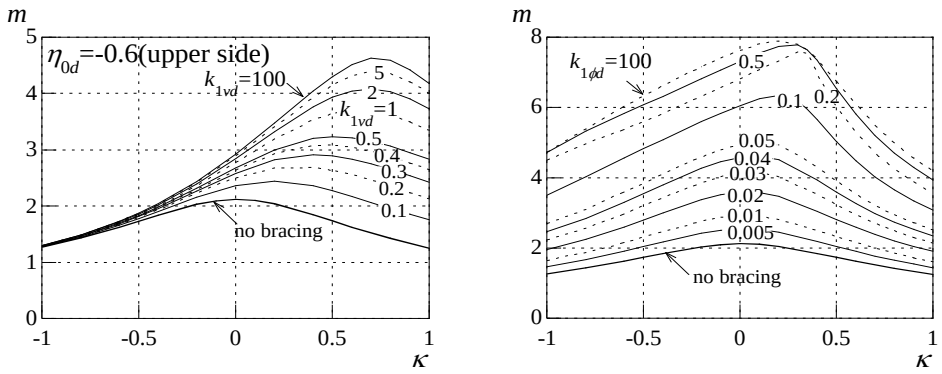

(a) One lateral brace **(b)** One torsional brace

Fig. 4.7 Effect of bracing stiffness (β=0.5)

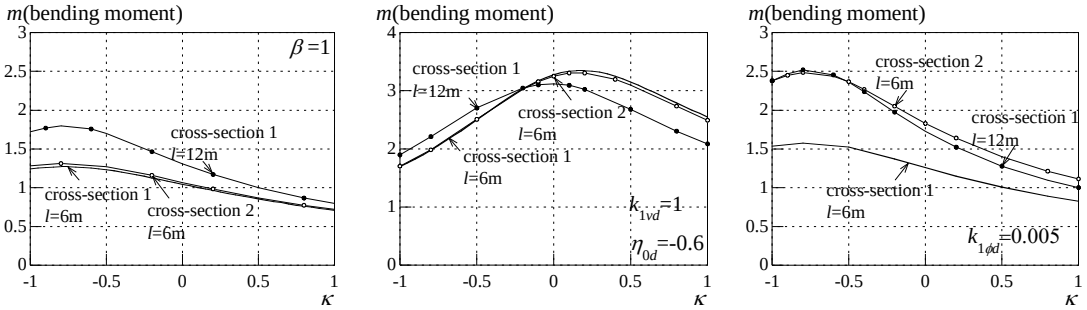

(a) No bracing **(b)** One lateral brace **(c)** One torsional brace

Fig. 4.8 Effect of size of cross section and length of member (β=1)

large enough to make the buckling strength m be maximum value. The uniformly distributed load ratio β is equal to 0, 0.5, 1 and 2 in Fig. 4.7(a), (b), (c) and (d), respectively. According to Fig. 4.7(a), setting lateral bracing at the compressive side or setting torsional bracing has roughly similar effect to increase the buckling strength when $\kappa \leqq 0.5$. And the buckling strength corresponding to torsional bracing is larger than that corresponding to lateral bracing when $\kappa > 0.5$. In Fig. 4.7(b) and (c), the effect to increase buckling strength of the case of torsional bracing is better than that of the case of lateral bracing. When β=2, the results of the cases of lateral bracing and torsional bracing are approximately consistent. Generally speaking, setting torsional bracing is better to develop buckling strength than that setting lateral bracing.

iii) Effect of cross section and length of member

Figure 4.8 shows the relation of m-κ by taking the cross section and length of member as parameters when one brace is attached at the member. The uniformly distributed load ratio β is set equal to unity. Figures 4.8(a), (b) and (c) show the cases of

no bracing, one lateral brace and one torsional brace, respectively. According to Figures 4.8(a), the relation of m-κ has little change when the cross section is different, and the buckling strength corresponding to the case of l=12m is larger than that corresponding to the case of l=6m when the cross section is set to be cross-section 1. In the case of one lateral brace (Figure 4.8(b)), the curves of m-κ of cross-sections 1 and 2 are almost same when the length of member is 6m. However, comparing the cases with different length, the relation of magnitude of m is not constant. In Figure 4.8(c), both cross section and length of member have much effect on the buckling strength.

iv) Effect of position of bracing

Figure 4.9(a), (b) and (c) show the relation of m-κ by taking the position of bracing η_{0d} as a parameter when the uniformly distributed load ratio β is set to equal 0, 0.5 and 2, respectively.

When the member is subjected to end moments only (Fig. 4.9(a), β=0), the lateral bracing set at the lower side is better than that set at the upper side because the lower side is subjected to compressive strength.

When β=0.5 (Fig. 4.9(b)), the portion subjected to compressive strength changes from the lower side only to the upper side as the end moment ratio κ increases. When $\eta_{0d} \geqq 0$ (lower side) and the value of κ is constant, the buckling strength increases as the value of η_{0d} increases. And the increase of m becomes smaller as the end moment ratio κ increases. When κ=1, the buckling strength m of η_{0d}>0 is smaller than that of η_{0d}=0 and the value of m is approximately equal to 1.3 regardless of the value of η_{0d}. The tendency of the situation of η_{0d}<0 is opposite to the situation of η_{0d}>0.

When β=2 (Fig. 4.9(c)), the portion subjected to compressive strength is wide so that the buckling strength m has little increase when $\eta_{0d} \geqq 0$. The effect of bracing on the buckling strength m when η_{0d}<0 is larger than that when $\eta_{0d} \geqq 0$.

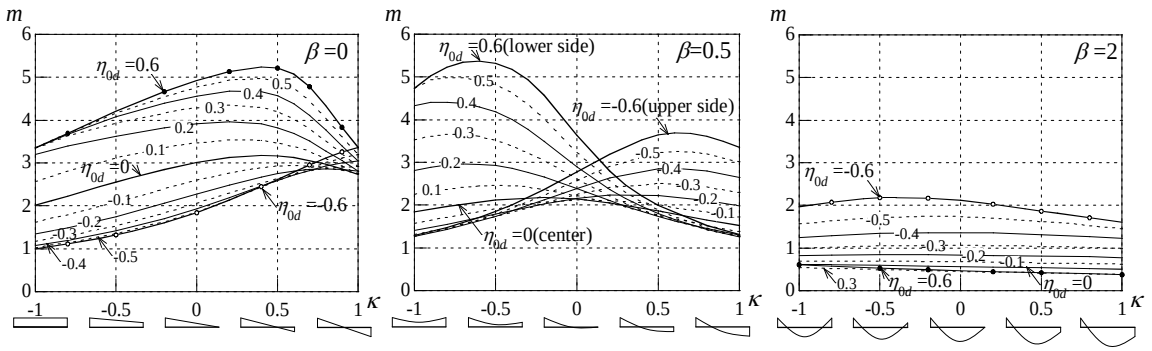

(a) β=0 **(b)** β=0.5 **(c)** β=2

Fig. 4.9 Effect of position of bracing（k_{1vd}=1）

4.3.3 Required bracing stiffness when buckling strength of beam member subjected to end moments and uniformly distributed load is equal to that of beam member subjected end moments only

The design equations of elastic buckling strength when the member is subjected to arbitrary end moments at both ends have been presented. In order to find the design equations of elastic buckling strength when the member with lateral bracing or torsional bracing is subjected to end moments and uniformly distributed load concurrently, this section aims to present the required bracing stiffness when the buckling strength of the beam member which is subjected to end moments and uniformly distributed load is equal to the buckling strength of the beam member which is subjected to end moments only. Because the main purpose is to present the idea and the method, the parameters used in following discussion are not arbitrarily.

Firstly, an example to obtain the required bracing stiffness is shown as Fig. 4.10. The cross section is set to H-600×200×11×17 (cross-section 1) and the length of member is

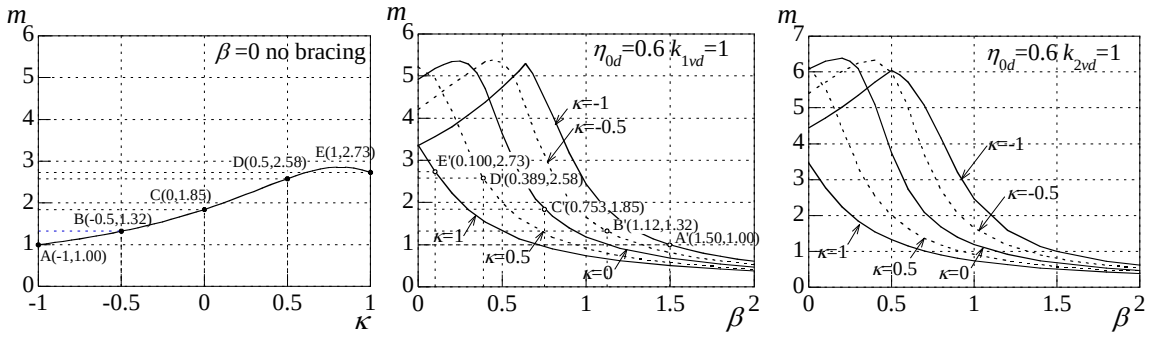

(a) Relation of m-κ when member is subjected to end moment only

(b) Relation of m-β of one lateral brace

(c) Relation of m-β of two lateral braces

Fig. 4.10 Method to obtain required bracing stiffness

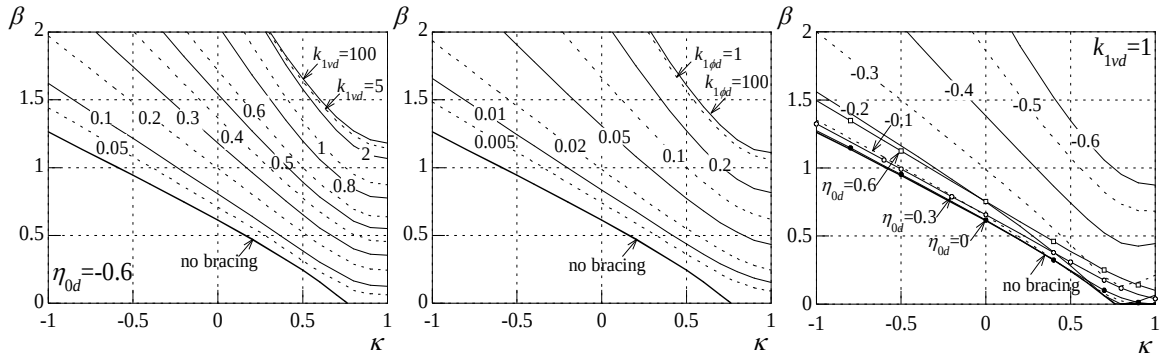

(a) One lateral brace (η_{0d}=-0.6)

(b) One torsional brace

(c) Effect of position of bracing

Fig.4.11 Examples of required bracing stiffness

6m. Figure 4.10(a) shows the elastic buckling strength when the member is subjected to end moments only. The coordinate values of Points A~E (κ, m) are shown in the brackets. Fig. 4.10(b) and (c) show the relation of m-β by taking the end moment ratio κ as a parameter when one and two lateral braces (k_{1vd}=k_{2vd}=1) are respectively attached at lower side (η_{0d}=0.6) of the member which is subjected to end moments and uniformly distributed load. Comparing these two figures, we can find the tendency of the case of two braces is almost same as the case of one brace. In Fig. 4.10(b), the coordinate values of Points A'~E' (β, m) whose vertical coordinate value m is identical to that of Points A~E shown in Fig. 4.10(a) are presented in the brackets. According to this figure, when the uniformly distributed load ratio β is smaller than the horizontal values shown in the brackets, the buckling strength m are always larger than the elastic buckling strength obtained in Fig. 4.10(a). For instance, when κ=-1 and β=1.5 (Point A'), if $\beta \leqq$ 1.5, the buckling strength in this condition can be evaluated in the safety margin by using the elastic buckling strength shown in Fig. 4.10(a) when the member is subjected to end moments only.

Based on this idea, we can obtain the values of β by determining the values of end moment ratio κ and the bracing stiffness k_{1vd} and $k_{1\phi d}$. and the relation of β-κ are presented in Fig. 4.11. The cross section is H-600×200×11×17 (cross-section 1) and the length of member is 6m. Fig. 4.11(a) and (b) respectively shows the cases of one lateral brace (η_{0d}=-0.6, upper side) and one torsional brace by taking the bracing stiffness as a parameter. Using this method, when the end moment ratio κ and the uniformly distributed load ratio β of beam member are determined, the required bracing stiffness when the buckling strength may be evaluated directly by the elastic buckling strength which is used to the case of the member subjected to end moments only.

4.4 Conclusions

The nondimensional elastic buckling strength of H-shaped member subjected to end moments and uniformly distributed load concurrently when discrete lateral or torsional bracing is attached at the member has been calculated by Rayleigh-Ritz method. The relation between end moment ratio κ and the nondimensional bending moment m has been presented by taking the number of brace, bracing stiffness, size of cross section, length of member and position of bracing as parameters.

In addition, the method to obtain the required bracing stiffness has also been presented. When the bracing has the required bracing stiffness, the buckling strength of the beam subjected to end moments and uniformly distributed load is equal to the buckling strength of the beam subjected to end moments only (Fig. 4.10). And some figures of required bracing stiffness as examples have been presented (Fig. 4.11). The main findings are shown as follows:

1) About the effect of number of bracing, when the uniformly distributed load β, the bracing stiffness k_{ivd} (i=1, 2) and the end moment ratio κ is identical, the elastic buckling strength of the case of one lateral brace is not always larger or smaller than that of the case of two lateral braces because of the variety of buckling modes (Fig. 4.4). Because the position of bracing has no influence on the torsional bracing, the buckling strength m become larger and the value of κ when the buckling strength m becomes the maximum value has a little change as the bracing stiffness increases. This is different from the case of lateral bracing whose result of κ has much change as the bracing stiffness increases (Fig. 4.7).
2) As for the effect of size of cross section and length of member on the buckling strength, the relation of m-κ in the case of lateral bracing is much the same even if the size of cross section is different and the buckling strength m in the case of l=12 is larger than that in the case of l=6m when the cross section is identical (Fig. 4.8(b)). In the case of torsional bracing, both the size of cross section and the length of member have much influence on the relation of m-κ (Fig. 4.8(c)).
3) As regards the effect of position of bracing, the part subjected to compressive stress is changed to the upper side from the lower side only as the end moment ratio κ increases (Fig. 4.9(b)). And in the case of β=2 (Fig. 4.9(c)), the buckling strength m is affected little by the position of bracing as the end moment ratio varies.

References for Chapter 4

1) Architectural Institute of Japan: Design Standard for Steel Structures -Based on Allowable Stress Concept-, 2005.09
2) Architectural Institute of Japan: Recommendation for Limit State Design of Steel Structures, 2010.02
3) Architectural Institute of Japan: Recommendations for the Plastic Design of Steel Structures, 2010.02
4) Architectural Institute of Japan: Recommendations for Stability Design of Steel Structures, 2009.11
5) Liu Mao and Kido Masae: Bracing for buckling of members with pinned ends subjected to bending moment and axial force –Part 1 Analysis and results of member subjected to axial force–, AIJ Kyushu Chapter Architectural Research Meeting, No53, pp.337-340, 2014.03
6) Liu Mao and Kido Masae: Bracing for buckling of members with pinned ends subjected to bending moment and axial force –Part 2 Results of member subjected to axial force and bending moment–, AIJ Kyushu Chapter Architectural Research Meeting, No53, pp.341-344, 2014.03
7) 藤本盛久，鈴木博：連続拘束を受ける H 形断面ばりの横座屈，日本建築学会大会学術講演梗概集， pp.961-962，1968.10
8) 藤本盛久：端モーメントと等分布荷重を受ける連続拘束された鉄骨 H 形断面梁の横座屈について, 日本建築学会大会学術講演梗概集, pp.1029-1030, 1969.8
9) 若林實，中村武：端モーメントと等分布荷重を受ける鉄骨 H 形はりの弾性横座屈に対する数値解析，日本建築学会論文報告集，第 208 号，pp.7-13，1973.6
10) 加藤勉, 秋山宏 : 上フランジを連続拘束された H 形断面鋼梁の弾性横座屈，日本建築学会論文報告集，第 232 号，pp41-49，1975.6
11) Yoshihiro Kimura and Yuki Yoshino: Required bracing capacity on lateral buckling strengh for h-shaped beams with bracings, Journal of Structural and Construction Engineering,Vol.76, No.670, pp.2143-2152, 2011.12
12) 日本建築学会：鋼構造物の座屈に関する諸問題 2013，2013.6

Chapter 5

Summary

5. Summary

This dissertation is concerned with the design methods for bracing of steel members and aimed at developing the methods for increasing the elastic buckling strength. The main findings for each chapter are shown as follows.

In Chapter 2, the buckling equations when the compressive member with one or two braces is subjected to varying axial force have been calculated by the buckling slope deflection method. The main findings concerned with the stiffness and the strength for bracing are summarized respectively.

As for the stiffness for bracing, the effective length factor γ_0 becomes larger as the ratio of axial forces increases, when the nondimensional bracing stiffness k is constant. The buckling modes are presented when the value of the nondimensional bracing stiffness k is equal to 0, 0.5 and 3. The ratio of axial forces plays an important role in the variation of buckling mode. In addition, the required bracing stiffness to take the effective length as the brace spacing is calculated and it decreases as the axial force ratio decreases. A specific example about the truss beam has been displayed in the final part of this section in order to present the application of this study in structural design.

As for the strength for bracing, the value of the nondimensional axial force p becomes larger as the value of the rotational angle R increases. The effect of the rotational angle R on the nondimensional axial force p becomes smaller as R increases. However, the value of p will not increase at all times, and it will approach constant as the value of p increases. When the value of F/N_1 is same, the value of the nondimensional axial force p increases as the axial force ratio a decreases and the value of p with k =1 is greater than that the value of p with k =0.5, in the case that the axial force ratio is same. According to Fig. 2.19(a) and (c), when the nondimensional bracing stiffness k is same, the value of F/N_E increases as the axial force ratio a increases, while the value of F/N_E decreases as the axial force ratio a increases. Moreover, as the nondimensional bracing stiffness k increases, the effect of the axial force ratio on the value of F/N_E becomes smaller when the axial force varies in a staircase pattern.

In Chapter 3, the general buckling equation of the H-shaped member pinned at both ends and subjected to the axial load, the end moments and the uniformly distributed load with the lateral bracing and torsional bracing is calculated by using the Rayleigh-Ritz method. The moment – axial force interaction of the elastic buckling strength when the lateral bracing or the torsional bracing are attached at the midspan of the member is presented.

When the lateral bracing is attached at the midspan of the member, the deflection and the torsional angle at the bracing point are zero as the bracing stiffness increases in case of the end moment ratio κ=-1 (symmetric end moment, Fig. 3.2(a)). As for the case of κ=1 (antisymmetric end moment), bracing is effective when the compressive force is large. However, the *m*-*n* interaction is same when the bracing stiffness is above a certain value (Fig. 3.2(c)).

There are two different buckling moments for one buckling axial force when the bracing is attached at the compressive flange (Fig. 3.3(a)).

When the length of the member is same, the effect of the cross section on the *m*-*n* interaction is not so remarkable (Fig. 3.4(a)). As for the influence of the member length, the difference of bucking modes affects the *m*-*n* interaction. The weak axis buckling or torsional buckling occurs depending on the member length when the member is subjected to axial force and the bracing stiffness increases.

About the effect of the torsional bracing, the deflection and the torsional angle at the bracing point are zero as the bracing stiffness increases in case of the end moment ratio κ=-1 (Fig. 3.5(a)).

When the lateral bracing or the torsional bracing is attached at the midspan of the member, the buckling mode that the deflection and the torsional angle at the bracing point are zero is referred to as full-bracing. The relation between the nondimensional buckling axial force and the required bracing stiffness for full-bracing is presented by Fig. 3.6 and Fig. 3.7. The simple equations to obtain the required bracing stiffness and the scope of the application are presented (Eq. (3.17), (3.18) and (3.20)).

In Chapter 4, the nondimensional elastic buckling strength of H-shaped member subjected to end moments and uniformly distributed load concurrently when discrete lateral or torsional bracing is attached at the member has been calculated by Rayleigh-Ritz method. The relation between end moment ratio κ and the nondimensional bending moment *m* has been presented by taking the number of brace, bracing stiffness, size of cross section, length of member and position of bracing as parameters.

As for the effect of number of bracing, when the uniformly distributed load β, the bracing stiffness k_{ivd} (i=1, 2) and the end moment ratio κ is identical, the elastic buckling strength of the case of one lateral brace is not always larger or smaller than that of the case of two lateral braces because of the variety of buckling modes (Fig. 4.4). Because the position of bracing has no influence on the torsional bracing, the buckling strength *m* become larger and the value of κ when the buckling strength *m* becomes the

maximum value has a little change as the bracing stiffness increases. This is different from the case of lateral bracing whose result of κ has much change as the bracing stiffness increases (Fig. 4.7).

As for the effect of size of cross section and length of member on the buckling strength, the relation of m-κ in the case of lateral bracing is much the same even if the size of cross section is different and the buckling strength m in the case of l=12 is larger than that in the case of l=6m when the cross section is identical (Fig. 4.8(b)). In the case of torsional bracing, both the size of cross section and the length of member have much influence on the relation of m-κ (Fig. 4.8(c)).

As regards the effect of position of bracing, the part subjected to compressive stress is changed to the upper side from the lower side only as the end moment ratio κ increases (Fig. 4.9(b)). And in the case of β=2 (Fig. 4.9(c)), the buckling strength m is affected little by the position of bracing as the end moment ratio varies.

In addition, the method to obtain the required bracing stiffness has also been presented. When the bracing has the required bracing stiffness, the buckling strength of the beam subjected to end moments and uniformly distributed load is equal to the buckling strength of the beam subjected to end moments only (Fig. 4.10). And some figures of required bracing stiffness as examples have been presented (Fig. 4.11).

In the future, the establishment of integrative evaluation method of bracing stiffness and bracing force for steel beams and steel beam-columns will be discussed as a continuation of my present research. Series of detail analysis on the H-shaped members with composite effect of lateral bracing and torsional bracing under general loading conditions will be carried out by considering several parameters, such as loading conditions, types of combination of bracing, bracing position, size of cross section, length of member and so on. The influence of these parameters will be given by the relation between lateral or flexural-torsional buckling strength and bracing stiffness. In addition, the relation between bracing force and deflection behavior should be discussed as well. Based on these analytical results, simple equations for evaluating bracing stiffness and bracing force will be developed for design.

Acknowledgement

Upon the completion of this dissertation, I would like to express my heartfelt gratitude to a number of people.

Firstly, my deepest gratitude goes foremost to Dr. Masae KIDO, Associate Professor of the University of Kitakyushu, for her effective guidance and encouragement. Without her consistent and illumination instruction, I could not have this dissertation reached its present form. I also wish to express my heartfelt gratitude to Dr. Keigo TSUDA, Professor of the University of Kitakyushu, who gave me a lot of valuable advices and encouragement for my research.

Moreover, I am also greatly indebted to Dr. Koji TAKASU, Professor of the University of Kitakyushu, and Dr. Kohji NAKAZAWA, Professor of the University of Kitakyushu, for their valuable advices on this dissertation. And I extend my faithful thanks to Dr. Kazuaki HOKI, Lecturer of the University of Kitakyushu, and Dr. Shintaro MATSUO, Associate Professor of Kyushu University, who gave me some valuable advices and helped me a lot on my research. And I also owe my sincere gratitude to Ms. Qingsong LIU, Mr. Guiqiu SHI, Mr. Sha LI, Ms. Misato KAMIJO, Ms. Aya NAI, the former Graduate School students of the university of Kitakyushu, and the present members of our lab who gave me their help and time in listening to me and helping me work out my problems during the difficult course of this dissertation.

Finally, my thanks would go to my beloved family for their loving considerations and great confidence in me all through these years.